Zoological Journal of the Linnean Society, 2022, **195**, 761–814. With 19 figures.

Combined phylogeny and new classification of catsharks (Chondrichthyes: Elasmobranchii: Carcharhiniformes)

KARLA D. A. SOARES*[✉] and KLEBER MATHUBARA

Departamento de Zoologia, Instituto de Biologia, Universidade Federal do Rio de Janeiro, Rio de Janeiro, RJ 21941-902, Brazil
Departamento de Zoologia, Instituto de Biociências, Universidade de São Paulo, SP 05508-900, Brazil

Received 26 October 2020; revised 19 October 2021; accepted for publication 5 November 2021

This is the first study to combine morphological and molecular characters to infer the phylogenetic relationships among catsharks. All currently valid genera classified in the family Scyliorhinidae *s.l.* and representatives of other carcharhinoid families plus one lamnoid and two orectoloboids were included as terminal taxa. A total of 143 morphological characters and 44 *NADH2* sequences were analysed. Parsimony analyses under different weighting schemes and strengths were used to generate hypotheses of phylogenetic relationships. The phylogenetic analysis of 78 terminal taxa, using the combined dataset and weighting each column separately (SEP; $k = 3$) resulted in one most-parsimonious cladogram of 4441 steps with the greatest internal resolution of clades and strongest support. The main changes in nomenclature and classification are the revised definition and scope of Scyliorhinidae, *Apristurus* and *Pentanchus* and the revalidation of Atelomycteridae. The monophyly of Pentanchidae is supported, as is that of most catshark genera. Two new subfamilies of the family Pentanchidae are defined: **Halaelurinae subfam. nov.** and **Galeinae subfam. nov.** Our analysis emphasizes the relevance of morphological characters in the inference of evolutionary history of carcharhinoids and sheds light on the taxonomic status of some genera in need of further exploration.

ADDITIONAL KEYWORDS: Atelomycteridae – Pentanchidae – Scyliorhinidae – total evidence.

INTRODUCTION

> "Variation in the catuloids is so extreme as to make distinction even between genera difficult, and a study of the phylogenetic characters is of the utmost importance, therefore, in establishing relationships. (White, 1936b)"
>
> "…[sub]divisions of the Scyliorhinidae should be based on broad pattern interrelationships rather than superficial similarities and differences in a few characters. (Compagno, 1988)"

Catsharks are a well-known group of carcharhiniforms traditionally grouped in the family Scyliorhinidae by sharing the character of a first dorsal fin situated posteriorly to the pelvic fins (Garman, 1913; Bigelow & Schroeder, 1948; Springer, 1979; Compagno, 1988; Compagno *et al.*, 2005; Ebert *et al.*, 2013). Scyliorhinidae *s.l.* comprises 18 genera and ~160 currently valid species of colourful and small-sized sharks found on and near the bottom in almost all seas, from cold to tropical waters, except the Antarctic (Compagno, 1988; Compagno *et al.*, 2005; Ebert *et al.*, 2013; Weigmann, 2016; Weigmann *et al.*, 2018; White *et al.*, 2019). Scyliorhinoids represent about a quarter of living shark species, and many new species have been described in recent years (42 were described over the past two decades; Weigmann, 2016).

Hypotheses regarding the phylogenetic relationships among catsharks diverge depending on the characters analysed (i.e. morphology or DNA), but no combined analysis has been performed so far. The combination of different datasets prior to phylogenetic analysis has been argued by different authors as a method with the potential to increase the descriptive efficiency and explanatory power of the data (e.g. Hillis, 1987; Kluge, 1989; Eernisse & Kluge, 1993; Dragoo & Honeycutt, 1997). Some arguments in favour of including all available data in a single analysis are

*Corresponding author E-mail: karlad.soares@yahoo.com.br
[Version of record, published online 3 March 2022; http://zoobank.org/ urn:lsid:zoobank.org:pub:7C65630E-BD2A-4A73-AFEF-AF9FC64C240B]

that different character classes might provide better levels of resolution at different nodes of a tree (Hillis, 1987), and phylogenetic analyses should explain all the data simultaneously (Kluge, 1989; Kluge & Wolf, 1993). Despite the great number of recent phylogenetic appraisals of elasmobranchs, most of them are based solely on molecular data (e.g. Douady *et al.*, 2003; Winchell *et al.*, 2004; Iglésias *et al.*, 2005; Naylor *et al.*, 2005, 2012a, b; Human *et al.*, 2006; Vélez-Zuazo & Agnarsson, 2011) and few are focused on relationships at or below the family level (Eitner, 1995; López *et al.*, 2006; Cavalcanti, 2007; Corrigan & Beheregaray, 2009).

Here, we combine morphological and molecular data of representatives of all catshark genera and analyse their relationships across carcharhinoids. We begin with the historical background of the family Scyliorhinidae.

Historical background

References on catsharks are found in the literature since pre-Linnaean works and have appeared on the pages of many classical studies of fishes (e.g. Rondelet, 1554; Salviani, 1554; Gesner, 1586; Artedi, 1738; Gronovius, 1756; Linnaeus, 1758; Berkenhout, 1769; Bloch, 1785, 1796; Hoffman & Jordan, 1892). In the earliest classifications, there were two genera, *Scyliorhinus* Blainville, 1816 and *Galeus* Rafinesque, 1810, differing mainly by the shape of the snout and presence or absence of caudal crests (Müller & Henle, 1841; Regan, 1908). Over time, detailed morphological studies and taxonomic reviews have enabled the proposition and inclusion of new catshark genera in the family Scyliorhinidae (Gill, 1862; Garman, 1913; Whitley, 1948; Springer, 1966, 1979; White *et al.*, 2019).

Scyliorhinoids and orectoloboids (wobbegong and carpet sharks) were grouped together by characters of the posterior position of first dorsal fins and morphology of nasal flaps and furrows until Regan (1908) separated these taxa into different families. Recent authors agree with the classification of catsharks within Carcharhiniformes based on their having a tripodal rostrum and a nictitating membrane with an associated postorbital musculature (Compagno, 1988; de Carvalho, 1996; Shirai, 1996). Nevertheless, the arrangement and scope of the family Scyliorhinidae has undergone several changes over the years, and phylogenetic relationships among these sharks remain uncertain (Garman, 1913; White, 1937; Compagno, 1973, 1988; Nakaya, 1975; Springer, 1979; Iglésias *et al.*, 2005; Naylor *et al.*, 2012a).

White (1936b) pointed out that scyliorhinids are difficult to classify because of their conservative morphology. She was the first to divide catsharks into different families: Catulidae, Atelomycteridae and Halaeluridae, based on the counts of heart and intestinal valves and the calcification pattern of vertebral centra (White, 1936a, b, 1937). However, these characters were not useful to distinguish unambiguously among her three families, and differences among scyliorhinoids, *Proscyllium* Hilgendorf, 1904 and *Pseudotriakis* Brito Capello, 1868, were overlooked (Nakaya, 1975; Compagno, 1988). Most subsequent workers recognized only one family of catsharks (e.g. Fowler, 1941; Bigelow & Schroeder, 1948; Springer, 1966, 1979; Bass *et al.*, 1975; Nakaya, 1975; Compagno, 1984, 1988; Compagno *et al.*, 2005; Ebert *et al.*, 2013; Nelson *et al.*, 2016). Like White, many authors have relied upon few characters for the division of groups in Scyliorhinidae, mostly from external morphology, such as size and position of fins, squamation, teeth, nasal flaps and labial furrows, while internal anatomy was represented only by the supraorbital crest on the neurocranium and the extrabranchial cartilages (Regan, 1908; Garman, 1913; Leigh-Sharpe, 1926; Springer, 1966, 1979; Nakaya, 1975). Maisey (1984) provided the first cladistic evidence of the paraphyly of scyliorhinids, resolving *Scyliorhinus* as a sister group of triakids + carcharhinids + *Galeus*. Even so, none of the subsequent morphological studies recognized that paraphyly, because no strict cladistic analysis was performed (Compagno, 1988; Herman *et al.*, 1990) or the group was undersampled (de Carvalho, 1996; Shirai, 1996; Douady *et al.*, 2003).

Compagno (1988) pointed out that Scyliorhinidae is a heterogeneous 'ragbag' diagnosed phenetically by the absence of higher carcharhinoid characters and would require extensive revision. Despite recognizing the absence of a well-defined autapomorphy for the family and that different groups of scyliorhinoids could have separate relationships to higher carcharhinoids, mainly to Proscylliidae, he followed the traditional classification of Scyliorhinidae (Bigelow & Schroeder, 1948; Springer, 1966, 1979; Compagno, 1984). Compagno (1988) also presented a large amount of morphological data for carcharhiniforms and proposed a classification of catsharks in four subfamilies (Atelomycterinae, Pentanchinae, Schroederichthyinae and Scyliorhininae), which are yet to be tested for cladistic monophyly.

Iglésias *et al.* (2005) analysed mitochondrial (12S, 16S and valine-tRNA) and nuclear (*RAG1*) genes and corroborated the paraphyly of Scyliorhinidae. The authors also resurrected the family Pentanchidae to include catshark genera with no supraorbital crest on the neurocranium and restricted Scyliorhinidae to *Scyliorhinus*, *Cephaloscyllium* Gill, 1862, *Poroderma* Smith, 1838, *Atelomycterus* Garman, 1913, *Aulohalaelurus* Fowler, 1934 and *Schroederichthys* Springer, 1966 (Scyliorhinidae *s.s.*). The paraphyly of the family was also corroborated by Human *et al.* (2006), who used different genes (*cytb*, *NADH2* and *NADH4*). However, representatives of only seven of the 18 genera assigned to Scyliorhinidae were included in both works.

Most recently, Vélez-Zuazo & Agnarsson (2011) and Naylor *et al.* (2012a) recovered three distinct paraphyletic lineages of catsharks: (1) *Apristurus* Garman, 1913, *Galeus*, *Asymbolus* Whitley, 1939, *Figaro* Whitley, 1928, *Bythaelurus* Compagno, 1988, *Halaelurus* Gill, 1862, *Haploblepharus* Garman, 1913, *Holohalaelurus* Fowler, 1934 and *Parmaturus xaniurus* (Gilbert, 1892); (2) *Atelomycterus*, *Aulohalaelurus*, *Schroederichthys* and *Parmaturus* sp.; and (3) *Cephaloscyllium*, *Poroderma* and *Scyliorhinus*. These results indicated that Scyliorhinidae *s.s.* as proposed by Iglésias *et al.* (2005) is still paraphyletic, and further investigation is needed. A summary of previous hypotheses of relationships among catshark genera based on morphological and molecular data is presented in Figure 1.

Doubts on the monophyly of the genera *Apristurus*, *Galeus*, *Halaelurus* and *Parmaturus* still persist (Vélez-Zuazo & Agnarsson, 2011; Naylor *et al.*, 2012a). *Galeus sauteri* (Jordan & Richardson, 1909) was placed separately from its congeners and the validity of *Halaelurus* and *Haploblepharus* was questioned by Naylor *et al.* (2012a). Different hypotheses regarding intragenus relationships of *Apristurus*, the largest genus among extant sharks, and the validity of *Pentanchus* as a genus distinct from *Apristurus* have been discussed, but without reaching overall consensus (Compagno, 1988; Nakaya & Sato, 1999; Nakaya & Séret, 2000; Sato, 2000; Iglésias *et al.*, 2005; Naylor *et al.*, 2012a; Weigmann, 2016). The scope of *Parmaturus* Garman, 1906 has undergone several reclassifications over the years, and relationships between its species and with other genera, such as *Figaro*, *Galeus* and *Apristurus*, are not fully understood (Springer, 1979; Compagno, 1988; Séret & Last, 2007; Vélez-Zuazo & Agnarsson, 2011; Naylor *et al.*, 2012a).

The present analysis is the first study to include all catshark genera, totalling 62 of the 160 species currently valid for Scyliorhinidae *s.l.* (Compagno, 1988); 22 species used in this study have never been included in any phylogenetic analysis. The goals of this study are as follows: (1) to provide a phylogenetic hypothesis among scyliorhinoids and other carcharhinoids, combining morphological and molecular data and shedding light on the taxonomic status of some genera in need of further exploration; (2) to test different weighting schemes and strengths, seeking the best internal resolution of clades and the strongest support; and (3) to investigate intrageneric relationships, especially within *Apristurus*, *Galeus* and *Scyliorhinus*. To summarize, we propose a phylogeny-based classification of catsharks.

MATERIAL AND METHODS

Selection of taxa

The phylogenetic analysis performed here included 78 terminal taxa. Species representing all currently valid genera assigned to the family Scyliorhinidae *s.l.* (Compagno, 1988) and the recently proposed *Akheilos* White, Fahmi & Weigmann, 2019 were included

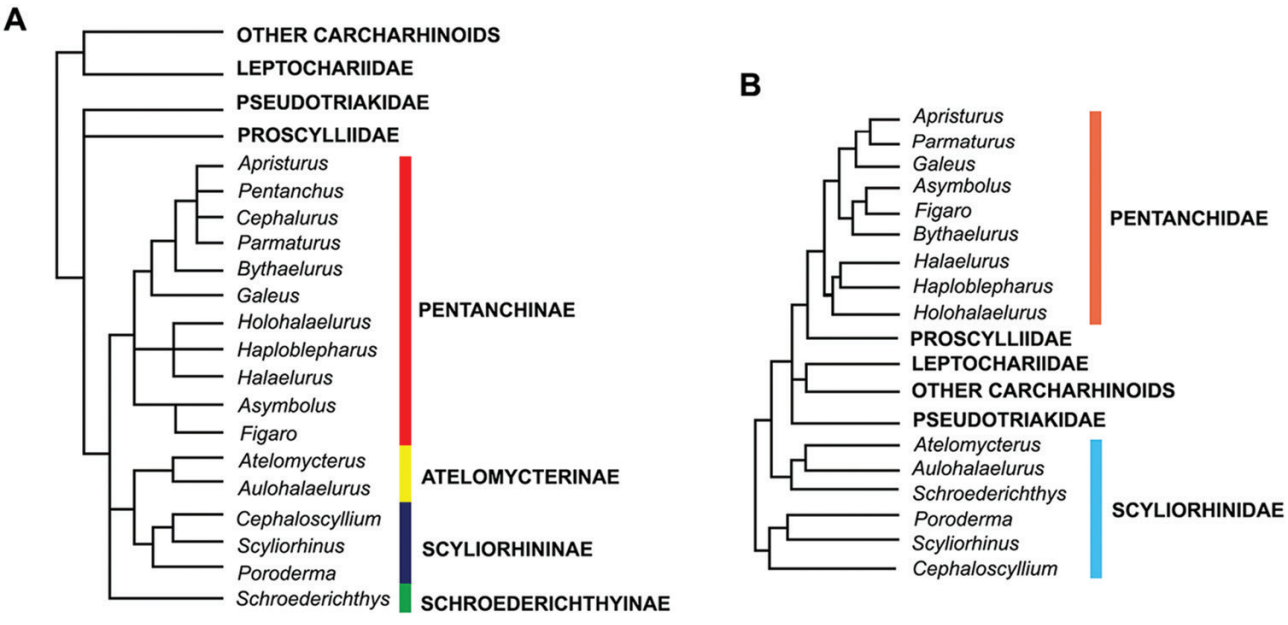

Figure 1. Summary of previous hypotheses on catsharks. A, morphology-based phylogeny from Compagno (1988). B, molecular-based phylogeny from Naylor *et al.* (2012a).

as ingroup taxa. Juveniles and adults, male and female specimens of 16 of the 18 catshark genera (excluding only *Akheilos*) were examined and some were dissected for anatomical investigation, totalling 221 specimens. Morphological data on *Akheilos suwartanai* White, Fahmi & Weigmann, 2019 and *Pentanchus profundicolus* Smith & Radcliffe, 1912 were extracted from the literature (Compagno, 1988; Nakaya & Séret, 2000; White *et al.*, 2019) owing to the lack of available material for study. Representatives of the four subfamilies proposed by Compagno (1988) were examined as follows (examined/valid species): Atelomycterinae, *Atelomycterus* (2/7) and *Aulohalaelurus* (2/3); Pentanchinae, *Apristurus* (8/31), *Asymbolus* (3/9), *Bythaelurus* (3/14), *Cephalurus* (1/1), *Figaro* (1/2), *Galeus* (5/18), *Halaelurus* (2/7), *Haploblepharus* (1/4), *Holohalaelurus* (1/5) and *Parmaturus* (5/11); Schroederichthyinae, *Schroederichthys* (3/5); Scyliorhininae, *Cephaloscyllium* (5/18), *Poroderma* (2/2) and *Scyliorhinus* (16/16). Complete specimens of *Aulohalaelurus* and *Bythaelurus* were not available for full dissection, but the neurocranium and claspers of a specimen of an *Aulohalaelurus* (MNHN 1988-1860) and claspers of two specimens of *Bythaelurus* (MNHN 1988-0355 and MNHN 1990-0726) were examined from material previously dissected by Séret (1990) and Soares (2020), respectively.

For comparative outgroup taxa, we examined representatives of other families of Carcharhiniformes (Compagno, 1988; Ebert *et al.*, 2013): Carcharhinidae [*Carcharhinus melanopterus* Quoy & Gaimard, 1824, *Loxodon macrorhinus* Müller & Henle, 1839, *Rhizoprionodon longurio* (Jordan & Gilbert, 1882) and *Triaenodon obesus* (Rüppell, 1837)], Hemigaleidae [*Paragaleus pectoralis* (Garman, 1906)], Proscylliidae [*Eridacnis barbouri* (Bigelow & Schroeder, 1944) and *Proscyllium habereri* Hilgendorf, 1904], Pseudotriakidae [*Gollum attenuatus* (Garrick, 1954)], Triakidae [*Galeorhinus galeus* (Linnaeus, 1758), *Hemitriakis japonica* (Müller & Henle, 1839), *Iago omanensis* (Norman, 1939), *Mustelus schmitti* Springer, 1939 and *Triakis semifasciata* Girard, 1855], in addition to one Lamniformes [*Alopias vulpinus* (Bonnaterre, 1788)] and two Orectolobiformes [*Chiloscyllium griseum* Müller & Henle, 1838 and *Hemiscyllium ocellatum* (Bonnaterre, 1788)].

The material examined for this study was previously fixed in formalin and then transferred to and preserved in 70–75% ethanol. Specimens are deposited in the following institutions: American Museum of Natural History, New York (AMNH); Australian Museum, Sydney (AMS); Natural History Museum, London (BMNH); California Academy Sciences, CA (CAS); Commonwealth Scientific & Industrial Research Organization, Hobart, Tasmania (CSIRO); Florida Museum of Natural History, Gainesville, FL (FLMNH); Hokkaido University, Hakodate (HUMZ); Museum of Comparative Zoology, Cambridge, MA (MCZ); Muséum National d'Histoire Naturelle, Paris (MNHN); Swedish Museum of Natural History, Stockholm (NRM); National Museum of Nature and Science, Tsukuba (NSMT); South African Institute for Aquatic Biodiversity, Grahamstown (SAIAB); South African Museum, Cape Town (SAM); Universidade do Estado do Rio de Janeiro, Rio de Janeiro (UERJ); National Museum of Natural History, Smithsonian Institution, Washington, DC (USNM); Zoological Museum Hamburg, Hamburg (ZMH); and Natural History Museum of Denmark, Copenhagen (ZMUC). Abbreviations followed Sabaj (2016). All specimens examined are listed in the Supporting Information (Supplementary Material 1).

Morphological data

The phylogenetic analysis was based on 143 morphological characters (134 qualitative and nine quantitative), including external morphology, branchiomeric and hypobranchial cranial muscles, clasper morphology, dermal denticles and skeleton. Terminology for the neurocranium follows Compagno (1988); jaws, Motta & Wilga (1995); gill arches, De Beer (1937) and Shirai (1992); claspers, Jungersen (1899) and Compagno (1988); neurocranial, hyoid and hypobranchial musculature, Huber *et al.* (2011); dermal denticles, Herman *et al.* (1990) and Cappetta (2012); and lateral line canals, Chu & Wen (1979) and Maruska (2001).

Specimens were dissected manually and, in some cases, with the aid of a stereomicroscope. To examine clasper anatomy, the left clasper was chosen to study the external morphology and the right clasper for the internal anatomy. Skeletal components and musculature were examined through dissection. Skin samples to examine dermal denticles were taken from the right side of the body above the pectoral fin, below the origin of the first dorsal fin and below the insertion of the second dorsal fin and were photographed using scanning electron microscopes (DSM 940 and ZEISS SIGMA VP) in Departamento de Zoologia of the Universidade de São Paulo. Meristic data were recorded directly from the examined specimens or taken from the paper by Compagno (1988) and other works (e.g. Compagno & Stevens, 1993a, b; Last *et al.*, 1999, 2008; Human, 2006a, b, 2007; Gledhill *et al.*, 2008; Last & White, 2008; Sato *et al.*, 2008; Nakaya *et al.*, 2013). Radiographs were taken in the Faculdade de Medicina Veterinária e Zootecnia of the Universidade de São Paulo (FMVZ-USP) and in the radiology facilities of the following institutions: BMNH, HUMZ, MCZ, NRM, NSMT, USNM and ZMUC. Counts

of monospondylous and diplospondylous vertebrae were based on the studies by Compagno (1988) and Soares & de Carvalho (2019).

Counts of vertebral centra, teeth, pectoral radials, intestinal valves, mandibular and hyomandibular pores of the lateral line system and the number of cusplets on dermal denticles were analysed as quantitative characters. A total of 87 characters analysed here were originally proposed or described by Soares & de Carvalho (2020), and other characters were compiled or modified from the works of White (1937), Compagno (1970, 1988), Nakaya (1975), Muñoz-Chápuli (1985), Raschi & Tabit (1992), Reif (1982, 1985), Shirai (1996), Goto (2001) and Soares (2020). In addition, 20 new characters (ch. 6, 7, 23, 25, 32–36, 52, 64, 65, 77, 80, 89, 94, 109–111 and 113) are proposed and defined herein. Characters are illustrated with photographs and schematic drawings made from digital photographs. Photographs were taken with a digital camera (Canon Power Shot SX610 HS) and edited with the aid of ADOBE ILLUSTRATOR CC and ADOBE PHOTOSHOP CS6.

Anatomical abbreviations: **acb**, accessory cartilage of the basibranchial copula; **anf**, anterior nasal flap; **bb**, basibranchial; **bh**, basihyal; **bp**, basal plate; **cab**, cardiobranchial cartilage of the basibranchial copula; **ch**, ceratohyal; **cnf**, circumnarial flap; **cor**, coracoid bar; **dr**, distal radial elements; **ecp**, ectodermal pits; **enc**, external nasal cartilage; **ethp**, ethmopalatine ligament; **exc**, excurrent aperture; **hb**, hypobranchials; **hf**, hyomandibular facet; **hpc**, hyomandibular pore canal; **icf**, internal carotid foramen; **inc**, incurrent aperture; **lcc**, lower caudal crest; **llf**, lower labial furrow; **lpq**, muscle levator palatoquadrati; **lrc**, lateral rostral cartilage; **mca**, muscle coracoarcualis; **mch**, muscle coracohyoideus; **mck**, Meckel's cartilage; **mep**, muscle epaxialis; **mes**, mesopterygium; **mih**, muscle interhyoideus; **mo**, mouth; **mr**, medial radial elements; **mrc**, medial rostral cartilage; **mtp**, metapterygium; **mtpax**, metapterygium axial; **mpc**, mandibular pore canal; **nc**, nasal capsule; **nf**, nasal fontanelle; **nle**, nictitating lower eyelid; **obp**, orbital process of the palatoquadrate; **pf**, parietal fossa; **pnf**, posterior nasal flap; **pog**, postorbital groove; **pos**, postorbital process; **pq**, palatoquadrate; **pr**, proximal radial elements; **pre**, preorbital process; **pro**, propterygium; **rf**, rostral fenestra; **sbp**, subnasal plate; **sc**, supraorbital crest; **sf**, stapedial foramen; **sop**, subocular pouch; **sp**, spiracle; **ss**, suborbital shelf; **ucc**, upper caudal crest; **ulf**, upper labial furrow.

DNA SEQUENCES

Cytochrome *c* oxidase subunit I (*COI*), the DNA barcode (e.g. Ward *et al.*, 2005, 2009; Zemlak *et al.*, 2009) has been used to identify species of elasmobranchs (e.g. Quattro *et al.*, 2006; Spies *et al.*, 2006; Ward *et al.*, 2007, 2008; Ward & Holmes, 2007; Smith *et al.*, 2008; Holmes *et al.*, 2009; Mariguela *et al.*, 2009; Richards *et al.*, 2009; Wong *et al.*, 2009; Wynen *et al.*, 2009; Serra-Pereira *et al.*, 2010; Straube *et al.*, 2010, 2011; White & Last, 2012; Griffiths *et al.*, 2013; Wyffels *et al.*, 2014; Madduppa *et al.*, 2016). Despite the great number of sequences deposited in GenBank and BOLD Systems, several sequences are not identified to the species level. Naylor *et al.* (2012a) justified not using *COI* in their phylogenetic analysis by misidentification of specimens, missing data, and methods of analysis that result in 'erroneous groupings'. In the study by Vélez-Zuazo & Agnarsson (2011), the large quantity of missing data and misidentification of samples in the phylogenetic analysis were evidenced by unsupported placements of some taxa on the tree presented.

Based on these arguments, we decided to use solely the 44 sequences of *NADH2* [length (*L*) = 1044 bp] generated by Naylor *et al.* (2012a, b). Photographs and information on voucher specimens were checked for outgroup taxa, and the identification of catshark DNA sequences relied mostly on the work of Naylor *et al.* (2012a). All sequences were obtained through the GenBank database (Table 1), edited and aligned in GENEIOUS PRIME 2020, implementing MUSCLE (Edgar, 2004) as an alignment tool. Sequences were translated to check stop codons and sequencing errors. Gaps were coded as missing entries (?) (Drummond *et al.*, 2010) in the same program in which the sequences were aligned.

PHYLOGENETIC ANALYSIS

Three data partitions (meristic, morphological and DNA) were combined in different ways in the following sets of characters: (1) quantitative and qualitative morphological characters; (2) molecular characters only; (3) qualitative morphological characters plus molecular data; and (4) combined dataset with all morphological and molecular data. Values for meristic data were normalized and included as the meristic partition (Goloboff *et al.*, 2006). The taxonomic composition of set 2 (molecular characters only) differed from the others because only taxa with available data were included (N = 44), aiming to avoid negative effects of missing data. Missing entries were used to represent two different instances in which characters could not be determined: (1) lack of appropriate study material; or (2) inapplicable character state. The complete dataset, containing all terminal taxa with quantitative and qualitative characters, and DNA sequences are provided in the Supporting Information (Supplementary Materials 2–4, respectively).

Table 1. Voucher information for the 44 specimens with available molecular data

Species	Database ID	GenBank ID
Alopias vulpinus	JQ518730	GN6200
Apristurus brunneus	JQ518667	GN1539
Apristurus laurussonii	JQ518666	GN1478
Apristurus macrostomus	KF927750	GN9994
Asymbolus analis	JQ518672	GN2478
Asymbolus rubiginosus	JQ518671	GN1936
Atelomycterus marmoratus	JQ519099	GN3705
Aulohalaelurus labiosus	JQ519192	GN2268
Bythaelurus dawsoni	JQ519146	GN6746
Carcharhinus melanopterus	KX172078	GN5508
Cephaloscyllium umbratile	JQ519177	GN982
Cephaloscyllium variegatum	JQ518997	GN4889
Chiloscyllium griseum	JQ518744	GN1702
Figaro boardmani	JQ518673	GN1946
Galeorhinus galeus	JQ518695	GN7236
Galeus melastomus	JQ519129	GN6627
Galeus nipponensis	KF927868	GN10093
Galeus polli	JQ518676	GN7116
Galeus sauteri	JQ519181	GN991
Gollum attenuatus	JQ518661	GN1470
Halaelurus sellus	JQ519034	GN4893
Haploblepharus edwardsii	JQ518679	GN7237
Hemiscyllium ocellatum	JQ518747	GN2587
Hemitriakis japonica	JQ519176	GN1000
Holohalaelurus regani	JQ518680	GN7178
Iago omanensis	JQ518699	GN6659
Loxodon macrorhinus	JQ518641	GN3646
Mustelus schmitti	JQ518704	GN2311
Paragaleus pectoralis	JQ518659	GN3212
Parmaturus xaniurus	JQ518681	GN1536
Pentanchus australis	JQ518995	GN4877
Pentanchus manis	JQ518663	GN1089
Poroderma africanum	JQ518682	GN1772
Poroderma pantherinum	JQ518683	GN7325
Proscyllium habereri	JQ519076	GN2601
Rhizoprionodon longurio	JQ518650	GN5298
Schroederichthys bivius	JQ518684	GN2305
Scyliorhinus canicula	JQ518686	GN2346
Scyliorhinus capensis	JQ518687	GN7186
Scyliorhinus retifer	JQ519117	GN2530
Scyliorhinus stellaris	JQ518685	GN2339
Triaenodon obesus	JQ518656	GN4420
Triakis semifasciata	JQ518713	GN1038

The degree of phylogenetic incongruence among the three data partitions (meristic, morphological and *NADH2*) was assessed using the maximum parsimony incongruence–length difference (ILD) method (Farris *et al.*, 1994) implemented by the script ild.run (http://phylo.wikidot.com/tntwiki) in TNT 1.1, with 1000 replications, using a heuristic tree search with five additional sequence replicates. All combinations of data partitions were considered.

All the analyses were done under parsimony using TNT 1.1 (Goloboff *et al.*, 2003, 2008b) and the 'Traditional Search' option, using the tree bisection–reconnection (TBR) algorithm for datasets 1 and 4, and the 'New Technology Search' option for sets 2 and 3. Character polarity was determined by outgroup comparison (Nixon & Carpenter, 1993). *Chiloscyllium griseum* was chosen to root the cladogram as a representative of Orectolobiformes, sister group of the clade formed by Carcharhiniformes and Lamniformes (Compagno, 1977, 1988; de Carvalho, 1996; Shirai, 1996; Goto, 2001; Naylor *et al.*, 2012a). Multistate qualitative characters (41, 42, 43, 57, 61 and 82) and quantitative characters (1–9) were analysed as ordered.

Given that the implied weighting method (Goloboff, 1993; Golboff *et al.*, 2008a) could artificially assign higher weights to missing entries in the molecular partition, we used the extended implied weighting herein (Goloboff, 2014; Mirande, 2019). Different values of concavity constant, k (1, 3, 7, 10 and 20) were combined with two weighting schemes for molecular characters, as proposed by Mirande (2019): (1) SEP, each column weighted separately according to its own homoplasy; and (2) BLK, all molecular characters weighted according to the average homoplasy of the whole marker. Morphological characters were weighted according to their own homoplasy under all the weighting schemes. The ten searches under extended implied weighting and one equal-weighting search (EQW) using the combined dataset were explored and submitted to a sensitivity analysis.

Values of the consistency and retention indices (CI and RI, respectively) and synapomorphies of nodes were obtained from the set of equally most-parsimonious trees. The relative degree of support for each node in the trees obtained with equal and extended implied weights was assessed with branch support indices (Bremer, 1994) and symmetric resampling (Goloboff *et al.*, 2003). Relative Bremer support was calculated using TBR and retaining suboptimal trees by seven steps. GC values: (differences of frequencies "Group present/Contradicted"; Goloboff *et al.*, 2003) were calculated using the strict consensus and 5000 replicates. Tree editing was performed with the aid of TreeGraph 2.15 and Adobe Photoshop CS6.

Taxon names in the Results and Discussion (e.g. atelomycterids, pentanchids and scyliorhinids) follow the new classification and arrangement proposed in this study, as summarized in Table 2. A description of each character and its variation within catsharks and the outgroup taxa, in addition to references to illustrations provided in other sources, are presented in the section 'Description and analysis of morphological characters'. The number preceding

Table 2. Phylogeny-based classification proposed in this study

Order Carcharhiniformes
Suborder Scyliorhinoidei
Family Scyliorhinidae Gill, 1862
Cephaloscyllium Gill, 1862 (18)
Poroderma Smith, 1837 (2)
Scyliorhinus Blainville, 1816 (16)
Suborder Carcharhinoidei
Infraorder Atelomycteroidea
Family Atelomycteridae White, 1936
Subfamily Atelomycterinae Compagno, 1988
Atelomycterus Garman, 1913 (6)
Aulohalaelurus Fowler, 1934 (2)
Subfamily Schroederichthyinae Compagno, 1988
Schroederichthys Springer, 1966
Infraorder Pentanchoidea
Family Pentanchidae Smith & Radcliffe, 1912
Akheilos White, Fahmi & Weigmann, 2019 (1)
Subfamily Halaelurinae subfam. nov.
Asymbolus Whitley, 1939 (9)
Bythaelurus Compagno, 1988 (14)
Figaro Whitley, 1928 (2)
Halaelurus Gill, 1862 (7)
Haploblepharus Garman, 1913 (4)
Holohalaelurus Fowler, 1934 (5)
Subfamily Galeinae subfam. nov.
Cephalurus Bigelow & Schroeder, 1941 (1)
Galeus Rafinesque, 1810 (18)
Parmaturus Garman, 1906 (11)
Apristurus Garman, 1913 (20)
Pentanchus Smith & Radcliffe, 1912 (19)

Numbers of species in each genus are presented in parentheses.

each character in the description corresponds to its number in the character matrix. The statement of each character and its states is followed by its recovered CI and RI.

RESULTS

Description and analysis of morphological characters

Quantitative characters

1. Number of monospondylous vertebrae: minimum = 28; maximum = 73 (CI = 25; RI = 44) [extracted from Soares & de Carvalho (2020): ch. 1].

Among the catsharks examined, the number of monospondylous vertebrae varies from 28 to 58. The lowest number of monospondylous vertebrae was found in *Holohalaelurus regani* (Gilchrist, 1922) (28) and the highest in *Cephaloscyllium isabella* (Bonnaterre, 1788) (58). In the orectoloboids examined, counts range from 26 to 40, and in the lamnid *Al. vulpinus*, from 72 to 73. In higher carcharhinoids, ranges vary from 34 to 72, with the highest value found for *Triaenodon obesus*.

2. Number of diplospondylous vertebrae: minimum = 67; maximum = 293 (CI = 41; RI = 52) [extracted from Soares & de Carvalho (2020): ch. 2].

In the catshark taxa examined, numbers of diplospondylous vertebrae range from 67 to 142, with the lowest values found for *Cephalurus cephalus* (Gilbert, 1892) (67–71), *Cephaloscyllium isabella* (71–72) and *Cephaloscyllium stevensi* Clark & Randall, 2011 (69–74) and the highest values for *Bythaelurus dawsoni* (Springer, 1971) (129–142). In the outgroups, numbers range from 87 to 293, with the highest values found for *Al. vulpinus* (278–293). According to our results, vertebral counts overlap among carcharhiniforms, and no transformation series between scyliorhinoids and other carcharhinoids can be proposed for this character, in contrast to the study by Compagno (1988).

3. Upper tooth counts: minimum = 20; maximum = 130 (CI = 31; RI = 63) [extracted from Soares & de Carvalho (2020): ch. 3].

4. Lower tooth counts: minimum = 20; maximum = 115 (CI = 22; RI = 56) [extracted from Soares & de Carvalho (2020): ch. 4].

In the catsharks examined, tooth row counts range from 29 to 130 considering both jaws; *Pentanchus longicephalus* Nakaya, 1975 presented the lowest values (29–53) and *Parmaturus albipenis* Séret & Last, 2007 the highest (130 in upper jaw; Séret *et al.*, 2007). In the outgroups, counts range from 20 to 115, with the highest values for the pseudotriakid *Gollum attenuatus* (96–115).

5. Number of intestinal valves: minimum = 4; maximum = 21 (CI = 24; RI = 30) [extracted from Soares & de Carvalho (2020): ch. 5].

Most catshark taxa have between five and 13 intestinal valves, with the exception of *Apristurus macrostomus* Zhu, Meng & Li, 1985 (18–21), *Aulohalaelurus labiosus* (Waite, 1905) (16), *Galeus polli* (Vaillant, 1888) (14) and *Pentanchus longicephalus* (13–17). In the outgroups, counts range from four to 15, with the highest values for *Chilloscyllium griseum* (15).

6. Number of mandibular pores: minimum = 2; maximum = 18 (CI = 21; RI = 30) [new character].

7. Number of hyomandibular pores: minimum = 6; maximum = 32 (CI = 25; RI = 59) [new character].

Hemigaleids and carcharhinids mostly present higher numbers of lateral line mandibular and hyomandibular pores compared with scyliorhinoids and some triakids. Differences in counts among and within catshark genera were also observed, and ranges are presented in the Supporting Information (Supplementary Material 2). For this reason, we

coded these characters as quantitative in order not to suppress any variation found.

8. Number of pectoral radials: minimum = 10; maximum = 38 (CI = 29; RI = 43) [modified from Goto (2001): ch. 58].

Nakaya (1975) suggested an increase in the number of pectoral radials in the transition from scyliorhinoids to carcharhinids and sphyrnids. However, we observed overlapping values among scyliorhinoids, proscylliids and triakids, as did Compagno (1988). Goto (2001) coded the number of pectoral radials for Orectolobiformes and considered two character states only (p. 62, ch. 58). We treat this character as quantitative and coded it as such herein.

9. Number of cusplets on dermal denticles: minimum = 0; maximum = 5 (CI = 33; RI = 40) [compiled from Reif (1985)].

Soares & de Carvalho (2020) coded the absence/presence of cusplets on dorsolateral dermal denticles (ch. 25); herein, we coded the number of cusplets as a quantitative character. Most taxa examined present two cusplets on dermal denticles (Fig. 2), with the exception of the carcharhinid *Carcharhinus melanopterus*, the hemigaleid *Paragaleus pectoralis* (Fig. 2C) and the lamnoid *Al. vulpinus*, which present up to five cusplets (Reif, 1982, 1985; Raschi & Tabit, 1992). Reif (1982, 1985) proposed that the high number of cusplets and crests on lateral dermal denticles would contribute to drag reduction, thus improving the hydrodynamics of pelagic sharks.

External morphology

10. Lateral extension of anterior nasal flap: (0) broad and entirely covering the excurrent nasal aperture; (1) slender and partially covering the excurrent nasal aperture (CI = 10; RI = 67) [modified from Soares & de Carvalho (2020): ch. 6].

Soares & de Carvalho (2020) coded both lateral extension and relative length of anterior nasal flap in the same character (p. 249, ch. 6). Here, we split the original character in two, aiming to provide better definition of the conditions observed and following the recommendations of Sereno (2007) in relationship to character construction. In most catsharks examined, the anterior nasal flap is broad and covers the excurrent aperture entirely (10:0; Fig. 3A, B), with the exception of species belonging to *Apristurus*, *Cephalurus*, *Figaro*, *Galeus*, *Pentanchus* and *Schroederichthys*. In these six genera, the flap is slender and covers the excurrent nasal aperture only in part (10:1; Fig. 3C). In the outgroups, broad anterior nasal flaps are found in the orectoloboids (Fig. 3D), the pseudotriakid *Gollum attenuatus*, the proscylliid *Proscyllium habereri*, the triakid *Hemitriakis japonica* and the carcharhinid *Triaenodon obesus*.

11. Relative length of anterior nasal flap: (0) short and not reaching the upper lip; (1) long, surpassing the posterior nasal flap and reaching the upper lip (CI = 20; RI = 43) [modified from Soares & de Carvalho (2020); ch. 6].

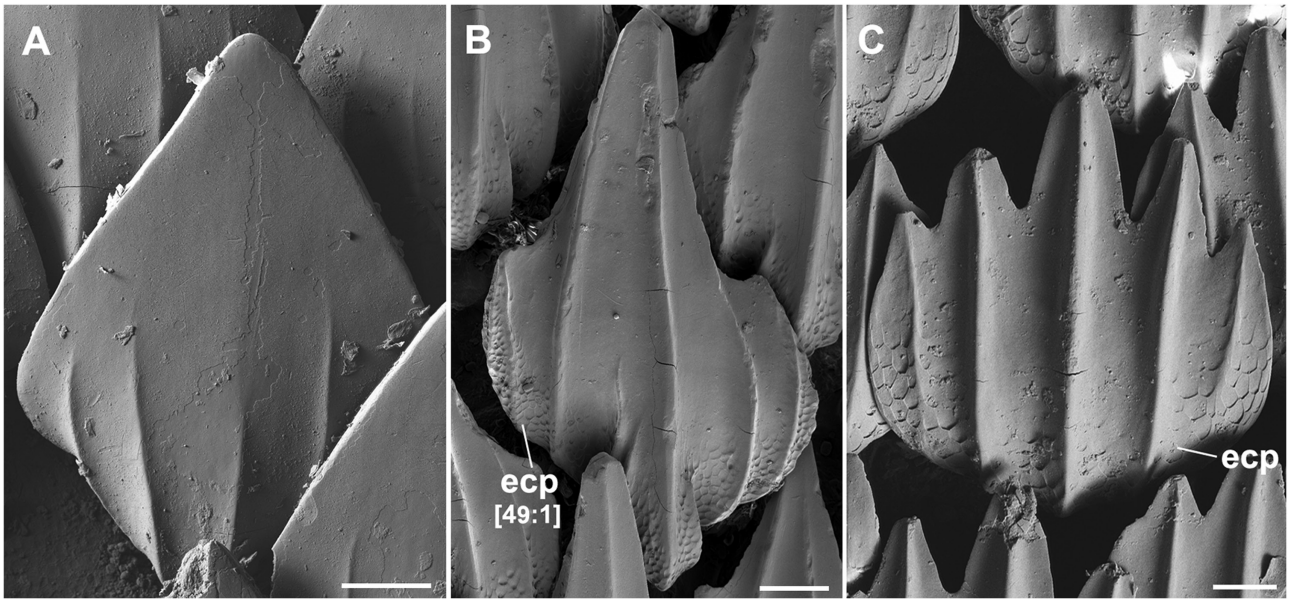

Figure 2. Dermal denticles above the origin of the first dorsal fin. A, *Hemiscyllium ocellatum*, USNM 176863, female, 490 mm TL. B, *Scyliorhinus capensis*, SAIAB 27577, male, 863 mm TL. C, *Paragaleus pectoralis*, USNM 197626, male, 470 mm TL. Abbreviations: ecp, ectodermal pits; TL, total length. Scale bars: 100 µm.

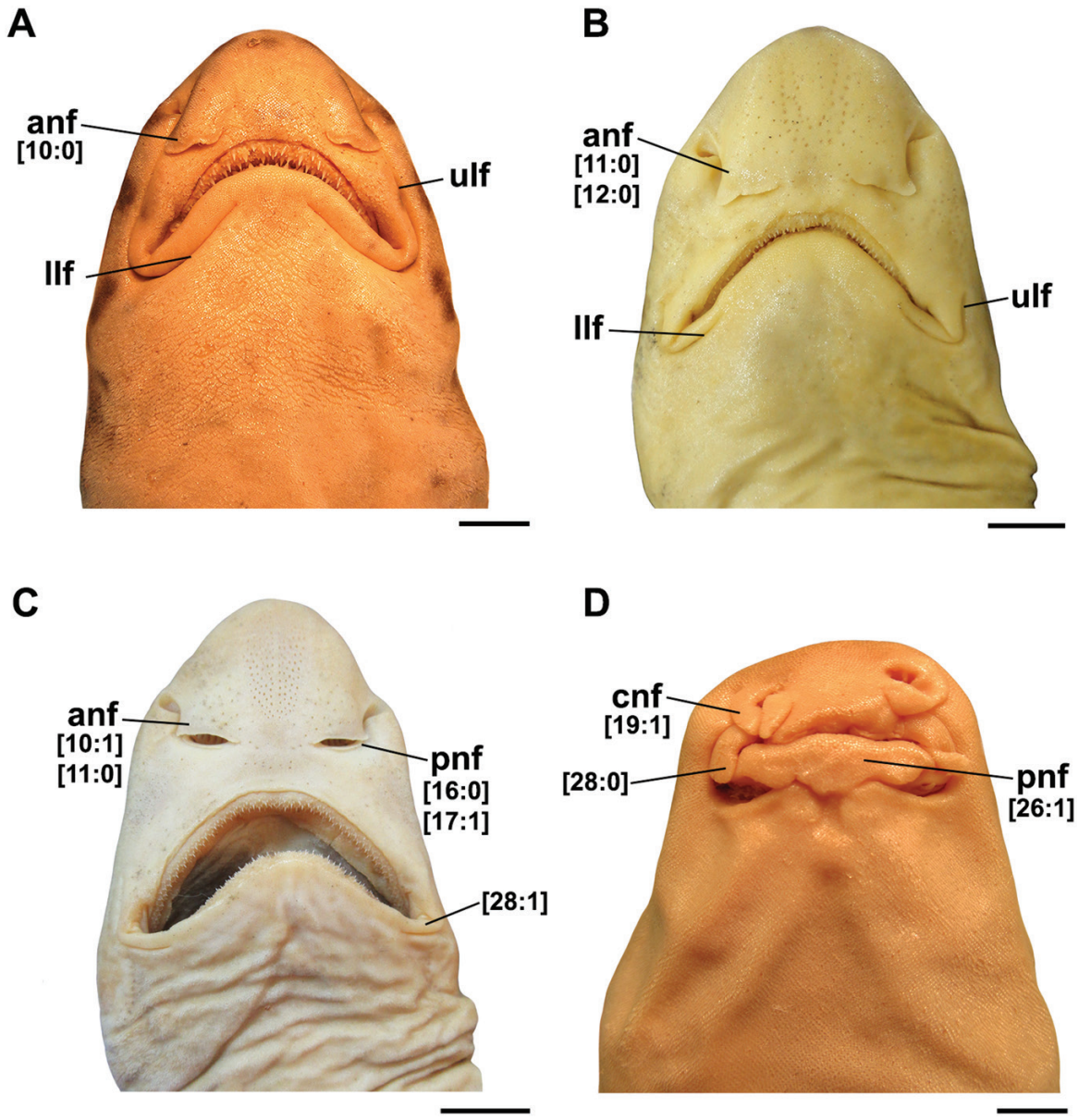

Figure 3. Ventral view of the head. A, *Asymbolus rubiginosus*, AMS I.34899-002, female, 390 mm TL. B, *Aulohalaelurus labiosus*, ZMH 2-1989, female, 480 mm TL. C, *Galeus sauteri*, MNHN 2013-0444, 328 mm TL. D, *Hemiscyllium ocellatum*, USNM 176863, female, 490 mm TL. Abbreviations: anf, anterior nasal flap; cnf, circumnarial flap; llf, lower labial furrow; pnf, posterior nasal flap; TL, total length; ulf, upper labial furrow. Scale bars: 20 mm.

A short anterior nasal flap restricted to the nasal region and not reaching the upper lip is found in most taxa examined, including the outgroups (11:0; Soares & de Carvalho, 2020). In the orectoloboids and the catshark species *Atelomycterus fasciatus* Compagno & Stevens, 1993, *Atelomycterus marmoratus* (Bennett, 1830), *Haploblepharus edwardsii* (Schinz, 1822), *Scyliorhinus canicula* (Linnaeus, 1758), *Scyliorhinus duhamelii* (Garman, 1913) and *Scyliorhinus garmani* (Fowler, 1934), the anterior nasal flap is distinctly long and reaches the upper lip, covering the lip in some specimens (11:1; Figs 3D, 4A).

12. Distance between anterior nasal flaps: (0) one-half or more of the width of the flap; (1) less than one-half of the width of the flap (CI = 33; RI = 50) [extracted from Soares & de Carvalho (2020): ch. 7].

Among all taxa examined, only in *Haploblepharus edwardsii*, *Scyliorhinus canicula*, *Scyliorhinus duhamelii* and *Atelomycterus* spp. are the anterior

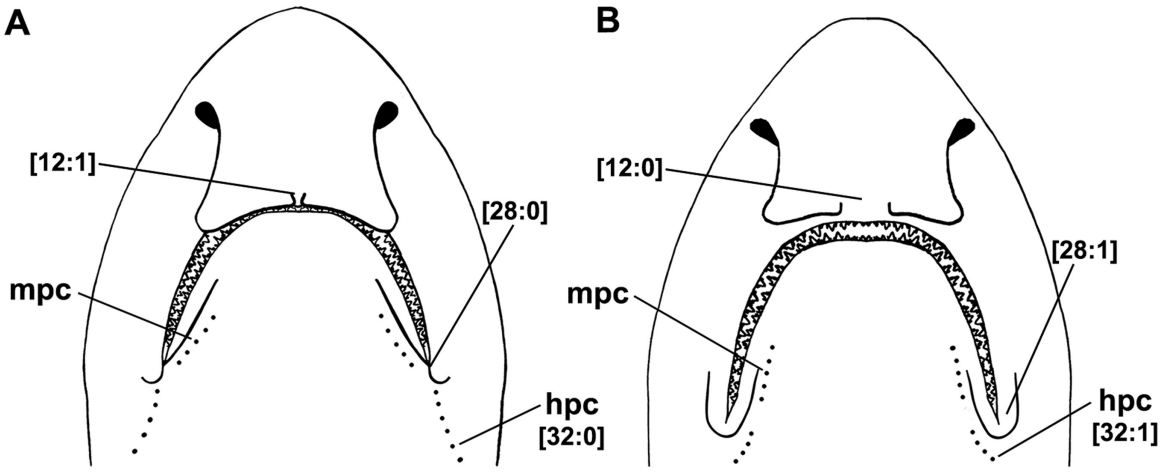

Figure 4. Detail of mandibular and hyomandibular pore canals. A, *Scyliorhinus canicula*, NRM 50183, male, 582.4 mm TL. B, *Asymbolus rubiginosus*, AMS I.34899-002, female, 390 mm TL (modified from Soares & de Carvalho, 2019). Abbreviations: hpc, hyomandibular pore canal; mpc, mandibular pore canal; TL, total length.

nasal flaps closely spaced, being separated by less than one-half of the width of the flap [12:1; Figs 3, 4; see also Soares & de Carvalho (2020): p. 350, fig. 3].

13. Morphology of the anterior nasal flap: (0) flap consisting of a single structure; (1) flap separated into lateral and medial two portions (CI = 25; RI = 50) [extracted from Soares & de Carvalho (2020): ch. 8].

Most taxa examined present a single anterior nasal flap (13:0; Fig. 3). In the catshark species *Cephalurus cephalus*, *Poroderma* spp. and *Schroederichthys* spp. [Soares & de Carvalho (2020): figs 1B, 2C] and in the orectoloboid *Hemiscyllium ocellatum* and the pseudotriakid *Gollum attenuatus* (13:1), the anterior nasal flap is divided into two portions.

14. Mesonarial crest: (0) absent; (1) present (CI = 20; RI = 85) [modified from Soares & de Carvalho (2020): ch. 9].

As defined by Soares & de Carvalho (2020), the mesonarial crest is a dermal notch situated on the anterior nasal flap, which corresponds to the extensions of the external nasal cartilage. This crest was observed only in the catshark species of *Cephaloscyllium*, *Schroederichthys* and *Scyliorhinus* [Soares & de Carvalho (2020): figs 1, 2] and the pseudotriakid *Gollum attenuatus* (14:1). It is absent in other taxa examined.

15. Muscular nasal barbel on anterior nasal flap: (0) absent; (1) present (CI = 100; RI = 100) [extracted from Soares & de Carvalho (2020): ch. 10].

Among all carcharhinoids examined, only species of *Poroderma* possess a muscular nasal barbel on the anterior nasal flap (Human, 2007; Soares & de Carvalho, 2020). As discussed by Compagno (1988) and Goto (2001), the nasal barbel observed in the orectolobiforms *Chiloscyllium* and *Hemiscyllium* is different from the barbel of *Poroderma*, because it originates on the rostral surface, medial and partly anterior to the anterior nasal flap, and has a cartilaginous base.

16. Posterior nasal flap: (0) present; (1) absent (CI = 14; CI = 65) [extracted from Soares & de Carvalho (2020): ch. 11].

A posterior nasal flap is observed in most catsharks examined (16:0; Fig. 3C; see also Soares & de Carvalho, 2020: fig. 2), with the exception of the species of *Apristurus*, *Atelomycterus*, *Aulohalaelurus*, *Haploblepharus* and *Pentanchus* (16:1). Most outgroup taxa examined present a posterior flap, except the triakids *Hemitriakis japonica* and *I. omanensis* and the carcharhinids *Carcharhinus melanopterus* and *R. longurio*.

17. Degree of development of posterior nasal flap: (0) corresponds to one-half or more of the area of the anterior nasal flap; (1) reduced and corresponds to less than one-half of the area of the anterior nasal flap (CI = 20; RI = 85) [extracted from Soares & de Carvalho (2020): ch. 12].

A well-developed posterior nasal flap that corresponds to one-half of the area of the anterior nasal flap is found in the scyliorhinids *Cephaloscyllium*, *Poroderma* and *Scyliorhinus* and the pentanchids *Asymbolus* and *Halaelurus* (17:0; Soares & de Carvalho, 2019, 2020). In all other catshark taxa that possess a posterior nasal flap, a reduced flap is observed, only bordering the posterior tip of the excurrent aperture (17:1; Fig. 3C). In the outgroups, only the orectoloboids, the pseudotriakid *Gollum attenuatus* and the procylliid *Proscyllium habereri* present a well-developed posterior nasal flap.

18. Position of the posterior nasal flap: (0) on the posterior border of the excurrent aperture; (1) lateral to the excurrent aperture (CI = 50; RI = 67) [extracted from Soares & de Carvalho (2020): ch. 13].

The posterior nasal flap of the catsharks *Scyliorhinus canicula* and *Scyliorhinus duhamelii* (Soares & de Carvalho, 2019) and the orectoloboids *Chilloscyllium griseum* and *Hemiscyllium ocellatum* (Goto, 2001) is uniquely situated at the lateral margin of the excurrent aperture (18:1), whereas in all other taxa this flap is positioned along the posterior border of the excurrent aperture (18:0; Soares & de Carvalho (2020): figs 2, 3).

19. Circumnarial flap: (0) absent; (1) present (CI = 100; RI = 100) [extracted from Shirai (1996): ch. 95].

Circumnarial flaps are situated laterally to the incurrent aperture in the orectoloboids examined (19:1; Fig. 3D; see also Goto, 2001) and in some batoids (Shirai, 1996). In all other taxa examined, circumnarial flaps are absent (19:0).

20. Nasoral groove: (0) absent; (1) present (CI = 25; RI = 50) [extracted from Soares & de Carvalho (2020): ch. 14].

Nasoral grooves linking the excurrent aperture and the mouth are observed only in *Scyliorhinus canicula*, *Scyliorhinus duhamelii*, *Atelomycterus* spp. and *Haploblepharus* spp. within carcharhiniforms [20:1; Soares & de Carvalho (2020): fig. 3]. Similar grooves are also observed in the orectoloboids but absent in the lamnoid *Al. vulpinus* (20:0).

21. Position of mouth: (0) entirely anterior to eye; (1) at the same level as the eye (CI = 100; RI = 100) [compiled from Compagno (1977, 1988)].

Only in the orectoloboids is the mouth positioned entirely anterior to the eye (21:0; Fig. 5A), in contrast to the more posterior condition observed in the lamniforms and carcharhiniforms examined (21:1; Fig. 5B–F).

22. Upper labial furrow: (0) present; (1) absent (CI = 14; RI = 78) [extracted from Soares & de Carvalho (2020): ch. 15].

An upper labial furrow is present in most catsharks examined (22:0; Fig. 3), with the exception of *Scyliorhinus*, *Cephaloscyllium*, *Holohalaelurus* and *Poroderma africanum* (Gmelin, 1789). In the outgroups, most carcharhinids examined (except *R. longurio*), the lamnoid *Al. vulpinus* and the triakid *Galeorhinus galeus* lack furrows along the upper jaw (Nakaya, 1975; Nakaya & Séret, 2000; Nakaya *et al.*, 2013; Soares & de Carvalho, 2019, 2020), whereas in the orectoloboids, proscylliids, all other triakids and the hemigaleid *Paragaleus pectoralis*, an upper furrow is present.

23. Length of upper labial furrow: (0) corresponds to one-half or more of mouth width; (1) corresponds to one-quarter to one-third of mouth width (CI = 20; RI = 80) [new character].

Reduced upper labial furrows are observed in most catshark genera (22:1; Figs 3B, C), but in species of *Apristurus*, *Atelomycterus*, *Aulohalaelurus* and *Pentanchus*, these furrows are well developed and exceed half of the mouth width (22:0; Fig. 3A). Among the outgroup taxa examined, triakids and orectoloboids present well-developed upper labial furrows.

24. Lower labial furrow: (0) present; (1) absent (CI = 25; RI = 62) [extracted from Soares & de Carvalho (2020): ch. 16].

A lower labial furrow is present in most scyliorhinoids examined (24:0; Fig. 3), except in the species of *Cephaloscyllium* and *Holohalaelurus regani* [Soares & de Carvalho, (2020): figs 1C, 2B]. In the carcharhinids *Carcharhinus melanopterus*, *L. macrorhinus* and *Triaenodon obesus*, furrows along the lower jaw are lacking.

25. Length of lower labial furrow: (0) corresponds to one-half or more of mouth width; (1) corresponds to one-quarter to one-third of mouth width (CI = 17; RI = 72) [new character].

Most scyliorhinoids present a poorly developed lower labial furrow corresponding to less than one-half of mouth width (24:1; Fig. 3B). In orectoloboids, the triakid *M. schmitti*, the catsharks *Scyliorhinus canicula* and *Scyliorhinus duhamelii* and scyliorhinoid species in the genera *Apristurus*, *Atelomycterus*, *Aulohalaelurus*, *Haploblepharus* and *Pentanchus*, well-developed lower furrows are observed (24:0; Fig. 3; see also Nakaya & Sato, 1999; Soares & de Carvalho, 2019, 2020).

26. Configuration of lower labial furrow: (0) separated in two furrows; (1) single and entirely across the lower jaw (CI = 33; RI = 33) [modified from Goto (2001): ch. 129].

Among taxa that possess lower labial furrows, only in the orectoloboid *Chiloscyllium griseum* do these furrows form a single unity extending entirely across the lower jaw (26:1; Fig. 3D). In all other taxa examined, lower furrows are distinctly separated from each other (26:0; Fig. 3A–C).

27. Projected flap on the upper lip margin: (0) absent; (1) present (CI = 50; RI = 94) [extracted from Soares & de Carvalho (2020): ch. 17].

A projected flap situated on the upper lip margin and covering laterally the lower labial furrow is found in *Scyliorhinus* species and *Poroderma africanum* (27:1; Soares & de Carvalho, 2019, 2020). The presence of this flap was hypothesized as a synapomorphic character for *Scyliorhinus* with an independent acquisition in *Poroderma africanum* by Soares & de Carvalho (2020). This flap is absent in all other taxa examined (27:0).

28. Configuration of labial furrows: (0) discontinuous and upper furrow ventral to the lower one; (1) continuous and fused laterally (CI = 14; RI = 62)

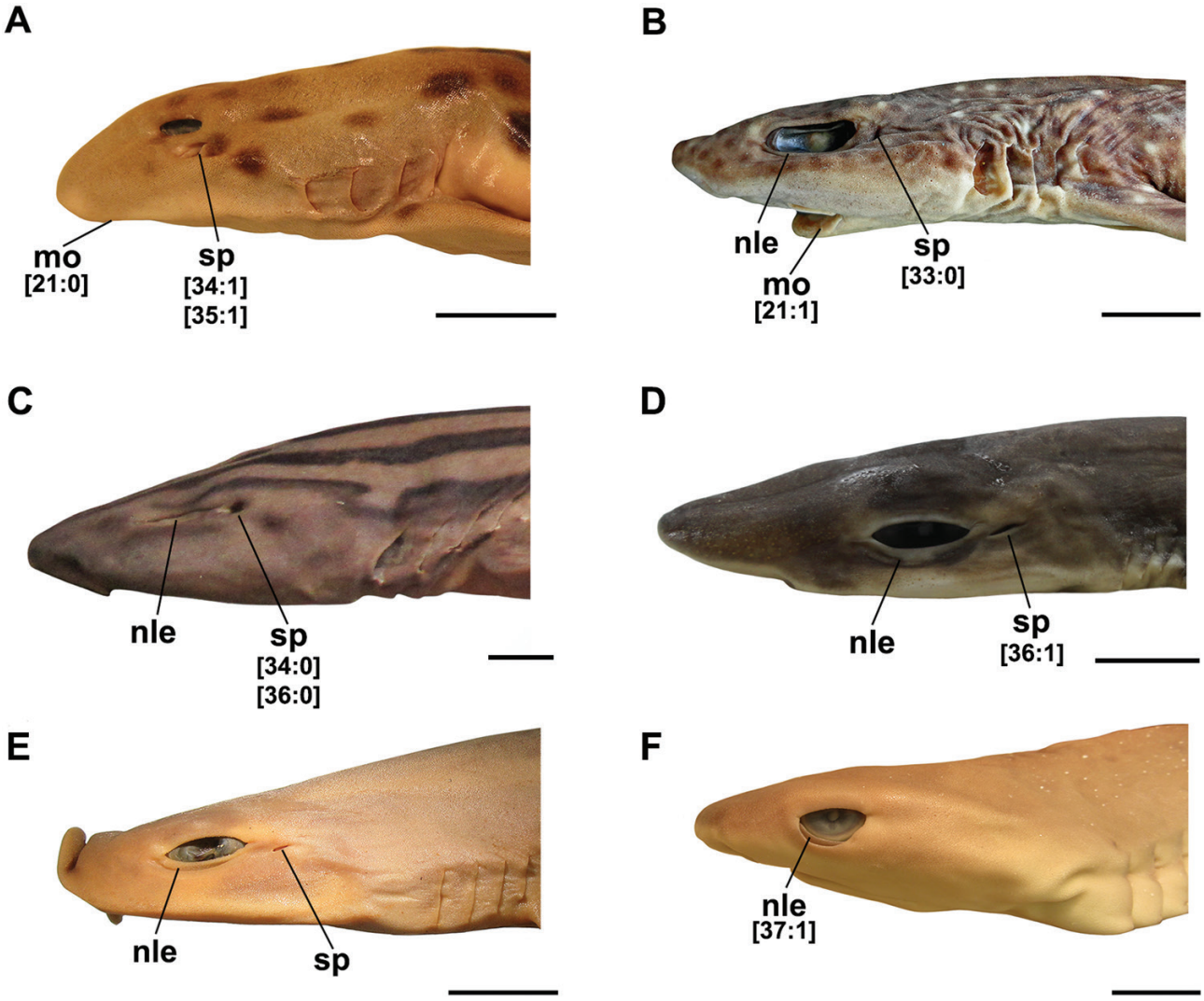

Figure 5. Lateral view of the head. A, *Hemiscyllium ocellatum*, USNM 176863, female, 490 mm TL. B, *Schroederichthys saurisqualus*, UERJ uncatalogued, female, 564 mm TL. C, *Poroderma africanum*, SAIAB 25343, male, 920 mm TL. D, *Galeus nipponensis*, HUMZ 90298, male, 550 mm TL. E, *Hemitriakis japonica*, NSMT 66856, female, 515 mm TL. F, *Triaenodon obesus*, USNM 216208, female, 610 mm TL. Abbreviations: mo, mouth; nle, nictitating lower eyelid; sp, spiracle; TL, total length. Scale bars: 20 mm.

[extracted from Soares & de Carvalho (2020): ch. 18].

Different configurations of the labial furrows are observed among taxa that present such furrows along upper and lower jaws. In most catsharks examined, the furrows are continuous and fused laterally (28:1; Figs 3, 4), with the exception of *Apristurus brunneus* (Gilbert, 1892), *Apristurus laurussonii* (Saemundsson, 1922), *Apristurus parvipinnis* Springer & Heemstra, 1979, *Parmaturus albipenis*, *Parmaturus angelae* Soares, Carvalho, Schwingel & Gadig, 2019, *Poroderma pantherinum* (Smith, 1838) and *Schroederichthys* spp., in which the upper furrow is ventral to the lower one [28:0; Soares & de Carvalho (2020): figs 1, 2]. Among outgroups, labial furrows are continuous in the pseudotriakid *Gollum attenuatus*, the triakid *I. omanensis*, the hemigaleid *Paragaleus pectoralis* and the carcharhinid *R. longurio*, but discontinuous in the other taxa.

29. Upper labial cartilages: (0) present; (1) absent (CI = 33; RI = 0) [compiled from Compagno (1988)].

Upper labial cartilages are observed in most taxa examined (29:0) but are lacking in the scyliorhinoid *Holohalaelurus regani* and the carcharhinids *L. macrorhinus* and *Triaenodon obesus* (29:1).

30. Number of upper labial cartilages: (0) two; (1) one (CI = 33; RI = 92) [extracted from Soares & de Carvalho (2020): ch. 19].

In taxa that present labial cartilages along the upper jaw, these can range from one to two cartilages in each side of the mouth. Two upper labial cartilages are observed in most taxa examined (30:0), with the exception of the carcharhinids *Carcharhinus melanopterus* and *R. longurio* and the scyliorhinoids *Scyliorhinus*, *Cephaloscyllium* and *Schroederichthys*, which present only one cartilage [30:1; Soares & de Carvalho (2020): fig. 4].

31. Postoral groove: (0) absent; (1) present (CI = 100; RI = 100) [extracted from Soares & de Carvalho (2020): ch. 20].

Postoral grooves are found only in *Cephaloscyllium* species (31:1; Last *et al.*, 2008; Last & White, 2008; Nakaya *et al.*, 2013). Their presence was proposed as a synapomorphy for this genus by Soares & de Carvalho (2020).

32. Position of hyomandibular canal pores: (0) continuous with the mouth commissure; (1) medial to the mouth commissure (CI = 33; RI = 50) [new character].

Hyomandibular pores extend posteriorly from the mouth commissure and are continuous with it in most taxa examined (32:0; Fig. 4A), whereas in the pseudotriakid *Gollum attenuatus*, the hemigaleid *Paragaleus pectoralis* and catshark species of *Asymbolus* (Fig. 4B), these pores are situated more medially in relationship to the mouth commissure (32:1).

33. Spiracle: (0) present; (1) absent (CI = 25; RI = 25) [new character].

The presence of a pair of modified openings located between the eyes and the first gill openings, known as spiracles (Compagno, 1988, 1999), has long been used in elasmobranch classifications by Müller & Henle (1838–1841) and subsequent workers (e.g. Regan, 1908; Garman, 1913; White, 1937) but has never been included in a cladistic analysis. The only references to these structures in systematic studies are the character 'spiracle valve' of Shirai (1996) and de Carvalho (1996), defined as a valvular structure probably with respiratory function and present in squalomorphs and batoids, and the 'spiracle tentacles' of Aschliman *et al.* (2012), described as projections on the inner margin of spiracles in some batoids. A spiracle is observed in most taxa examined (33:0; Fig. 5), with the exception of the lamnoid *Al. vulpinus*, the triakid *I. omanensis* and the carcharhinids *Carcharhinus melanopterus*, *R. longurio* and *Triaenodon obesus* (Fig. 5F). A vestigial spiracle is observed in the carcharhinid *L. macrorhinus* and coded as present herein.

34. Position of spiracle: (0) posterior to eye; (1) ventral to eye (CI = 00; RI = 100) [new character].

In carcharhinoids that have a spiracle, this aperture is situated posteriorly to the posterior eye margin (34:0; Fig. 5B–E). In the orectoloboids *Chiloscyllium griseum* and *Hemiscyllium ocellatum*, the spiracle is situated below the eye and anterior to the vertical that passes through its posterior margin (34:1; Fig. 5A).

35. Size of spiracle: (0) half-length or larger than the eye; (1) less than half the length of the eye (CI = 100; RI = 100) [new character].

In the orectoloboids *Chiloscyllium griseum* and *Hemiscyllium ocellatum*, the spiracle corresponds to more than half the length of the eye (35:0; Fig. 5A), whereas all other taxa examined have a much smaller spiracle (35:1; Fig. 5B–E). Compagno (1988) noted a gradual decrease in spiracle size relative to the eyes and body from scyliorhinoids, proscylliids and pseudotriakids to hemigaleids and carcharhinids. However, spiracle size varies among the carcharhinoids examined, and we are unable to define discrete states for the variation observed unambiguously.

36. Shape of spiracle: (0) circular; (1) horizontally elongated (CI = 25; RI = 67) [new character].

Most catshark genera examined present a spiracle circular in shape (36:0; Fig. 5B, C), with the exception of *Galeus melastomus* Rafinesque, 1810, *Galeus nipponensis* Nakaya, 1975 and *Galeus polli* in which a horizontally elongated spiracle is found (36,1; Fig. 5D). The spiracle is also horizontally elongated in the triakids *Galeorhinus galeus*, *Hemitriakis japonica* (Fig. 5E), *M. schmitti* and *Triakis semifasciata*, the proscylliid *E. barbouri*, the hemigaleid *Paragaleus pectoralis* and the carcharhinid *L. macrorhinus*.

37. Nictitating lower eyelid: (0) absent; (1) present (CI = 100; RI = 100) [compiled from White (1937) and Compagno (1970, 1988)].

A true nictitating lower eyelid with postocular eyelid muscles is found in all carcharhinoids (37:1; Figs 5, 6), and the presence of this eyelid has already been proposed as an autapomorphy for the order Carcharhiniformes (Compagno, 1970, 1977, 1988; Maisey, 1984). This structure is absent in the lamnoid and orectolobids examined herein (37:0).

38. Relationship between the nictitating lower eyelid and the subocular pouch: (0) eyelid rudimentary and slightly differentiated from the subocular pouch; (1) eyelid well developed and with well-defined edges in relationship to the subocular pouch (CI = 50; RI = 90) [compiled from White (1937) and Compagno (1970, 1988)].

Compagno (1970) proposed four different states to describe the morphological gradient of the nictitating lower eyelid in carcharhinoids: (1) rudimentary type, weakly differentiated and with shallow subocular pouches; (2) external type, characterized by a strong secondary lower eyelid with a well-defined edge; (3) internal type not connected to the upper eyelid; and (4) transitional type. Here, we propose two distinct characters to account for the conditions observed among taxa examined, one referring to the

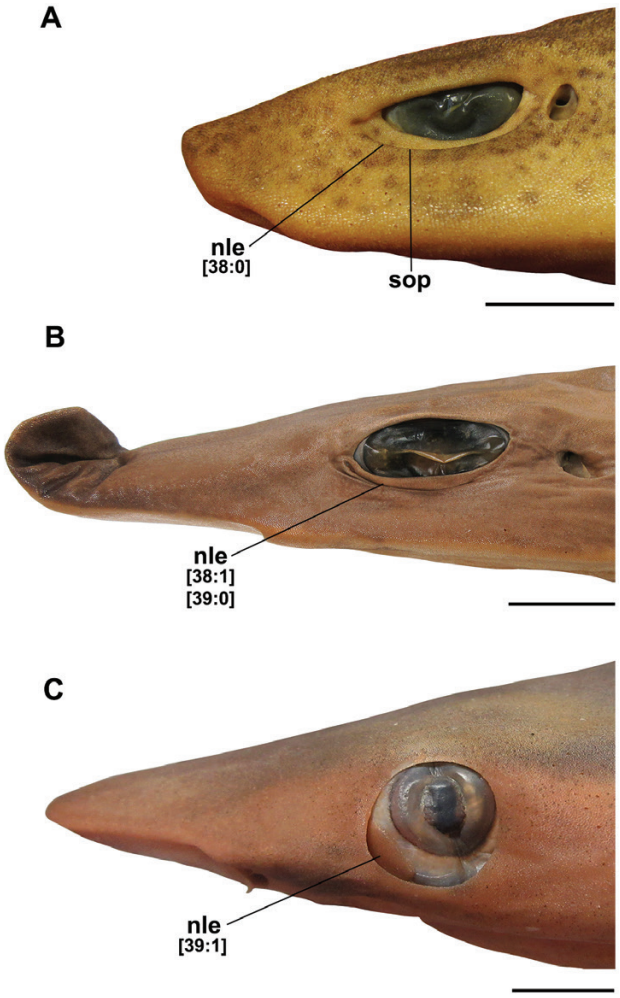

Figure 6. Detail of nictitating lower eyelid (nle). A, *Scyliorhinus canicula*, NRM 49164, male, 677.4 mm TL. B, *Gollum attenuatus*, NSMT 42855, female, 950 mm TL. C, *Rhizoprionodon longurio*, CAS 56628, female, 428 mm TL. Abbreviation: TL, total length. Scale bars: 10 mm.

relationship between the nictitating lower eyelid and the subocular pouch and another regarding the eyelid position under character 39. All scyliorhinoids and the procylliids *E. barbouri* and *Proscyllium habereri* (Fig. 6A) present a rudimentary nictitating lower eyelid slightly differentiated from the subocular pouch (38:0). In other carcharhinoids, the eyelid is well developed and displays well-defined edges in relationship to the subocular pouch (38:1; Fig. 6B, C).

39. Position of the nictitating lower eyelid: (0) external to the palpebral structure and continuous with the upper eyelid; (1) internal to the palpebral structure and not continuous with the upper eyelid (CI = 33; RI = 67) [compiled from Compagno (1970, 1988)].

In all scyliorhinoids, the pseudotriakid *Gollum attenuatus* and the triakids *Hemitriakis japonica*, *M. schmitti* and *Triakis semifasciata*, the nictitating lower eyelid is situated externally to the palpebral structure and is continuous with the upper eyelid (39:0; Fig. 6A, B). In the triakids *Galeorhinus galeus* and *I. omanensis*, the hemigaleid *Paragaleus pectoralis* and all carcharhinids examined, the eyelid lies internally to the palpebral structure and is not continuous with the upper eyelid (39:1; Fig. 6C). Garman (1913), White (1937), Bigelow & Schroeder (1948) and Garrick & Schultz (1963) used the type of nictating lower eyelid to distinguish triakids from carcharhinids, but as observed here and stated by Compagno (1970, 1988), the morphology of this structure varies widely among family groups and needs to be investigated further.

40. Pelvic apron: (0) absent; (1) present (CI = 33; RI = 89) [extracted from Soares & de Carvalho (2020): ch. 21].

In males of species of *Scyliorhinus*, *Asymbolus* and *Holohalaelurus*, a fusion between the pelvic inner margins that covers the claspers partly or entirely, known as the pelvic apron, is present (40:1; Soares & de Carvalho, 2019, 2020). In all other taxa

examined, the pelvic inner margins are not fused; there is no pelvic apron (40:0).

41. Extension of pelvic apron: (0) fusion extends to less than one-half the length of pelvic inner margins; (1) fusion extends to more than one-half to up two-thirds of the length of pelvic inner margins; (2) pelvic inner margins almost entirely fused (CI = 67; RI = 83) [extracted from Soares & de Carvalho (2020): ch. 22].

In *Asymbolus* and *Holohalaelurus*, the pelvic apron is short and extends to less than one-half of the length of the pelvic inner margins (41:0). Within *Scyliorhinus*, most species present a more developed pelvic apron, ranging from up to two-thirds the length of the pelvic inner margins (41:1), whereas in *Scyliorhinus canicula*, *Scyliorhinus capensis* (Müller & Henle, 1838), *Scyliorhinus duhamelii*, *Scyliorhinus torazame* (Tanaka, 1908) and *Scyliorhinus torrei* Howell Rivero, 1936, the pelvic inner margins are almost entirely fused (41:2). In the paper by Soares & de Carvalho (2020), the presence of a long pelvic apron was hypothesized to support a clade formed comprising *Scyliorhinus canicula*, *Scyliorhinus capensis*, *Scyliorhinus duhamelii*, *Scyliorhinus garmani*, *Scyliorhinus torazame* and *Scyliorhinus torrei*.

42. Origin of the first dorsal fin: (0) closer to the vertical line that passes through the insertion of pelvic fins; (1) closer to the vertical line that passes through the origin of pelvic fins; (2) closer to the vertical line that passes through the insertion of pectoral fins (CI = 25; RI = 82) [modified from Soares & de Carvalho (2020): ch. 23].

This character corresponds to character 23 of Soares & de Carvalho (2020: p. 354, fig. 6) and is modified to include an additional character state (2). All scyliorhinoids and the two orectoloboids examined present a posteriormost origin of the first dorsal fin, although it varies in its position relative to pelvic fins; in *Cephaloscyllium* and *Parmaturus*, this fin is closer to the origin than to the insertion of pelvics [42:1; Soares & de Carvalho (2020): fig. 6B]. In all other carcharhinoids and the lamnoid *Al. vulpinus*, the first dorsal fin originates closer to the pectoral fins than to the pelvics (42:2; Compagno, 1988).

43. Origin of second dorsal fin: (0) posterior to the vertical line that passes through the midpoint of the anal fin base; (1) anterior to the vertical line that passes through the midpoint of the anal fin base; (2) closer to the vertical line that passes through the insertion of pelvic fins (CI = 18; RI = 77) [modified from Soares & de Carvalho (2020): ch. 24].

This character corresponds to character 24 of Soares & de Carvalho (2020: p. 354, fig. 6) and is modified to include an additional character state that is observed in all carcharhinoids and the lamnoid examined, in which the anteriormost position of the second dorsal fin is closer to the pelvics than to the anal fin (43:0). In the orectoloboids and most scyliorhinoids, the origin of second dorsal fin is posterior to the half-length of the anal fin base (43:2), whereas in the catsharks *Cephaloscyllium*, *Cephalurus* and *Parmaturus* and the proscylliid *Proscyllium habereri*, this fin is positioned more anteriorly (43:1).

44. Insertion of anal fin: (0) close to the lower caudal fin lobe; (1) distinctly separate from the lower caudal fin lobe (CI = 20; RI = 73) [extracted from Goto (2001): ch. 136].

In the orectoloboids, *Apristurus*, *Pentanchus*, *Galeus melastomus* and *G. polli*, *G. sauteri*, the insertion of the anal fin is situated close to the lower caudal fin lobe (44:0; Nakaya & Sato, 1999; Goto, 2001), whereas in all other taxa examined, both fins are distinctly separate from each other (44:1).

45. Lower caudal fin lobe: (0) indistinct; (1) distinct (CI = 100; RI = 100) [compiled from Goto (2001)].

Uniquely in the orectoloboids, the lower caudal fin lobe is weakly developed and indistinct from the dorsal lobe (45:0; Goto, 2001).

46. Precaudal notch: (0) absent; (1) present (CI = 50; RI = 83) [extracted from Shirai (1996): ch. 103].

All catsharks examined lack a precaudal notch, which is also absent in the orectoloboids, proscylliids triakids (except *Hemitriakis japonica*) and the pseudotriakid *Gollum attenuatus* (46:0). Prominent notches are observed in *Hemitriakis japonica*, the hemigaleid *Paragaleus pectoralis* and all carcharhinids examined (46:1; Compagno, 1988).

47. Upper caudal crest of enlarged dermal denticles: (0) absent; (1) present (CI = 14; RI = 57) [modified from Soares & de Carvalho (2020): ch. 28].

48. Lower caudal crest of enlarged dermal denticles: (0) absent; (1) present (CI = 25; RI = 50) [modified from Soares & de Carvalho (2020): ch. 28].

Soares & de Carvalho (2020: p. 358, fig. 8) coded the presence of caudal crests of enlarged denticles (ch. 28) without differentiating between upper and lower crests. We code both crests separately. An upper caudal crest is found in the pseudotriakid *Gollum attenuatus* and the scyliorhinoids *Pentanchus manis* (Springer, 1979), *Pentanchus stenseni* (Springer, 1979), *Figaro boardmani* and all *Galeus* and *Parmaturus* species examined (Whitley, 1928, 47:1; Fig. 7). A lower caudal crest is observed in *Pentanchus manis*, *F. boardmani* and all species of *Parmaturus* (48:1) except *Parmaturus xaniurus*. Caudal crests are absent in all other carcharhinoids, orectoloboids and the lamnoid examined (47:0; 48:0).

49. Ectodermal pits on dermal denticles on dorsolateral surfaces of the body: (0) absent; (1) present (CI = 100; RI = 100) [compiled from Muñoz-Chápuli (1985) and Reif (1985)].

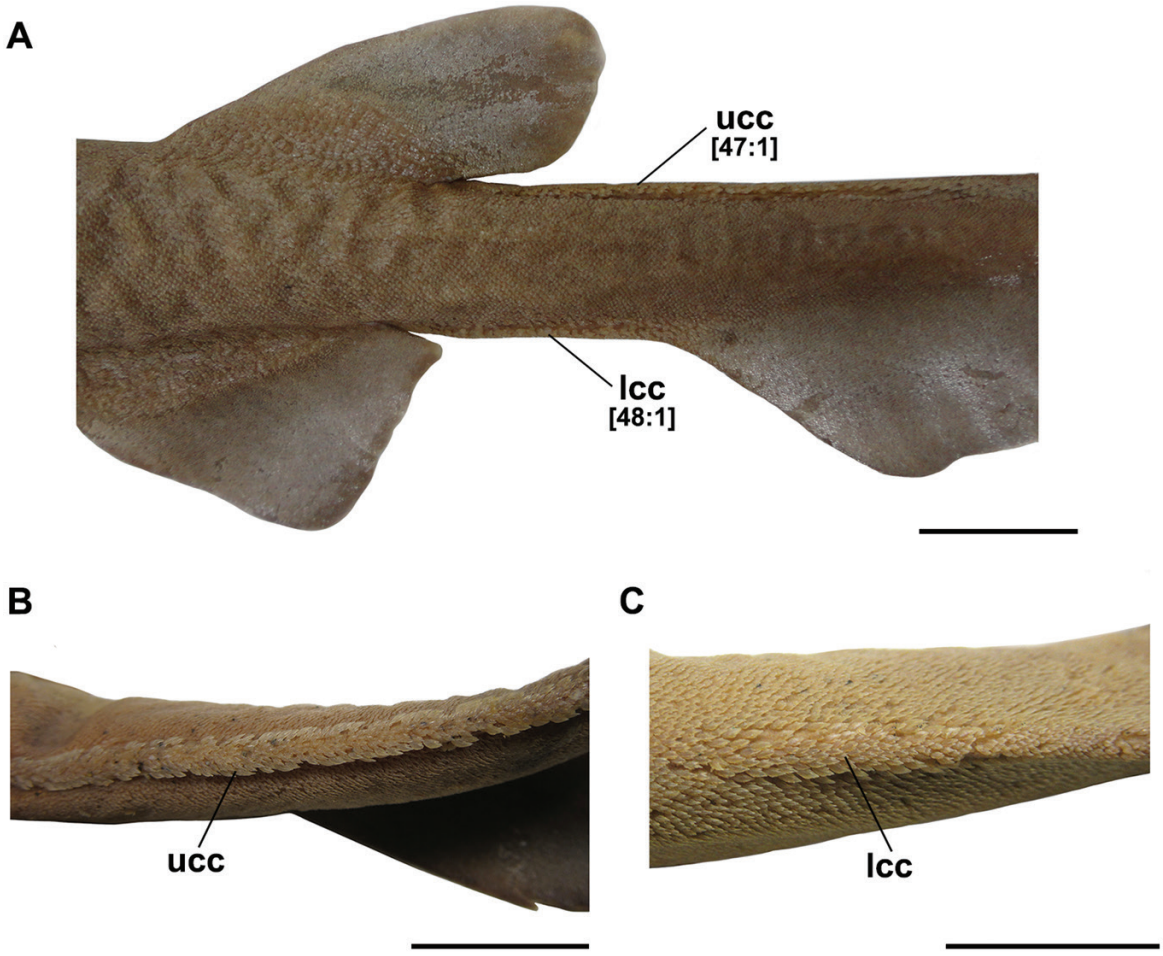

Figure 7. Detail of caudal crests. A, *Parmaturus angelae*, MZUSP 124001, female, 390 mm TL. B, C, *Parmaturus pilosus*, AMNH 49523, male, 593 mm TL. Abbreviations: lcc, lower caudal crest; TL, total length; ucc, upper caudal crest. Scale bars: 20 mm.

Muñoz-Chápuli (1985) described the presence of ectodermal pits on scales of the carcharhinoids *Scyliorhinus canicula*, *Galeus melastomus* (p. 394, fig. 1), *Galeus atlanticus* (Vaillant, 1888), *Mustelus mustelus* (Linnaeus, 1758) (p. 394, fig. 1), *Prionace glauca* (Linnaeus, 1758) (p. 395, fig. 3) and *Carcharhinus brachyurus* (Günther, 1870). Ectodermal pits are also observed in the scanning electron microscope scale images of *Galeorhinus galeus* (pl. 33), *Carcharhinus falciformis* (Bibron, 1839) (pls 34–37), *Carcharhinus obscurus* (Lesueur, 1818) (pls 40, 41), *Carcharhinus plumbeus* (Nardo, 1827) (pls 42–47), *Sphyrna lewini* (Griffith & Smith, 1834) (pl. 67), *Sphyrna tudes* (Valenciennes, 1822) (pls 68–70) and *Sphyrna zygaena* (Linnaeus, 1758) (pls 71–74) provided by Reif (1985). Here, these pits were observed on scales of all carcharhinoids examined, but were absent in orectoloboids and the lamnoid examined (Fig. 2A).

50. Extension of ectodermal pits on dorsal surface of the crown denticles: (0) restricted to anterior portion of the crown; (1) extending through more than one-half of the crown length (CI = 17; RI = 69) [extracted from Soares & de Carvalho (2020): ch. 26].

In all scyliorhinids, atelomycterids and the pentanchid *Haploblepharus edwardsii* and in the proscylliid *E. barbouri*, the pseudotriakid *Gollum attenuatus*, the hemigaleid *Paragaleus pectoralis* and the carcharhinid *Triaenodon obesus*, ectodermal pits are restricted to the anterior portion of the crown (50:0; Fig. 2B, C). In all other pentanchids, carcharhinids and triakids examined, the crown surface of dermal denticles is almost entirely covered by ectodermal pits [50:1; Soares & de Carvalho (2020): fig. 7].

51. Number of median ridges on dermal denticles: (0) one; (1) two (CI = 14; RI = 67) [extracted from Soares & de Carvalho (2020): ch. 27].

In scyliorhinids and the pentanchids *Apristurus*, *Cephalurus*, *Holohalaelurus*, *Halaelurus sellus* White, Last & Stevens, 2007, *Galeus antillensis*

Springer, 1979, *Galeus melastomus* and *Parmaturus angelae*, only one median ridge is observed on the crown surface (51:0; Fig. 2B). In other taxa examined, two ridges were observed [51:1; Soares & de Carvalho (2020): fig. 7].

Musculature

52. Muscles levator and retractor palpebrae nictitantis: (0) absent; (1) present (CI = 100; RI = 100) [new character].

The muscles levator and retractor palpebrae nictitantis are part of the postorbital musculature and are present in all carcharhinoids [52:1; Compagno (1988): fig. 2.6; Soares & de Carvalho (2020): p. 358, fig. 9] and absent in the orectoloboids and the lamnoid examined (52:0).

53. Muscle depressor palpebrae nictitantis: (0) absent; (1) present (CI = 100; RI = 100) [extracted from Soares & de Carvalho (2020): ch. 29].

Three muscles (levator, retractor and depressor) are responsible for elevating the nictitating lower eyelid and compose the postorbital musculature of most carcharhiniforms, except in *Cephaloscyllium*, *Poroderma* and *Scyliorhinus*, which lack a depressor palpebrae nictitantis [53:0; Compagno (1988): fig. 2.6; Soares & de Carvalho (2020): p. 358, fig. 9].

54. Origin of m. preorbitalis: (0) from the posterior border of nasal capsule; (1) from the dorsal surfaces of the orbito-nasal process [Goto (2001): ch. 85] (CI = 100; RI = 100).

In all carcharhiniforms and lamnoids examined, the muscle preorbitalis originates from the posterior border of nasal capsule (54:0), whereas in the orectoloboids, it originates from the dorsal surfaces of the orbito-nasal process [54:1; Goto (2001): figs 46–49].

55. Insertion of m. preorbitalis: (0) entirely inserts on the mandibula via a long tendon; (1) inserts on the adductor dorsal, extending until the mouth commissure (CI = 100; RI = 100) [extracted from Goto (2001): ch. 87].

Among taxa examined, only in the orectolobids does the m. preorbitalis insert on the mandibula via a long tendon [55:0; Goto (2001): figs 46–49], whereas in other taxa this muscle inserts on the adductor dorsal and extends until the mouth commissure (55:1).

56. Muscle spiracularis: (0) present; (1) absent (CI = 100; RI = 100) [extracted from Goto (2001): ch. 94].

A muscle spiracularis distinctly separated from the m. palatoquadrate is observed only in the orectoloboids [56:0; Goto (2001): fig. 52].

57. Origin of m. levator palatoquadrati: (0) on the ventral surface of the postorbital process; (1) extending along the posterior wall of the orbit; (2) extending from the postorbital process to the dorsal surface of the preorbital process (CI = 100; RI = 100) [compiled from Nakaya (1975) and Compagno (1988)].

The muscle levator palatoquadrati originates on the otic capsule of the neurocranium and inserts on the posterodorsal surface of the palatoquadrate, acting in the elevation of the upper jaw (Compagno, 1988; Huber *et al.*, 2011). Nakaya (1975) described three conditions for this muscle in carcharhinoids, from the restricted condition found in scyliorhinoids to the well developed and expanded muscle in cacharhinids; these conditions are analysed cladistically in this study. All scyliorhinoids, the proscylliids *E. barbouri* and *Proscyllium habereri*, the triakid *I. omanensis* and the pseudotriakid *Gollum attenuatus* exhibit a small m. levator palatoquadrati with origin restricted to the postorbital process (57:0; Fig. 8A); this condition is also observed in the orectoloboids and lamnoid examined. In the triakids *Galeorhinus galeus*, *M. schmitti* and *Triakis semifasciata*, the muscle invades the orbit and extends along its posterior wall (57:1; Fig. 8B). All carcharhinids examined and the hemigaleid *Paragaleus pectoralis* present a well-developed levator palatoquadrati with a broad origin that extends ventral and anterior to the postorbital process to attach on the lateral wall of the orbit and the cranial roof (57:2; Fig. 8C).

58. Divisions of m. adductor mandibulae: (0) three or more subdivisions; (1) two subdivisions, one dorsal and one ventral (CI = 100; RI = 100) [extracted from Shirai (1996): ch. 36].

The muscle adductor mandibulae in all carcharhiniforms and the lamnoid examined is divided in two subunits, one dorsal and one ventral [58:1; Compagno (1988): fig. 8.1]. Only in the orectolobiformes does this muscle present three or more subdivisions [58:0; Goto (2001): fig. 46].

59. Origin of m. coracomandibularis: (0) on the fascia of the coracoarcualis; (1) on the lateral borders of the coracoid (CI = 100; RI = 100) [compiled from Soares & de Carvalho (2020)].

Soares & de Carvalho (2020) described the muscle coracomandibularis originating directly from the coracoid bar in *Apristurus longicephalus* (= *Pentanchus longicephalus*) (p. 358, fig. 11D). The same condition is also observed in other species of *Pentanchus* (*Pentanchus australis*, *Pentanchus manis* and *Pentanchus stenseni*). In all other taxa examined, the coracomandibularis originates on the fascia of the coracoarcualis (59:0).

60. Insertion of m. coracomandibularis: (0) near the mid-length of the lower jaws, on their anteromedial borders; (1) on the articular region of the antimeres of Meckel's cartilage (CI = 14; RI = 40) [extracted from Soares & de Carvalho (2020): ch. 30].

In most catsharks examined, the m. coracomandibularis inserts on the articular region of the antimeres of Meckel's cartilage (60:1), as it

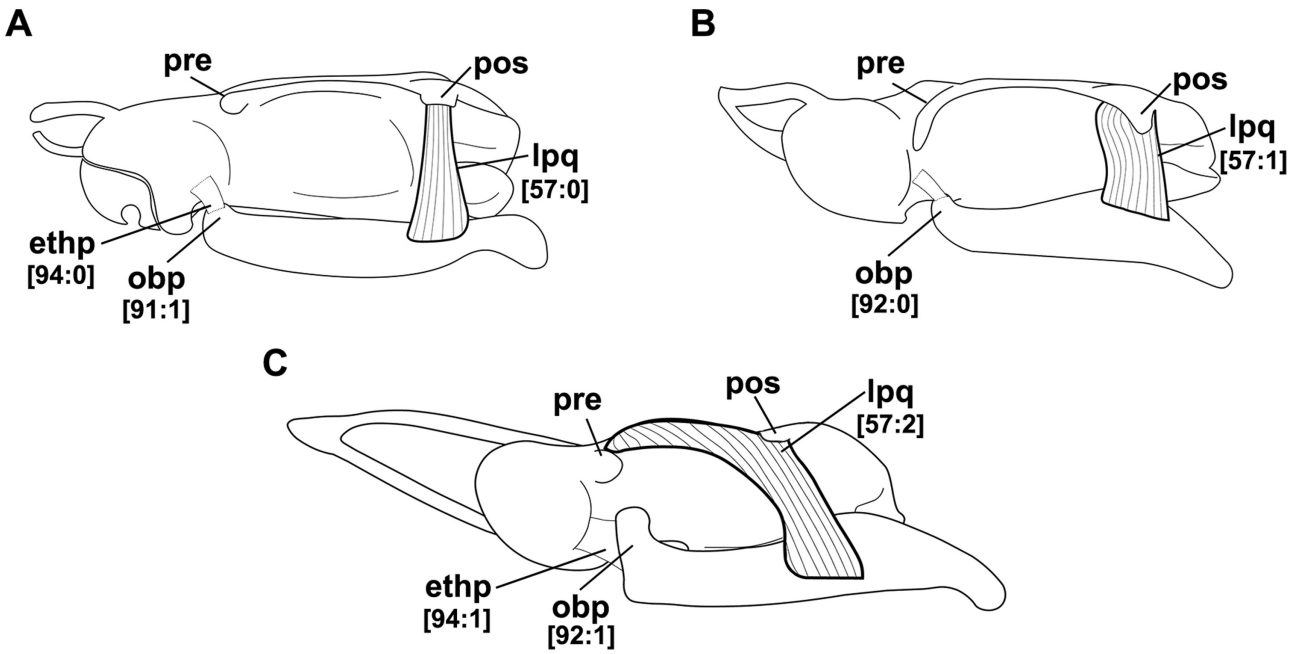

Figure 8. Detail of muscle levator palatoquadrati and palatoquadrate. A, *Scyliorhinus cabofriensis*, UERJ 1427, female, 446 mm TL. B, *Hemitriakis japonica*, NSMT 66856, female, 515 mm TL. C, *Rhizoprionodon longurio*, CAS 56628, female, 428 mm TL. Abbreviations: ethp, ethmopalatine ligament; lpq, muscle levator palatoquadrati; obp, orbital process of the palatoquadrate; pos, postorbital process; pre, preorbital process; TL, total length.

does also in the carcharhinids, most triakids, the pseudotriakid *Gollum attenuatus*, the hemigaleid *Paragaleus pectoralis* and the lamnoid *Al. vulpinus*. In the scyliorhinoids *Haploblepharus edwardsii*, *Halaelurus* spp., *Poroderma africanum*, *Parmaturus xaniurus* and *Cephalurus cephalus*, the proscylliids, the triakid *M. schmitti* and the orectoloboids, this muscle is divided into two portions anteriorly, each of which inserts on the anteromedial borders of the antimeres of Meckel's cartilage [60:0; Soares & de Carvalho (2020): fig. 10].

61. Muscle bundles of *coracohyoideus*: (0) united; (1) divided anteriorly; (2) separated throughout their extension (CI = 50; RI = 82) [modified from Soares & de Carvalho (2020): ch. 32].

All scyliorhinoids, proscylliids and the pseudotriakid *Gollum attenuatus* present muscle bundles of the coracohyoideus separated throughout their extension (61:2; Fig. 9A). The muscle bundles are united in orectoloboids, the lamnoid *Al. vulpinus*, all the carcharhinids examined and the triakid *I. omanensis* (61:0; Fig. 9C), whereas in the remaining triakids and the hemigaleid *Paragaleus pectoralis*, these are divided only posteriorly (61:1; Fig. 9B).

62. Distance between muscle bundles of coracohyoideus: (0) juxtaposed; (1) distance similar to half of the width of muscle bundle (CI = 25; RI = 62) [modified from Soares & de Carvalho (2020): ch. 32].

In taxa in which the muscle bundles of coracohyoideus are separated throughout their extension, there is variation regarding the distance between these. In most taxa examined, these bundles are juxtaposed (62:0), whereas in the pseudotriakid *Gollum attenuatus*, the scyliorhinid *Cephaloscyllium* spp., the pentanchids *Halaelurus* spp. and *Cephalurus cephalus*, the muscle bundles are separated by a distance of at least half the width of each bundle [62:1; Soares & de Carvalho (2020): fig. 11].

63. Origin of m. coracobranchialis II, III and IV: (0) on the pericardial membrane; (1) on the coracoid bar (CI = 20; RI = 81) [modified from Soares & de Carvalho (2020): ch. 33].

In most catsharks examined, the muscles coracobranchialis II, III and IV originate on the coracoid bar, in addition to the coracobranchialis I and V (63:1). In the scyliorhinoids *Cephalurus*, *Halaelurus*, *Haploblepharus*, *Holohalaelurus* and *Schroederichthys*, the orectoloboid *Hemiscyllium ocellatum* and the lamnoid *Al. vulpinus*, these muscles originate on the pericardial membrane [63:0; Soares & de Carvalho (2020): fig. 12].

64. Extension of m. interhyioideus: (0) posterior third of Meckel's cartilage; (1) half the length of Meckel's cartilage (CI = 20; RI = 78) [new character].

In the lamnoid *Al. vulpinus*, the orectolobid *Chiloscyllium griseum* and most scyliorhinoids, except *Galeus* and *Haploblepharus*, the muscle

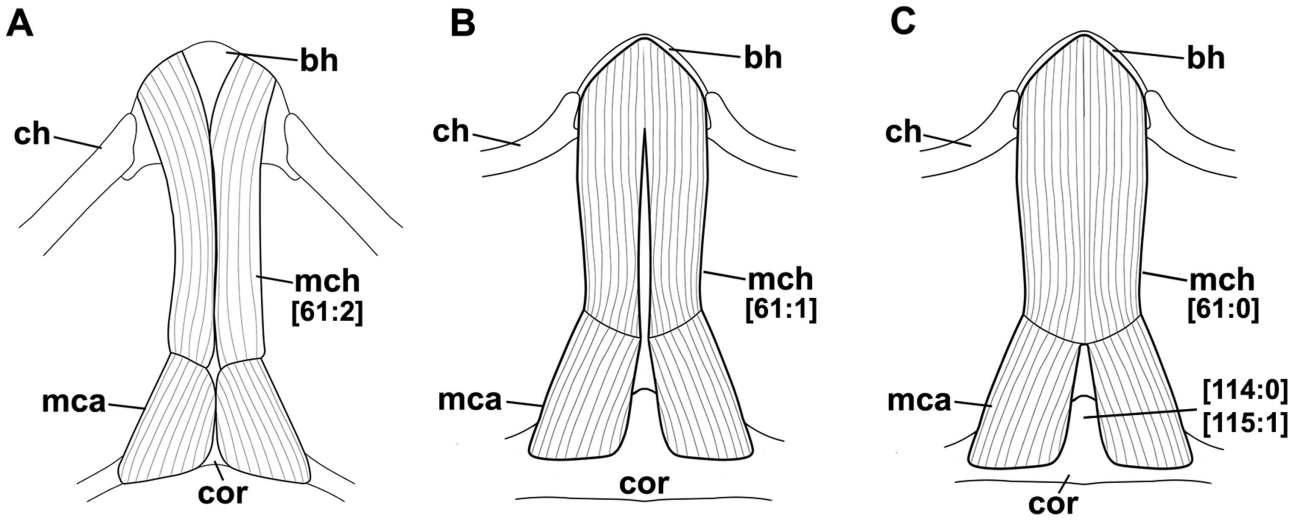

Figure 9. Detail of muscle coracohyoideus. A, *Holohalaelurus regani*, SAIAB 25717, male, 610 mm TL. B, *Mustelus schmitti*, UERJ 393, male, 390 mm TL. C, *Rhizoprionodon longurio*, CAS 56628, female, 428 mm TL (modified from Soares & de Carvalho, 2020). Abbreviations: bh, basihyal; ch, ceratohyal; cor, coracoid bar; mca, muscle coracoarcualis; mch, m. coracohyoideus; TL, total length.

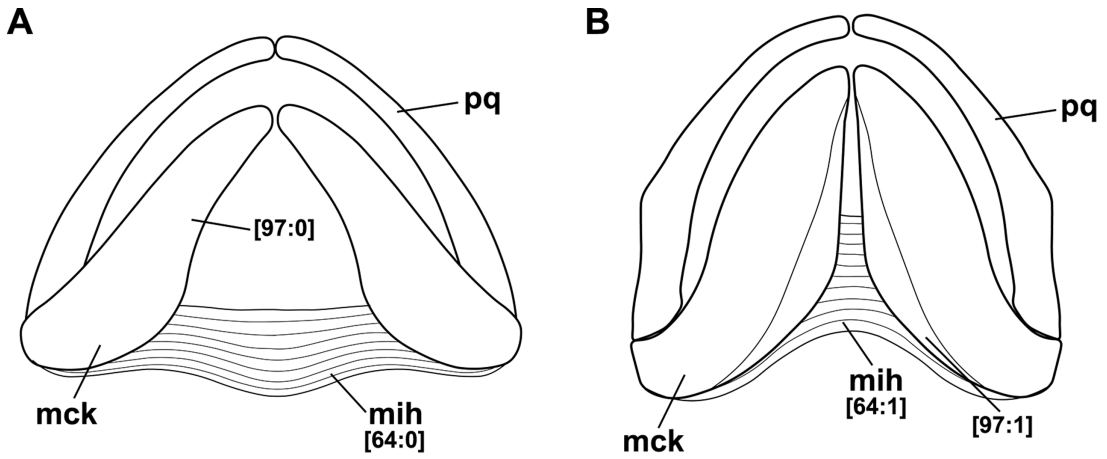

Figure 10. Detail of muscle interhyoideus. A, *Cephaloscyllium isabella*, USNM 320594, female, 390 mm TL. B, *Galeus antillensis*, UF 77853, female, 370 mm TL. Abbreviations: mck, Meckel's cartilage; mih, muscle interhyoideus; pq, palatoquadrate; TL, total length.

interhyoideus is restricted to the posterior third of Meckel's cartilage (64:0; Fig. 10A). All other carcharhinoids exhibit a well-developed interhyoideus extending up to half the length of Meckel's cartilage (64:1; Fig. 10B).

65. Extension of m. epaxialis: (0) expanded anteriorly and almost reaching the postorbital process; (1) posterior to the parietal fossa (CI = 14; RI = 74) [new character].

The m. epaxialis extends from the posterior margin of the neurocranium to the caudal fin. Its anterior extension varies across the specimens examined (Fig. 11). In most scyliorhinoids, the proscylliids *E. barbouri* and *Proscyllium habereri*, the triakids *Galeorhinus galeus* and *Hemitriakis japonica* and the carcharhinid *L. macrorhinus*, this muscle lies posterior to the parietal fossa and does not extend anteriorly (65:1; Fig. 11B). In the orectoloboids and lamnoid examined, the catshark genera *Apristurus*, *Asymbolus* and *Galeus*, the triakids *I. omanensis*, *M. schmitti* and *Triakis semifasciata*, the hemigaleid *Paragaleus pectoralis* and all carcharhinids apart from *Loxodon*, the same muscle extends past the posterior margin of the parietal fossa and almost reaches the postorbital process (65:0; Fig. 11A).

66. Muscle parietalis: (0) present; (1) absent (CI = 100; RI = 100) [extracted from Goto (2001): ch. 79].

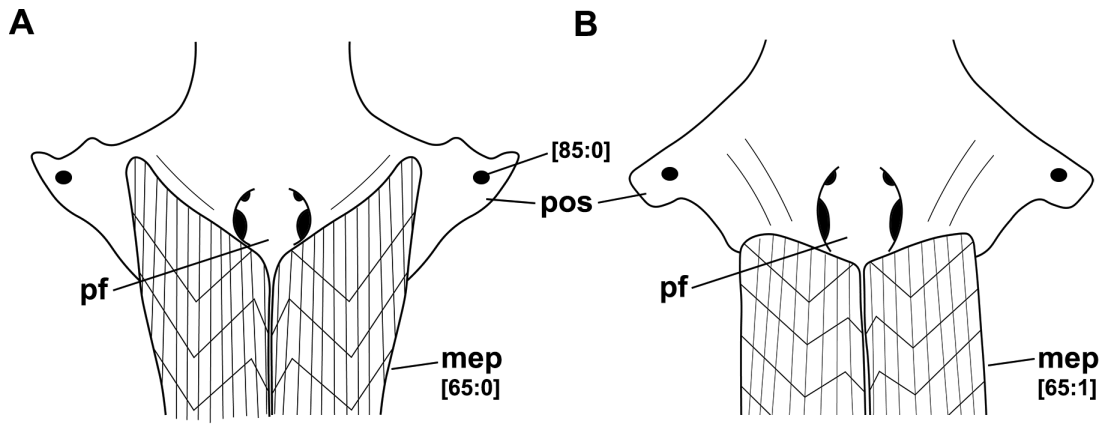

Figure 11. Detail of muscle epaxialis. A, *Asymbolus rubiginosus*, AMS I.30393-004, male, 527 mm TL. B, *Holohalaelurus regani*, SAIAB 25717, male, 610 mm TL. Abbreviations: mep, muscle epaxialis; pf, parietal fossa; pos, postorbital process; TL, total length.

A muscle parietalis is found only in the orectoloboids examined (Goto, 2001: 39).

Neurocranium

67. Rostral process: (0) composed of ventral and median rostral cartilage; (1) composed of lateral and median cartilages to form a tripodal rostrum (CI = 100; RI = 100) [compiled from Shirai (1996): ch. 1].

A rostral process composed of only one rostral cartilage, medially situated to the nasal capsules, is observed in the orectoloboids (67:0; Goto, 2001). In carcharhinoids and lamnoids, the rostrum is formed by three rostral cartilages, one medial and two lateral (67:1; Figs 12, 13); this condition was hypothesized to support a close relationship between the Lamniformes and Carcharhiniformes (Compagno, 1988; Shirai, 1996).

68. Rostral cartilages: (0) fused; (1) united only by connective tissue (CI = 50; RI = 96) [extracted from Soares & de Carvalho (2020): ch. 34].

In scyliorhinids, *Atelomycterus* and *Aulohalaelurus*, the rostral cartilages are united only by connective tissue (68:1; Figs 12A, 13A), whereas in all other carcharhinoids and the lamnoid *Al. vulpinus*, these cartilages are fused anteriorly (68:0; Fig. 13B–D).

69. Rostral fenestra: (0) absent; (1) present (CI = 100; RI = 100) [compiled from Compagno (1988) and Lana *et al.* (2021)].

A rostral fenestra limited anteriorly by a transverse bar is found in the carcharhinids *Carcharhinus melanopterus* (Fig. 12D), *L. macrorhinus* and *R. longurio* and the hemigaleid *Paragaleus pectoralis* (69:1), as recently described and illustrated by Lana *et al.* (2021: figs 1, 4, 7). In all other carcharhinoids examined that present a rostral node, a fenestra is lacking (69:0).

70. Rostral length: (0) corresponding to less than one-half of nasobasal length; (1) corresponding to one-half or more of nasobasal length (CI = 17; RI = 44) [new character].

The lamnoid *Al. vulpinus* and most scyliorhinoids present a short rostrum (70:0), with the exception of *Pentanchus* species (Figs 12B, 13B), *Galeus melastomus* and *Galeus polli* (70:1). Nakaya & Sato (1999) used the rostral length to diagnose their *Apristurus longicephalus* group using only the terms 'long' and 'short'. A long rostrum is also found in the pseudotriakid *Gollum attenuatus*, the triakids *I. omanensis* and *Triakis semifasciata* and the carcharhinids *L. macrorhinus* and *R. longurio*. In the orectoloboids *Chiloscyllium griseum* and *Hemiscyllium ocellatum*, only a median rostral cartilage is found, which corresponds to less than one-half of nasobasal length (70:0).

71. Relationship between lateral rostral cartilages and anterior fontanelle: (0) rostral cartilages separated from anterior fontanelle; (1) rostral cartilages confluent with lateral borders of anterior fontanelle (CI = 12; RI = 70) [extracted from Soares & de Carvalho (2020): ch. 35].

In *Apristurus*, *Galeus*, *Pentanchus*, *F. boardmani* and *Parmaturus xaniurus*, the rostral cartilages are confluent with the lateral borders of the anterior fontanelle, connected to it through ridges that extend from the base of the rostral cartilages to the border of the fontanelle [71:1; Soares & de Carvalho (2020): fig. 13F, G]; this condition is also observed in the lamnoid *Al. vulpinus*, all carcharhinids examined, the hemigaleid *Paragaleus pectoralis* and the triakids *Galeorhinus galeus*, *I. omanensis* and *Triakis semifasciata*. In all other taxa, rostral cartilages are separated from the anterior fontanelle (71:0; Soares & de Carvalho (2020): fig. 13A–E].

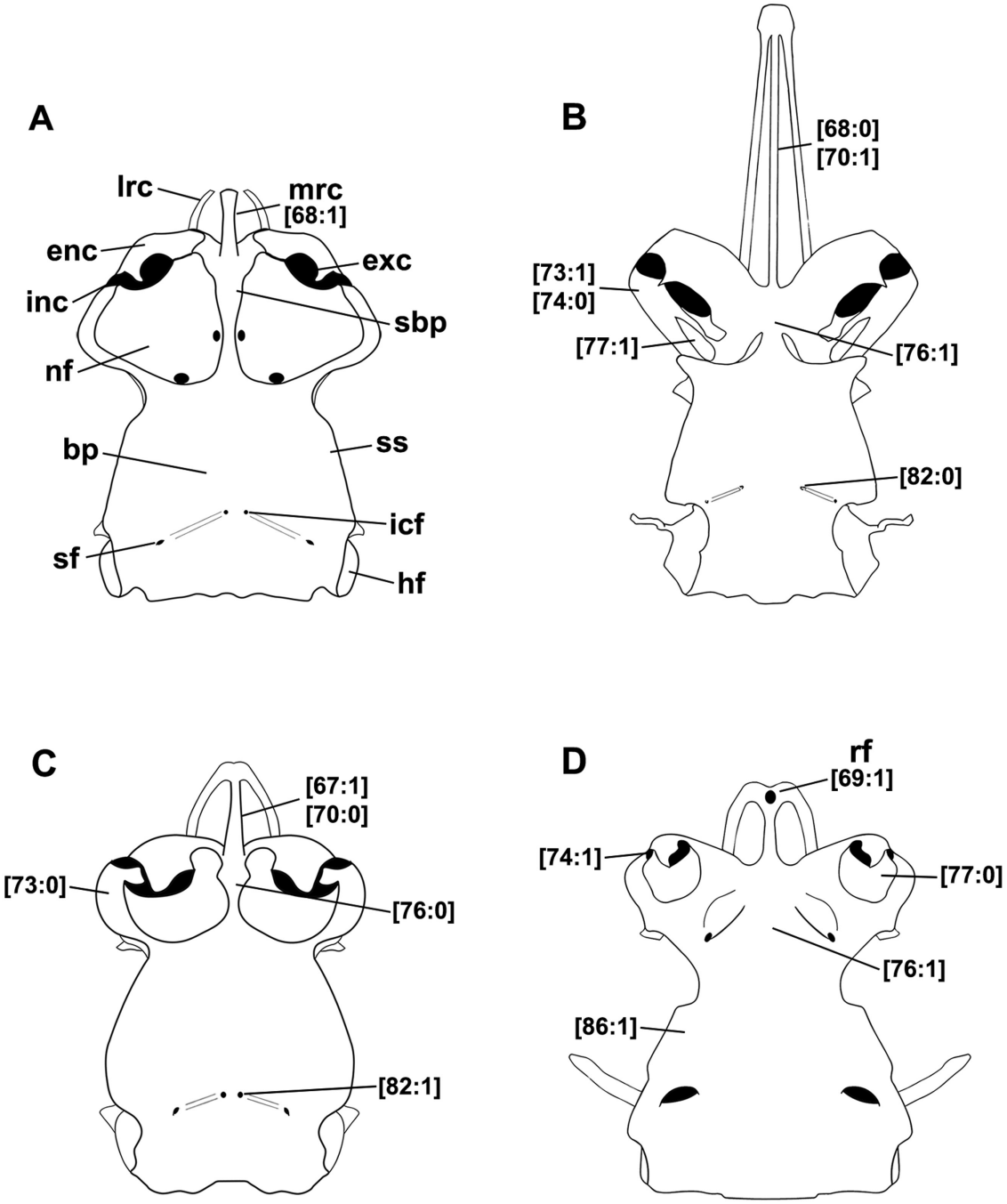

Figure 12. Neurocranium; ventral view. A, *Poroderma pantherinum*, SAIAB 34577, male, 640 mm TL. B, *Pentanchus australis*, CSIRO H1287-2, male, 510 mm TL. C, *Proscyllium habereri*, CAS 57189, male, 410 mm TL. D, *Carcharhinus melanopterus*, CAS 232592, male, 460 mm TL. Abbreviations: bp, basal plate; enc, external nasal cartilage; exc, excurrent aperture; hf, hyomandibular facet; icf, internal carotid foramen; inc, incurrent aperture; lrc, lateral rostral cartilage; mrc, medial rostral cartilage; nf, nasal fontanelle; rf, rostral fenestra; sbp, subnasal plate; sf, stapedial foramen; ss, suborbital shelf; TL, total length.

72. Relationship between median rostral cartilage and anterior fontanelle: (0) median rostral cartilage and anterior fontanelle separated by internasal space; (1) median rostral cartilage confluent with anterior fontanelle (CI = 20; RI = 69) [extracted from Soares & de Carvalho (2020): ch. 36].

In most catsharks examined and in the orectoloboids, the lamnoid *Al. vulpinus* and the triakids *Galeorhinus*

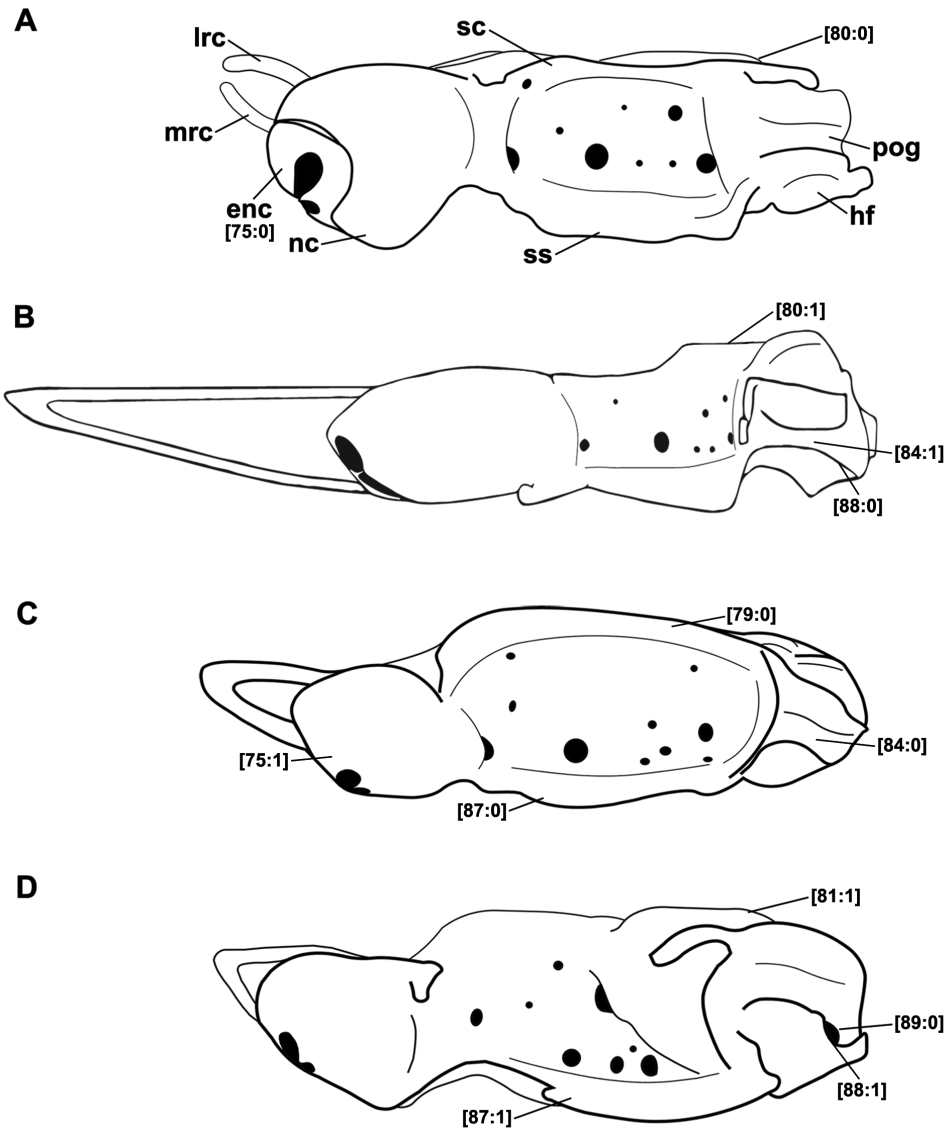

Figure 13. Neurocranium; lateral view. A, *Poroderma pantherinum*, SAIAB 34577, male, 640 mm TL. B, *Pentanchus australis*, CSIRO H1287-2, male, 510 mm TL. C, *Proscyllium habereri*, CAS 57189, male, 410 mm TL. D, *Carcharhinus melanopterus*, CAS 232592, male, 460 mm TL. Abbreviations: enc, external nasal cartilage; hf, hyomandibular facet; lrc, lateral rostral cartilage; mrc, medial rostral cartilage; nc, nasal capsule; pog, postorbital groove; sc, supraorbital crest; ss, suborbital shelf; TL, total length.

galeus and *M. schmitti*, the median rostral cartilage is separated from the anterior fontanelle by an internasal space (72:0). In the scyliorhinoids *Cephalurus*, *Haploblepharus* and *Holohalaelurus*, carcharhinids, proscylliids, the hemigaleid *Paragaleus pectoralis*, the pseudotriakid *Gollum attenuatus* and the triakids *Hemitriakis japonica*, *I. omanensis* and *Triakis semifasciata*, the median rostral cartilage and anterior fontanelle are confluent with each other, with no internasal space separating them [72:1; Soares & de Carvalho (2020): fig. 13; Lana *et al.* (2021): figs 1, 7].

73. Orientation of nasal capsules: (0) nasal capsules perpendicular to the anteroposterior axis of the neurocranium; (1) nasal capsules oblique (CI = 33; RI = 83) [extracted from Soares & de Carvalho (2020): ch. 37].

Nasal capsules are oriented perpendicularly to the anteroposterior axis of the neurocranium in most taxa examined (73:0; Fig. 12) except for the scyliorhinoids *Apristurus*, *Pentanchus* (Fig. 12B) and *Galeus*, the lamnoid *Al. vulpinus* and the carcharhinids *Carcharhinus melanopterus*, *L. macrorhinus* and

R. longurio, in which these capsules are obliquely oriented (73:1).

74. Relative position between nasal apertures: (0) incurrent aperture anterior to excurrent one; (1) nasal apertures parallel (CI = 14; RI = 79) [extracted from Soares & de Carvalho (2020): ch. 38].

Incurrent and excurrent nasal apertures are parallel in scyliorhinids, *Schroederichthys* spp., the triakids *M. schmitti* and *Triakis semifasciata*, the carcharhinid *Carcharhinus melanopterus* and the lamnoid *Al. vulpinus* (74:1; Fig. 12A, D). In all other taxa examined, the incurrent aperture is anterior to the excurrent one (74:0; Fig. 12B, C).

75. Relationship of the external nasal cartilage to the dorsal position of the nasal capsule: (0) not fused; (1) fused (CI = 100; RI = 100) [extracted from Soares & de Carvalho (2020): ch. 39].

In the orectoloboids, the lamnoid *Al. vulpinus*, the atelomycterids and scyliorhinids, the external nasal cartilage is separated from the anterodorsal portion of nasal capsule by a narrow strip of connective tissue (75:0; Fig. 13A), whereas in all other carcharhinoids, the nasal cartilage and capsule are fused (75:1; Fig. 13B–D).

76. Degree of development of the subnasal plate: (0) restricted to the medial portion of the nasal capsules and ventral to the internasal septum; (1) laterally expanded and united to the lateral border of the nasal capsule (CI = 50; RI = 95) [extracted from Soares & de Carvalho (2020): ch. 40].

In all examined scyliorhinoids except *Apristurus*, *Galeus* and *Pentanchus* and in the orectoloboids and the lamnoid and proscylliids examined (Fig. 12C), a subnasal plate restricted to the medial portion of the nasal capsules is observed (76:0; Fig. 12A), In the pentanchids *Apristurus*, *Galeus* and *Pentanchus* (Fig. 12B) and all other carcharhinoids, the subnasal plate extends laterally and unites to the lateral border of the nasal capsule (76:1).

77. Nasal fontanelle: (0) continuous and undivided, (1) divided into two units (CI = 33; RI = 88) [new character].

The nasal fontanelle, a ventral aperture of nasal capsule closely associated with the nasal apertures, is covered by a layer of connective tissue and presents different extensions among carcharhiniforms (Compagno, 1988). It is continuous and undivided in most catsharks examined (77:0; Fig. 12A, C, D) and in the carcharhinids, proscylliids, orectoloboids and the lamnoid *Al. vulpinus*. In the scyliorhinoids *Apristurus*, *Galeus* and *Pentanchus*, the hemigaleid *Paragaleus pectoralis* and all triakids examined, the nasal fontanelle is divided into anterior and posterior units by a lateral extension of the subnasal plate (77:1; Fig. 12B).

78. Epiphyseal notch: (0) absent; (1) present (CI = 12; RI = 73) [extracted from Soares & de Carvalho (2020): ch. 41].

An epiphyseal notch is present on the posterior border of the anterior fontanelle in the scyliorhinoids *Atelomycterus*, *Halaelurus*, *Haploblepharus*, *Holohalaelurus*, *Schroederichthys* and *Scyliorhinus*, the proscylliid *E. barbouri*, the pseudotriakid *Gollum attenuatus* and the triakids *Hemitriakis japonica* and *I. omanensis* [78:1; Soares & de Carvalho (2020): fig. 13A, C, D], whereas it is absent in all other taxa examined.

79. Supraorbital crest: (0) present; (1) absent (CI = 50; RI = 97) [extracted from Soares & de Carvalho (2020): ch. 42].

A supraorbital crest is observed in the orectoloboids, scyliorhinids, atelomycterids, the lamnoid *Al. vulpinus* and all other carcharhinoids examined (79:0; Fig. 13A, C), except pentanchids, carcharhinids and the hemigaleid *Paragaleus pectoralis* (Fig. 13B, D). This crest is absent in all pentanchids and was proposed as a synapomorphic character to group all crestless catsharks (Iglésias *et al.*, 2005).

80. Relationship between anterior fontanelle and parietal fossa: (0) at the same level; (1) parietal fossa dorsal to anterior one (CI = 33; RI = 71) [new character].

A parietal fossa higher than the anterior fontanelle is observed in the lamnoid *Al. vulpinus*, the pentanchid genera *Apristurus* and *Pentanchus*, the triakids *Hemitriakis japonica* and *I. omanensis* and all carcharhinids examined (80:1; Fig. 13B, D). In all other taxa examined, both structures are parallel in lateral view (80:0; Fig. 13A, C).

81. Otic capsules: (0) same width in relationship to the anterior portion of neurocranium; (1) inflated and broader than the anterior portion of neurocranium (CI = 50; RI = 90) [compiled from Compagno (1988)].

All carcharhinids examined exhibit well-developed otic capsules greatly expanded dorsally and laterally (81:1; Fig. 13D). Compagno (1988) pointed out that the inflation of the otic capsules might be related to an increase in length of the semicircular canals, representing a derived condition for these sharks. In other taxa examined, the otic capsules are narrower than the anterior portion of neurocranium (81:0).

82. Distance between internal carotid foramina: (0) greater than the distance between internal carotid and stapedial foramina; (1) smaller than the distance between internal carotid and stapedial foramina; (2) equal to the distance between internal carotid and stapedial foramina (CI = 17; RI = 68) [extracted from Soares & de Carvalho (2020): ch. 43].

The internal carotid foramina are separated by a distance greater than that between the internal carotid and stapedial foramina in the scyliorhinoids *Apristurus*, *Asymbolus*, *Figaro*, *Galeus*, *Haploblepharus*,

Pentanchus and *Poroderma*, all carcharhinids examined, the triakids *I. omanensis*, *M. schmitti* and *Triakis semifasciata* and the hemigaleid *Paragaleus pectoralis* (82:0; Fig. 12B). In *Cephaloscyllium*, *Holohalaelurus*, *Schroederichthys*, *Scyliorhinus*, the proscylliids, the triakid *Hemitriakis japonica* and the pseudotriakid *Gollum attenuatus*, foramina to the internal carotid artery are close to each other (82:1; Fig. 12A, C). In the catsharks *Atelomycterus*, *Aulohalaelurus*, *Cephalurus*, *Halaelurus* and *Parmaturus* and the triakid *Galeorhinus galeus*, the internal carotid foramina are separated by a distance similar to that between the internal carotid and stapedial foramina (82:2).

83. Postorbital groove: (0) absent; (1) present (CI = 33; RI = 33) [compiled from Compagno (1988)].

A postorbital groove, situated posteriorly to the orbits and ventral to the postorbital processes, is observed in most taxa examined (83:1; Fig. 13), with the exception of the orectoloboids, the triakid *M. schmitti* and the carcharhinid *Triaenodon obesus*.

84. Height of postorbital groove: (0) similar to or more than one-half the height of the hyomandibular facet; (1) less than one-half the height of the hyomandibular facet (CI = 25; RI = 70) [extracted from Soares & de Carvalho (2020): ch. 44].

In most taxa with a postorbital groove, the groove is more than one-half of the height of the hyomandibular facet (84:0; Fig. 13). In *Aulohalaelurus*, *Cephalurus*, *Pentanchus*, the hemigaleid *Paragaleus pectoralis* and all carcharhinids, this groove is narrow, corresponding to less than one-half the height of the hyomandibular facet (84:1; Fig. 13B).

85. Fenestra for the infraorbital canal of the lateral line: (0) present; (1) absent (CI = 20; RI = 43) [extracted from Soares & de Carvalho (2020): ch. 45].

A fenestra for the infraorbital canal of the lateral line is observed in most taxa examined [85:0; Fig. 11; see also Soares & de Carvalho (2020): fig. 13], except the scyliorhinoids *Pentanchus* and *Schroederichthys* spp., the lamnoid *Al. vulpinus* and the carcharhinids *Carcharhinus melanopterus*, *L. macrorhinus* and *R. longurio*. As described and illustrated by Soares & de Carvalho (2020: fig. 13C), the infraorbital canal passes through a bifurcation at the distal tip of the postorbital process in *Schroederichthys*. In *Pentanchus* spp., *Al. vulpinus* and the carcharhinids, the infraorbital canal of the lateral line passes posteriorly to the postorbital process.

86. Suborbital shelf: (0) absent; (1) present (CI = 50; RI = 0) [compiled from Compagno (1988)].

The suborbital shelf is a horizontal plate that forms the floor of the orbit and runs from the nasal capsules to the otic capsules in most carcharhinoids and some orectoloboids (86:1; Compagno, 1988, 1999; Goto, 2001). A suborbital shelf is present in most taxa examined (Figs 12, 13), except in the orectolobid *Hemiscyllium ocellatum* and the lamnoid *Al. vulpinus* (86:0).

87. Extension of suborbital shelf: (0) from the orbitonasal process; (1) from the posterior half of the orbit (CI = 100; RI = 100) [compiled from Compagno (1988)].

Variations regarding the extension of the suborbital shelf were observed among carcharhiniforms. In most taxa examined, this shelf extends from the orbitonasal process to the anterior edge of otic capsules (87:0; Fig. 13A–C). A distinct condition is observed in carcharhinids and the hemigaleid *Paragaleus pectoralis*, which present a short suborbital shelf that extends from the posterior half of the orbit to the otic capsules (87:1; Fig. 13D).

88. Posterior border of the hyomandibular facet: (0) continuous; (1) notched (CI = 50; RI = 86) [compiled from Compagno (1988)].

In all catsharks examined and in the orectoloboids, the lamnoid *Al. vulpinus*, proscylliids, the pseudotriakid *Gollum attenuatus* and the triakid *Galeorhinus galeus*, the posterior border of the hyomandibular facet is continuous (88:0; Fig. 13A–C). In all other carcharhinoids, a prominent notch is found on the posterior border of the hyomandibular facet (88:1; Fig. 13D).

89. Position of foramen for glossopharyngeal (IX) nerve: (0) on the lateral wall; (1) on the posterior wall of the otic capsule (CI = 20; RI = 56) [new character].

In all scyliorhinoids, the triakids *Triakis semifasciata* and *Galeorhinus galeus*, the proscylliid *E. barbouri*, the pseudotriakid *Gollum attenuatus* and the carcharhinid *L. macrorhinus*, the foramen for the glossopharyngeal (IX) nerve is situated on the posterior wall of the otic capsule (89:1; Fig. 13A–C). In the orectoloboids and lamnoid examined, the carcharhinids *Carcharhinus melanopterus* (Fig. 13D), *R. longurio* and *Triaenodon obesus*, the triakids *Hemitriakis japonica* and *M. schmitti* and the hemigaleid *Paragaleus pectoralis*, this foramen is situated on the lateral wall and adjacent to the hyomandibular facet (89:0).

Visceral arches

90. Labial ridge of the quadrate process: (0) present; (1) absent (CI = 10; RI = 56) [extracted from Soares & de Carvalho (2020): ch. 46].

A prominent ridge on the labial surface measuring about one-half of the length of the quadrate process is present in some scyliorhinoids, such as *Asymbolus*, *Aulohalaelurus*, *Atelomycterus*, *Cephalurus*, *Galeus*, *Halaelurus*, *Haploblepharus* and *Parmaturus* [90:0; Soares & de Carvalho (2020): fig. 17]. A similar condition is also observed in the orectoloboids, the pseudotriakid *Gollum attenuatus*, the triakid *I. omanensis*, the

hemigaleid *Paragaleus pectoralis* and the carcharhinid *Triaenodon obesus*. This ridge is absent in the lamnoid *Al. vulpinus* and all other carcharhinoids.

91. Orbital process: (0) absent; (1) present (CI = 25; RI = 25) [compiled from Compagno (1988)].

The orbital process of the palatoquadrate articulates with the preorbital wall, posterior portion of the nasal capsules and anterior end of the suborbital shelves and is involved in the palatoquadrate–neurocranial articulation in carcharhinoids (Compagno, 1988). Herein, we adopt the definition and terminology proposed by Compagno (1977, 1988) rather than the term 'ethmoidal articulations' as defined by Maisey (1980). An orbital process is present in most taxa examined (Fig. 8), with the exception of the pentanchid *Cephalurus cephalus*, the orectoloboids, the proscylliid *E. barbouri* and the pseudotriakid *Gollum attenuatus* [91:0; Soares & de Carvalho (2020): fig. 17].

92. Degree of development of orbital process: (0) reduced and not invading the orbit; (1) well developed, occupying the anterior one-quarter of the orbit (CI = 100; RI = 100) [compiled from Compagno (1988)].

The orbital process varies from a reduced condition, as observed in most carcharhinoids (92.0; Fig. 8A, B), to a well-developed structure that occupies the anterior one-quarter of the orbit in all carcharhinids, except *Triaenodon obesus*, the triakids *Galeorhinus galeus*, *Hemitriakis japonica*, *M. schmitti* and *Triakis semifasciata* and the hemigaleid *Paragaleus pectoralis* (92:1; Fig. 8C).

93. Position of the orbital process of the palatoquadrate: (0) at the anterior one-quarter of each antimere; (1) closer to half the length of each antimere (CI = 20; RI = 73) [extracted from Soares & de Carvalho (2020): ch. 47].

In most taxa examined, the orbital process is situated at the anterior one-quarter of the palatoquadrate (93:0). In the pentanchids *Apristurus*, *Galeus*, *Haploblepharus*, *Holohalaelurus*, *Parmaturus* and *Pentanchus* and the triakid *I. omanensis*, this process is more posteriorly situated, close to one-half the length of the palatoquadrate (93:1; Soares & de Carvalho, 2020: fig. 17).

94. Insertion point of the ethmopalatine ligament: (0) on the dorsal surface of the orbital process; (1) on the anterior surface of orbital process (CI = 100; RI = 100) [new character].

In all catsharks, the lamnoid *Al. vulpinus*, the proscylliid *Proscyllium habereri* and the triakids *I. omanensis* and *Triakis semifasciata*, the ethmopalatine ligament inserts on the dorsal surface of the orbital process (94:0; Fig. 8A, B). A different insertion point is observed in all carcharhinids, the hemigaleid *Paragaleus pectoralis* and the triakids *Galeorhinus galeus*, *Hemitriakis japonica* and *M. schmitti*, in which the ligament inserts on the anterior edge of the orbital process (94:1; Fig. 8C).

95. Relative distance between the orbital process and the ethmoidal region of the neurocranium: (0) separated by a long and well-developed ethmopalatine ligament; (1) close to each other and slightly separated by a short ethmopalatine ligament (CI = 20; RI = 20) [modified from Goto (2001): ch. 35].

Goto (2001) coded three conditions for the ethmoidal articulation within orectolobiforms, mixing in the information on the thickness of the ethmopalatine ligament (loose vs. massive), the degree of development of the orbital process (prominent vs. low) and the articular surface of the ethmoidal region of the neurocranium. Herein, we modified this character to consider the relative distance between the orbital process and the ethmoidal region of the neurocranium. Soares & de Carvalho (2020) described a unique condition for *Haploblepharus*, in which short ethmopalatine ligaments were found and the orbital process articulates directly with the orbital notch; this condition is also observed in the triakids *Hemitriakis japonica* and *M. schmitti*, the hemigaleid *Paragaleus pectoralis* and the carcharhinids *L. macrorhinus* and *Triaenodon obesus* (95:1). In all other taxa, the orbital process is separated from the ethmoidal region by a long and well-developed ethmopalatine ligament (95:0).

96. Accessory cartilage on symphysis of mandibula: (0) absent (1) present (CI = 25; RI = 0). [extracted from Goto (2001): ch. 32].

An accessory cartilage on the mandibular symphysis is present in the orectoloboid *Chiloscyllium griseum*, the scyliorhinid *Poroderma africanum* and the pentanchids *Pentanchus longicephalus* and *Haploblepharus edwardsii* [95:1; Goto (2001): fig. 21]. This cartilage was not depicted in the illustration of *Pentanchus longicephalus* provided by Soares & de Carvalho (2020: fig. 17B).

97. Degree of calcification of the medial portion of Meckel's cartilage: (0) uniformly calcified throughout; (1) medial portion less calcified than the rest of Meckel's cartilage (CI = 25; RI = 79) [extracted from Soares & de Carvalho (2020): ch. 48].

Most taxa examined possess a Meckel's cartilage uniformly calcified throughout its extension (97:0; Fig. 10A). In the pentanchids *Apristurus*, *Cephalurus*, *Figaro*, *Galeus*, *Parmaturus* and *Pentanchus*, the pseudotriakid *Gollum attenuatus* and the triakid *I. omanensis*, the medial portion of the Meckelian antimeres is less calcified than the rest of the cartilage (97:1; Fig. 10B).

98. Number of Meckelian condyles on the articular region of the quadratomandibular joint: (0) two,

(1) one (CI = 12; RI = 74) [modified from Soares & de Carvalho (2020): ch. 49].

Soares & de Carvalho (2020) coded three character states for the condyles found in the Meckel's cartilage, merging the condition in which anterior and posterior condyles are distinct from each other with the one in which both condyles form a unit. Herein, we divided this character into two, coding separately the number of condyles and the relative position of the posterior and anterior condyles and the facet of the quadratomandibular joint. Only one condyle is observed in scyliorhinids, the atelomycterid *Schroederichthys*, the pentanchids *Cephalurus*, *Haploblepharus*, *Holohalaelurus* and *Parmaturus*, the lamnoid *Al. vulpinus*, the triakid *I. omanensis* and the carcharhinid *Triaenodon obesus* [98:1; Soares & de Carvalho (2020): fig. 18A], whereas in all other taxa examined two condyles are observed [98:0; Soares & de Carvalho (2020): fig. 18B, C].

99. Relative position of the posterior condyle on the articular region of the quadratomandibular joint of Meckel's cartilage: (0) between anterior labial condyle and facet; (1) opposite the facet (CI = 25; RI = 66) [modified from Soares & de Carvalho (2020): ch. 49].

In taxa that possess two distinct condyles on the articular region of Meckel's cartilage, the posterior and lingual condyle is situated between the anterior labial condyle and facet in the scyliorhinoids *Asymbolus*, *Atelomycterus*, *Figaro*, *Galeus* and *Halaelurus*, the proscylliid *Proscyllium*, the pseudotriakid *Gollum attenuatus* and all triakids examined [99:0; Soares & de Carvalho (2020): fig. 18B]. In the pentanchids *Apristurus* and *Pentanchus*, the proscylliid *E. barbouri*, the hemigaleid *Paragaleus pectoralis* and the carcharhinid *R. longurio*, the posterior condyle is situated more posteriorly and opposite the facet [99:1; Soares & de Carvalho (2020): fig. 18C].

100. Connective tissue adjacent to the basihyal cartilage: (0) absent; (1) present (CI = 33; RI = 70) [compiled from Soares & de Carvalho (2020)].

Soares & de Carvalho (2020) described the presence of connective tissue surrounding the basihyal in *Pentanchus longicephalus* and *Holohalaelurus regani* that would serve as insertion surfaces for the muscle coracohyoideus [Soares & de Carvalho (2020): fig. 11D]. However, the character states proposed by those authors were not independent because the m. coracohyoideus also inserts on the ventral surface of the basihyal cartilage in taxa that present such adjacent connective tissues. For this reason, we code the occurrence of connective tissues adjacent to the basihyal cartilage herein to express the condition observed better. In addition to the taxa mentioned above, connective tissues are also present in *Pentanchus australis*, *Pentanchus manis*, *Pentanchus stenseni* and the proscylliid *E. barbouri* (100:1).

101. Thyroid foramen: (0) absent; (1) present (CI = 20; RI = 83) [extracted from Soares & de Carvalho (2020): ch. 50].

An opening at the anterior portion of the basihyal cartilage, known as the thyroid foramen, is present in scyliorhinids, the atelomycterids *Atelomycterus* and *Schroederichthys* and the pentanchids *Apristurus*, *Asymbolus*, *Figaro*, *Halaelurus* and *Holohalaelurus* [101:1; Soares & de Carvalho (2020): fig. 19], whereas it is absent in all other taxa examined (101:0).

102. Internal surface of the hyomandibular cartilage: (0) uniform; (1) concave (CI = 33; RI = 75) [extracted from Soares & de Carvalho (2020): ch. 51].

In most taxa examined, the internal surface of the hyomandibular cartilage is uniform (102:0), with the exception of the pentanchids *Apristurus*, *Parmaturus* and *Pentanchus* and the pseudotriakid *Gollum attenuatus*, in which a prominent concavity is observed [102:1; Soares & de Carvalho (2020): fig. 20B].

103. Anterior border of the basihyal cartilage: (0) not bifurcated; (1) bifurcated (CI = 25; RI = 62) [extracted from Soares & de Carvalho (2020): ch. 52].

The anterior border of the basihyal cartilage is bifurcated in the scyliorhinoids *Atelomycterus*, *Halaelurus*, *Holohalaelurus* and *Schroederichthys* and the triakid *Hemitriakis japonica* (103:1; Soares & de Carvalho, 2020, fig. 19B). In other taxa examined, the basihyal cartilage is uniform, and no bifurcation is observed [103:0; Soares & de Carvalho (2020): fig. 19A].

104. Lateral processi rastriformis: (0) absent; (1) present (CI = 33; RI = 82) [extracted from Soares & de Carvalho (2020): ch. 53].

As described and illustrated by Soares & de Carvalho (2020: fig. 21), processi rastriformis greater than dermal papillae and situated on the anterior surface of the articular region between cerato- and epibranchial cartilages are observed in *Asymbolus*, *Atelomycterus*, *Halaelurus*, *Poroderma* and *Schroederichthys* [104:1; Soares & de Carvalho (2020): fig. 21].

105. Oropharyngeal denticles: (0) small and not forming rows on internal face of gill components; (1) large and forming rows on internal face of gill components (CI = 17; RI = 50) [extracted from Soares & de Carvalho (2020): ch. 54].

Rows of oropharyngeal denticles greater than the surrounding ones and similar in shape and size to the dermal denticles of dorsolateral surfaces of the body were found on the internal surface of gill components in the scyliorhinoids *Cephaloscyllium sufflans* (Regan, 1921), *Cephaloscyllium variegatum* Last & White, 2008, *Halaelurus natalensis* (Regan, 1904), *Halaelurus*

sellus and *Parmaturus xaniurus*, *Pentanchus australis*, *Pentanchus longicephalus*, *Pentanchus manis* and *Poroderma* spp. and the carcharhinid *R. longurio* (105:1; Soares & de Carvalho, 2020: fig. 22). In all other taxa, oropharyngeal denticles are small and do not form rows (105:0).

106. Shape of the gill pickax: (0) short and triangular; (1) elongated and sling-like (CI = 20; RI = 73) [extracted from Soares & de Carvalho (2020): ch. 55].

The gill pickax is a plate formed by the fusion between the dorsal tips of gill arches IV and V (Shirai, 1992), which varies from short and triangular (scyliorhinoids *Cephaloscyllium* and *Poroderma*, the orectoloboids, the lamnoid *Al. vulpinus*, the triakid *Hemitriakis japonica* and all carcharhinids; 106:0) to elongated and sling-like [all other scyliorhinoids, proscyliids, the pseudotriakid *Gollum attenuatus*, the triakids *Galeorhinus galeus*, *I. omanensis* and *M. schmitti* and the hemigaleid *Paragaleus pectoralis*; 106:1; Soares & de Carvalho (2020): fig. 23].

107. Ventral extrabranchial cartilages: (0) four; (1) three (CI = 100; RI = 100) [extracted from Soares & de Carvalho (2020): ch. 56].

Only in scyliorhinids (*Cephaloscyllium*, *Poroderma* and *Scyliorhinus*) are three ventral extrabranchial cartilages observed (107:1) rather than four as in all other taxa examined. This character was listed by Compagno (1988) and hypothesized by Soares & de Carvalho (2020) as a synapomorphy for the subfamily Scyliorhininae (= family Scyliorhinidae in the present study; Table 2).

108. Accessory cartilage of basibranchial copula: (0) not differentiated from the cardiobranchial cartilage; (1) separated from the cardiobranchial cartilage (CI = 33; RI = 50) [modified from Goto (2001): ch. 50].

An accessory cartilage is not differentiated from the cardiobranchial cartilage of the basibranchial copula in the orectoloboids examined and the pentanchids *Ap. parvipinnis*, *Pentanchus australis* and *Pentanchus longicephalus* (108:0; Fig. 14A). In all other taxa examined, this cartilage is distinctly separated from the cardiobranchial cartilage (108:1; Fig. 14B, C).

109. Length of accessory cartilage of basibranchial: (0) one-quarter of the cardiobranchial cartilage; (1) one-third of the cardiobranchial cartilage (CI = 17; RI = 76) [new character].

A well-developed accessory cartilage of the basibranchial corresponding to one-third of the cardiobranchial cartilage is observed in most scyliorhinoids examined and the triakids *Hemitriakis japonica* and *M. schmitti* (109:1; Fig. 14C). In *At. fasciatus*, *Cephaloscyllium* spp., *Cephalurus cephalus*, *F. boardmani*, *Parmaturus xaniurus* and *Schroederichthys* spp., this cartilage is short and corresponds to one-quarter of the cardiobranchial cartilage, as in most of the remaining carcharhinoids (109:0; Fig. 14B).

Pectoral skeleton

110. Pectoral propterygium and mesopterygium proximal segments: (0) isolated; (1) fused, forming a plate (CI = 50; RI = 86) [new character].

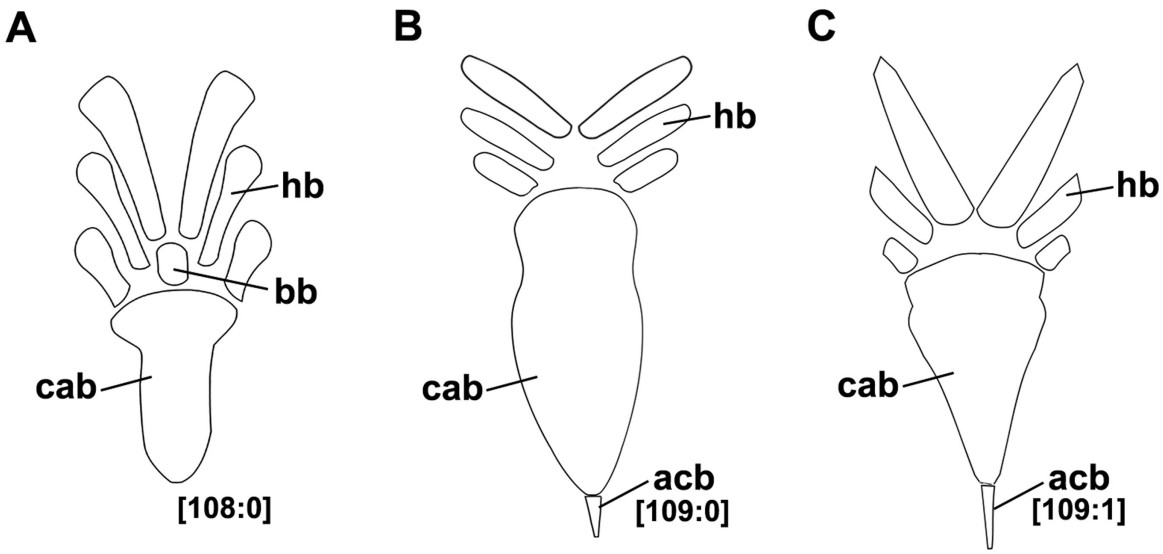

Figure 14. Detail of hypobranchials and copula basibranchial. A, *Pentanchus australis*, CSIRO H1287-2, male, 510 mm TL. B, *Holohalaelurus regani*, SAIAB 25717, male, 610 mm TL. C, *Carcharhinus melanopterus*, CAS 232592, male, 460 mm TL. Abbreviations: acb, accessory cartilage of the basibranchial copula; bb, basibranchial; cab, cardiobranchial cartilage of the basibranchial copula; hb, hypobranchials; TL, total length.

Compagno (1988) stated that fusions of adjacent mesopterygial radials are common in carcharhinoids, as noted also by White (1937) and Nakaya (1975). Fusions between mesopterygial and propterygial proximal radial segments are less common and have been reported only for *Apristurus japonicus* by Nakaya (1975: p. 74, fig. 36c). Among the taxa examined here, similar fusions were observed only in species of *Apristurus* and *Pentanchus* (110:1; Fig. 15B) and in the triakid *Hemitriakis japonica*.

111. Relative size of the propterygium and mesopterygium: (0) propterygium smaller than mesopterygium; (1) same size (CI = 33; RI = 78) [new character].

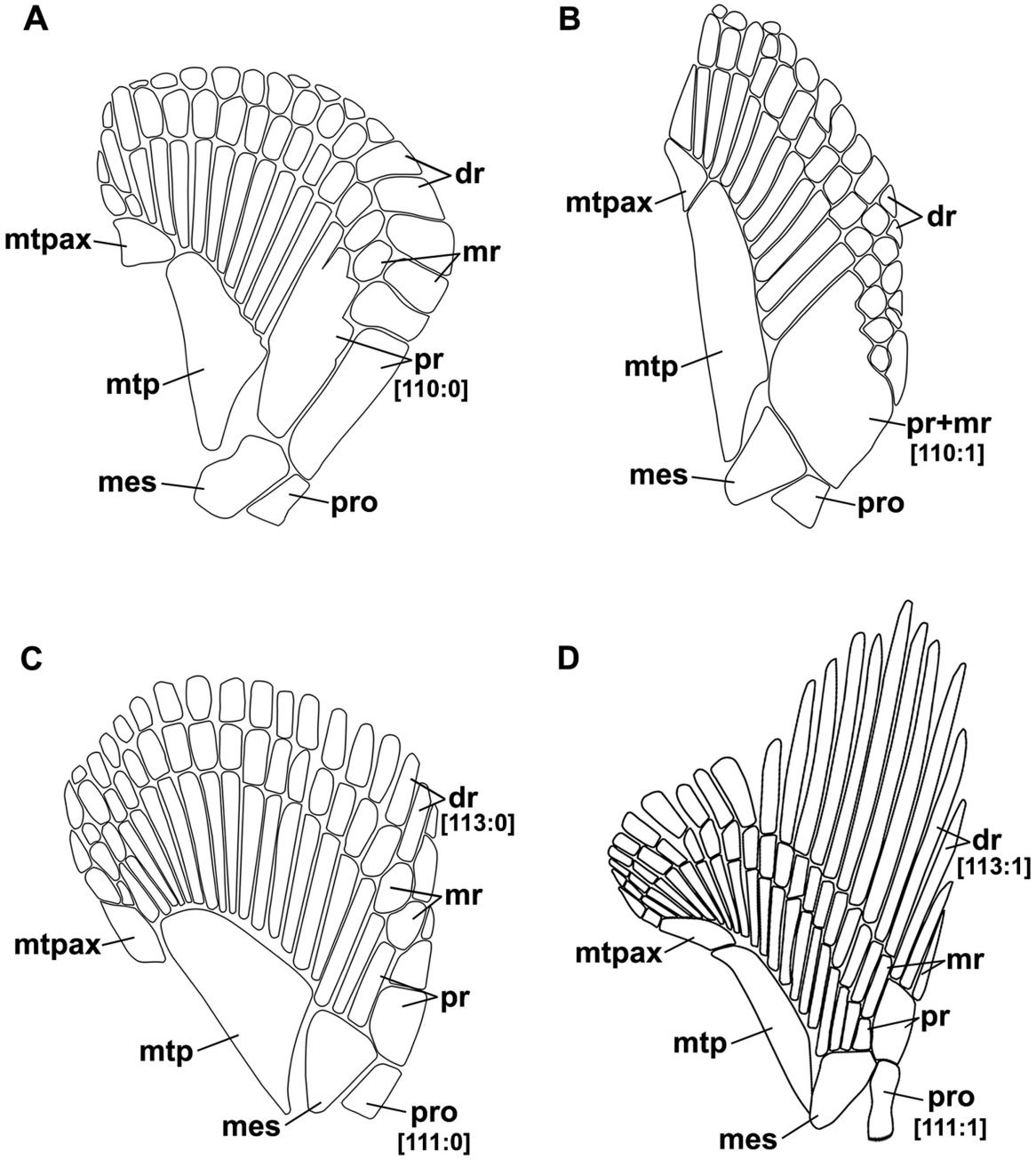

Figure 15. Pectoral fin skeleton. A, *Poroderma pantherinum*, SAIAB 34577, male, 640 mm TL. B, *Apristurus laurussonii*, UF 185652, male, 480 mm TL. C, *Gollum attenuatus*, NSMT 42855, female, 950 mm TL. D, *Loxodon macrorhinus*, HUMZ 37632, male, 750 mm TL. Abbreviations: dr, distal radial elements; mes, mesopterygium; mr, medial radial elements; mtp, metapterygium; mtpax, metapterygium axial; pr, proximal radial elements; pro, propterygium; TL, total length.

In all catshark genera, the proscylliids *E. barbouri* and *Proscyllium habereri*, the pseudotriakid *Gollum attenuatus* and the orectolobids examined, a propterygium smaller than the mesopterygium is observed (111:0; Fig. 15A–C). All carcharhinids examined, the hemigaleid *Paragaleus pectoralis*, the triakids *Hemitriakis japonica*, *I. omanensis*, *M. schmitti* and *Triakis semifasciata* and the lamnoid *Al. vulpinus* possess a propterygium and mesopterygium that are similar in size (111:1; Fig. 15D).

112. Pectoral-fin radials: (0) aplesodic; (1) plesodic (CI = 50; RI = 83) [compiled from Compagno (1988) and Shirai (1996)].

As proposed by Stensiö (1959) and described by Compagno (1988), two types of pectoral fins are observed within carcharhinoids: aplesodic (pectoral radials extending up to half-length or less of the pectoral anterior margin and distal web supported only by ceratotrichia) and plesodic (radials extending well into the fin web and supplementing the support of its ceratotrichia). Aplesodic pectoral radials are found in all catshark genera examined and in the orectoloboids, proscylliid *Proscyllium habereri*, the pseudotriakid *Gollum attenuatus* and the triakids *Galeorhinus galeus*, *I. omanensis* and *Triakis semifasciata* (112:0). In the lamnoid *Al. vulpinus*, the triakid *Hemitriakis japonica*, the hemigaleid *Paragaleus pectoralis* and all carcharhinids examined, pectoral-fin radials are plesodic [112:1; Compagno (1988): fig. 4.1].

113. Distal radial elements of propterygium and mesopterygium: (0) shorter than proximal radial elements; (1) same length or longer than proximal radial elements (CI = 33; RI = 82) [new character].

Differences in relative length of the pectoral proximal and distal radial segments among carcharhinoids were reported and explored by White (1937), Compagno (1970, 1988) and Nakaya (1975). Compagno (1988) pointed out that a gradient increase in length of distal radial segments could be noted from scyliorhinoids, proscylliids and pseudotriakids to hemigaleids and carcharhinids. In the present study, we restricted our observations to the radial segments associated with the propterygium and mesopterygium. Distal radial elements similar in length or longer than the proximal ones are observed in all carcharhinids and triakids examined, the hemigaleid *Paragaleus pectoralis*, the proscylliid *E. barbouri* and the lamnoid *Al. vulpinus* (113:1; Fig. 15D). In all catshark genera, the orectoloboids examined, the pseudotriakid *Gollum attenuatus* and the proscylliid *Proscyllium habereri*, distal segments are shorter than proximal radial elements (113:0; Figs 15A–C).

114. Medial projection of the coracoid bar: (0) present; (1) absent (CI = 33; RI = 0) [extracted from Goto (2001): ch. 53; Soares & de Carvalho (2020): ch. 57].

A medial projection of the coracoid bar is present in most taxa examined (114:0; Fig. 9), except *Haploblepharus*, *Holohalaelurus* and *Schroederichthys saurisqualus* Soto, 2001 [114:1; Soares & de Carvalho (2020): fig. 24C].

115. Degree of development of the medial projection of the coracoid bar: (0) reduced to less than twice the size of the lateral portion of the coracoid bar; (1) well developed, more than twice the size of the lateral portion of the coracoid bar (CI = 33; RI = 90) [extracted from Soares & de Carvalho (2020): ch. 58].

In the scyliorhinoids *Cephalurus*, *Cephaloscyllium* and *Scyliorhinus* and the carcharhinid *L. macrorhinus*, the medial projection of the coracoid bar is well developed and corresponds to more than two times the size of the lateral portion of the coracoid bar [115:1; Soares & de Carvalho (2020): fig. 24A]. In *Cephaloscyllium* and *Scyliorhinus*, this projection entirely covers the heart ventrally, whereas in *Cephalurus* and *Loxodon* it is slender and covers the heart only in part (Soares & de Carvalho, 2020: fig. 24D). In all other taxa examined, the medial projection is not prominent (115:0).

116. Lateral processes on pectoral girdle: (0) present; (1) absent (CI = 12; RI = 69) [extracted from Soares & de Carvalho (2020): ch. 59].

Lateral processes on each side of the coracoid bar were observed in the catshark genera *Cephaloscyllium*, *Halaelurus*, *Haploblepharus*, *Schroederichthys* and *Scyliorhinus*, the orectoloboid *Chilloscyllium griseum*, the proscylliid *E. barbouri* and the triakids *Hemitriakis japonica*, *I. omanensis* and *M. schmitti* [116:0; Soares & de Carvalho (2020): fig. 24A, B). These processes are absent in other taxa examined (116:1).

Clasper

117. Dermal denticles on the dorsomedial surface of clasper glans: (0) absent; (1) present (CI = 33; RI = 80) [extracted from Soares & de Carvalho (2020): ch. 60].

In most taxa examined, the dorsomedial surface of the clasper glans is covered by dermal denticles in varying degrees and distribution patterns (117:1; Soares & de Carvalho, 2019, 2020; Soares, 2020). Only in the scyliorhinoids *Cephalurus cephalus*, *Halaelurus* spp., *Haploblepharus edwardsii* and *Parmaturus* spp., the proscylliid *Proscyllium habereri*, the triakids *Hemitriakis japonica* and *I. omanensis* and the carcharhinid *L. macrorhinus* are the dermal denticles lacking on the dorsomedial surface [117:0; Soares (2020): fig. 2A, B].

118. Dermal denticles on the cover rhipidion of the clasper: (0) absent; (1) present (CI = 10; RI = 61)

[modified from Soares & de Carvalho (2020): ch. 61].

In taxa that present dermal denticles on the dorsomedial surface of the clasper glans, their distribution varies from covering most of the surface except the rhipidion and terminal dermal cover or only some portions of the exorhipidion (Soares, 2020). Character 61 and its character states as proposed by Soares & de Carvalho (2020) are modified here to restrict the observations to the occurrence of dermal denticles on the cover rhipidion. In the proscylliid *E. barbouri*, scyliorhinoids *Ak. suwartanai*, *Ap. brunneus*, *Asymbolus* spp., *Aulohalaelurus kanakorum* Séret, 1990, *Bythaelurus* spp., *F. boardmani*, *Galeus nipponensis*, *Parmaturus* spp., *Pentanchus australis*, *Pentanchus longicephalus*, *Schroederichthys* spp., *Scyliorhinus cervigoni* Maurin & Bonnet, 1970, *Scyliorhinus boa* Goode & Bean, 1892, *Scyliorhinus hesperius* Springer, 1966 and *Scyliorhinus retifer* (Garman, 1881), the dorsal surface of cover rhipidion is smooth and lacks dermal denticles (118:0; Soares, 2020; Soares & de Carvalho, 2020: fig. 25A, D). In all other species of *Scyliorhinus* and in *Ap. laurussonii*, *Ap. macrostomus*, *Atelomycterus* spp., *Au. labiosus*, *Cephaloscyllium* spp., *Galeus antillensis*, *Galeus polli*, *Galeus sauteri*, *Holohalaelurus regani* and *Poroderma* spp., denticles cover the surface of the cover rhipidion or at least on its posterior portion [118:1; Soares (2020): figs 1–7].

119. Clasper hooks on the medial border of the exorhipidion: (0) absent; (1) present (CI = 14; RI = 25) [modified from Soares & de Carvalho (2020): ch. 62].

Specialized hooks were observed on the medial border of the exorhipidion in claspers of the catsharks *Ap. laurussonii*, *Ap. macrostomus*, *F. boardmani*, *Galeus antillensis*, *Galeus nipponensis*, *Halaelurus natalensis*, *Poroderma pantherinum* and *Scyliorhinus torazame* [Soares & de Carvalho (2020): fig. 25F] and the proscylliids *E. barbouri* and *Proscyllium habereri* (119:1).

120. Terminal dermal cover of clasper glans: (0) present; (1) absent (CI = 25; RI = 40) [extracted from Soares & de Carvalho (2020): ch. 63].

A terminal dermal cover of the clasper glans as described by Compagno (1988) and Soares et al. (2015) is found in proscylliids and most scyliorhinoids examined [120:0; Soares, (2020): figs 1–7] except *Bythaelurus clevai* (Séret, 1987), *Cephalurus cephalus*, *Halaelurus sellus* and *Pentanchus longicephalus*. This dermal cover is also absent in the triakids *Hemitriakis japonica* and *I. omanensis* and the carcharhinid *L. macrorhinus* (120:1).

121. Extension of the terminal dermal cover: (0) restricted to the distal tip of the clasper glans; (1) corresponding to up to one-third of clasper glans (CI = 14; RI = 74) [extracted from Soares & de Carvalho (2020): ch. 64].

The terminal dermal cover extends to one-third of the clasper glans in all scyliorhinids and the petanchids *Asymbolus*, *F. boardmani*, *Galeus nipponensis*, *Galeus polli* and *Holohalaelurus regani* (121:1). A more restricted dermal cover is observed in the scyliorhinoids *Asymbolus rubiginosus* Last, Gomon & Gledhill, 1999, *At. fasciatus*, *Au. labiosus*, *Halaelurus natalensis*, *Haploblepharus edwardsii*, *Parmaturus xaniurus* and *Schroederichthys saurisqualus* and the proscylliids examined (121:0).

122. Surface of the terminal dermal cover of the clasper: (0) smooth; (1) rough (CI = 33; RI = 0) [extracted from Soares & de Carvalho (2020): ch. 65].

In taxa with a terminal dermal cover, the cover may be smooth, as in most taxa examined (122:0), or rough in texture, as observed in *Holohalaelurus regani* [Soares (2020): fig. 2C], *Scyliorhinus canicula* [Soares & de Carvalho (2020): fig. 25B] and *Scyliorhinus capensis* (122:1).

123. Degree of development of the rhipidion of the clasper: (0) reduced and in a narrow strip; (1) well developed and presenting a prominent posterior margin (CI = 12; RI = 71) [extracted from Soares & de Carvalho (2020): ch. 66].

The rhipidion is an elongated flap attached to the floor of the clasper glans, with its free edge directed laterally (Soares, 2020). It is well developed and with a prominent posterior margin in *Asymbolus* spp., *Cephaloscyllium sufflans*, *Galeus polli*, *Halaelurus* spp., *Holohalaelurus regani*, *Schroederichthys* spp. and most *Scyliorhinus* species (except *Scyliorhinus canicula*, *Scyliorhinus duhamelii* and *Scyliorhinus torazame*); a similar condition is also present in the proscylliid *E. barbouri* and the triakid *Hemitriakis japonica* (123:1). In the scyliorhinoids *Scyliorhinus canicula*, *Scyliorhinus duhamelii*, *Scyliorhinus torazame*, *Apristurus* spp., *Atelomycterus* spp., *Aulohalaelurus* spp., *Bythaelurus* spp., *F. boardmani*, *Galeus antillensis*, *Galeus nipponensis*, *Galeus sauteri*, *Haploblepharus edwardsii*, *Parmaturus*, *Pentanchus*, *Poroderma* and *Schroederichthys*, the rhipidion is reduced and not prominent, in addition to the proscylliid *Proscyllium habereri*, the triakid *I. omanensis* and the carcharhinid *L. macrorhinus* [123:0; Soares & de Carvalho (2020): fig. 26].

124. Cover rhipidion of the clasper: (0) poorly developed; (1) well developed and medially expanded (CI = 17; RI = 74) [extracted from Soares & de Carvalho (2020): ch. 68].

A cover rhipidion medially expanded that covers the clasper groove is found in the scyliorhinids the atelomycterids *Atelomycterus* and *Aulohalaelurus*, the pentanchids *Asymbolus*, *Bythaelurus*, *F. boardmani*,

Halaelurus natalensis, *Holohalaelurus regani* and *Schroederichthys* (124:1). In all other taxa examined, the cover rhipidion is poorly developed and restricted to the dorsolateral margin of the claspers (124:0; Soares, 2020).

125. Exorhipidion of the clasper: (0) poorly developed; (1) medially expanded (CI = 33; RI = 82) [extracted from Soares & de Carvalho (2020): ch. 69].

In most catsharks examined and in the proscylliids, a well-developed and medially expanded exorhipidion was observed on the claspers (125:1). A poorly developed exorhipidion restricted to the posterior portion of the ventral terminal 2 cartilage and not reaching the cover rhipidion medially is found in the scyliorhinoids *Apristurus*, *Cephalurus*, *Galeus* and *Pentanchus*, the triakids *Hemitriakis japonica* and *I. omanensis* and the carcharhinid *L. macrorhinus* (125:0).

126. Envelope of the clasper: (0) absent; (1) present (CI = 9; RI = 58) [extracted from Soares & de Carvalho (2020): ch. 70].

An envelope, described as a projected flap anterior to the exorhipidion on claspers (Soares, 2020; Soares & de Carvalho, 2020), is present in the pentanchids *Asymbolus*, *Bythaelurus*, *Figaro*, *Halaelurus natalensis*, *Parmaturus* and *Pentanchus longicephalus*, the scyliorhinids *Scyliorhinus boa*, *Scyliorhinus cervigoni*, *Scyliorhinus haeckelii* Miranda Ribeiro, 1907, *Scyliorhinus hesperius*, *Scyliorhinus retifer*, *Scyliorhinus torrei* and *Scyliorhinus ugoi* Soares, Gadig & Gomes, 2015, the atelomycterid *Schroederichthys*, the proscylliid *Proscyllium habereri* and the carcharhinid *L. macrorhinus* (126:1). This structure is absent in other taxa examined (126:0).

127. Degree of development of the envelope of the clasper: (0) poorly developed; (1) medially expanded (CI = 33; RI = 50) [extracted from Soares & de Carvalho (2020): ch. 71].

Only in *Scyliorhinus boa*, *Scyliorhinus retifer* and *Scyliorhinus hesperius* a well-developed envelope that extends medially and extends past the anterior border of the cover rhipidion is observed (127:1; Soares & de Carvalho, 2019); this condition was hypothesized by Soares & de Carvalho (2020) as a synapomorphy for the clade composed by those three species .

128. Accessory terminal cartilage of the clasper: (0) present; (1) absent (CI = 8; RI = 31) [extracted from Soares & de Carvalho (2020): ch. 72].

An accessory terminal cartilage situated at the anterior end of the clasper glans (Soares, 2020) is present in most taxa examined (128:0), except the atelomycterids *At. marmoratus* and *Au. labiosus*, the pentanchids *Galeus antillensis*, *Galeus nipponensis*, *Holohalaelurus regani*, *Parmaturus albimarginatus* and *Parmaturus xaniurus* and the scyliorhinids *Poroderma* spp., *Scyliorhinus cabofriensis* Soares, Gomes & Carvalho, 2016, *Scyliorhinus cervigoni*, *Scyliorhinus comoroensis* Compagno, 1988, *Scyliorhinus duhamelii*, *Scyliorhinus haeckelii*, *Scyliorhinus stellaris* (Linnaeus, 1758), *Scyliorhinus torrei* and *Scyliorhinus ugoi* (128:1; Soares & de Carvalho, 2019; Soares, 2020).

129. Accessory dorsal marginal cartilage of the clasper: (0) present; (1) absent (CI = 25; RI = 84) [extracted from Soares & de Carvalho (2020): ch. 73].

An accessory dorsal marginal cartilage located at the distal tip of the dorsal marginal cartilage on claspers is present in most taxa examined (129:0), with the exception of all scyliorhinids examined and the pentanchids *Cephalurus cephalus*, *Galeus antillensis*, *Galeus nipponensis* and *Galeus sauteri* (129:1; Soares & de Carvalho, 2019; Soares, 2020).

130. Dorsal marginal 3 cartilage of the clasper: (0) absent; (1) present (CI = 50; RI = 75) [extracted from Soares & de Carvalho (2020): ch. 74].

Soares (2020) stated that the presence of a dorsal marginal 3 cartilage on claspers could suggest a close relationship between *Halaelurus* and *Holohalaelurus* (130:1); illustrations of this cartilage can be found in the paper by Soares (2020: figs 10, 12). The same cartilage is also present in the carcharhinid *L. macrorhinus*.

131. Ventral marginal 2 cartilage of the clasper: (0) present; (1) absent (CI = 17; RI = 58) [extracted from Soares & de Carvalho (2020): ch. 75].

A ventral marginal 2 cartilage adjacent to the ventral marginal cartilage and opposite to the accessory dorsal marginal cartilage was observed in the scyliorhinoids *Apristurus*, *Galeus nipponensis*, *Halaelurus*, *Haploblepharus edwardsii*, *Holohalaelurus regani*, *Parmaturus xaniuris*, *Pentanchus* and *Poroderma* [Soares (2020): figs 8–15] and the proscylliid *Proscyllium habereri* (131:0). This cartilage is absent in all other taxa examined (131:1).

132. Position of the ventral marginal 2 cartilage on claspers: (0) continuous to the posterior border of the ventral marginal cartilage; (1) lateral to the posterior border of the ventral marginal cartilage (CI = 100; RI = 100) [extracted from Soares & de Carvalho (2020): ch. 76].

In taxa that possess a ventral marginal 2 cartilage, only in *Poroderma* this cartilage is lateral to the posterior border of the ventral marginal cartilage [132:1; Soares (2020): fig. 8C]. This condition was listed as a synapomorphy for the genus by Soares & de Carvalho (2020). In all other taxa, the ventral marginal 2 cartilage is continuous to the posterior border of the ventral marginal cartilage (132:0).

133. Ventral marginal 3 cartilage of the clasper: (0) absent; (1) present (CI = 50; RI = 80) [compiled from Soares (2020)].

A ventral marginal 3 cartilage dorsal to the ventral marginal 2 cartilage was observed only in claspers of *Apristurus* and *Pentanchus* species (Soares, 2020: fig. 9) and in the carcharhinid *L. macrorhinus* (133:1).

134. Dorsal terminal 2 cartilage of the clasper: (0) present; (1) absent (CI = 20; RI = 33) [extracted from Soares & de Carvalho (2020): ch. 77].

Most taxa examined (including the outgroups) possess a dorsal terminal 2 cartilage on the lateral border of the dorsal terminal cartilage (134:0), with the exception of *Ap. brunneus*, *Ap. laurussonii*, *B. dawsoni*, *Cephaloscyllium sufflans*, *Halaelurus* spp. and *Schroederichthys saurisqualus* [134:1; Soares (2020): figs 8–15].

135. Shape of the dorsal terminal 2 cartilage of the clasper: (0) elongated and rod-like; (1) rhomboidal (CI = 100; RI = 100) [extracted from Soares & de Carvalho (2020): ch. 78].

The dorsal terminal 2 cartilage consists in an elongated and rod-like structure in most taxa examined (135:0), whereas in *Scyliorhinus cabofriensis*, *Scyliorhinus capensis*, *Scyliorhinus haeckelii* and *Scyliorhinus ugoi* it is poorly developed and rhomboidal (135:1; Soares & de Carvalho, 2019; Soares, 2020). Soares & de Carvalho (2020) resolved these four *Scyliorhinus* species, forming a clade supported by the presence of a rhomboidal dorsal terminal cartilage.

136. Ventral terminal 2 cartilage of the clasper: (0) present; (1) absent (CI = 11; RI = 11) [extracted from Soares & de Carvalho (2020): ch. 79].

A ventral terminal 2 cartilage is present in the claspers of most taxa examined [136:0; Soares (2020): figs 8–15], except the scyliorhinoids *Ap. laurussonii*, *Ap. macrostomus*, *At. marmoratus*, *Cephaloscyllium sufflans*, *Cephalurus cephalus*, *Halaelurus* spp. and *Scyliorhinus comoroensis*, the proscylliid *Proscyllium habereri* and the triakid *Hemitriakis japonica* (136:1).

137. Position of the ventral terminal 2 cartilage on claspers: (0) anteriorly situated and sometimes attached to the anterior tip of the ventral terminal cartilage; (1) posteriorly situated, posterior to the half-length of the ventral terminal cartilage (CI = 100; RI = 100) [extracted from Soares & de Carvalho (2020): ch. 80].

Soares & de Carvalho (2020) reported a unique condition for *Poroderma* spp. and *Au. labiosus*, in which the ventral terminal 2 cartilage is situated in the posterior portion of the ventral terminal cartilage. However, according to the description and illustration provided by Soares (2020: fig. 11C), the ventral terminal 3 cartilage of *Au. labiosus* was misidentified as the ventral terminal 2 cartilage by those authors. The condition observed in *Poroderma* species is confirmed by our observations (137:1). In all other taxa examined that present a ventral terminal 2 cartilage, it is anteriorly situated and closer to the anterior tip of the ventral terminal cartilage (137:0).

138. Shape of ventral terminal 2 cartilage of the clasper: (0) trapezoidal or rod-like and not concave ventrally; (1) sigmoid and concave ventrally (CI = 33; RI = 60) [compiled from Soares (2020)].

In *Asymbolus galacticus* Séret & Last 2008, *As. rubiginosus*, *B. dawsoni*, *F. boardmani*, *Galeus antillensis* and *Galeus polli*, ventral terminal 2 cartilage is sigmoid in shape, concave ventrally and involves the anterior portion of terminal cartilages [138:1; Soares (2020): figs 10A, B, 12B, 13A, 14A]. In all other taxa examined, the ventral terminal 2 cartilage is trapezoidal or rounded but never sigmoid in shape (138:0).

139. Ventral terminal 3 cartilage of the clasper: (0) absent; (1) present (CI = 12; RI = 30) [compiled from Soares (2020)].

A ventral terminal 3 cartilage dorsally or posteriorly situated to the ventral terminal cartilage 2 is found in the scyliorhinoids *Asymbolus* spp., *At. fasciatus*, *Aulohalaelurus* spp., *Galeus antillensis*, *Galeus nipponensis*, *Galeus sauteri* and *Schroederichthys maculatus* Springer, 1966 and the proscylliid *E. barbouri* [139:1; Soares (2020): figs 10A, B, 11B, C, 13A, D].

140. Extension of the clasper siphon: (0) extending beyond the half distance between the coracoid and cloaca; (1) shorter than half the distance between the coracoid and cloaca (CI = 25; RI = 87) [extracted from Soares & de Carvalho (2020): ch. 81].

Long clasper siphons extending beyond half the distance between the coracoid and cloaca were observed in the catsharks *Asymbolus*, *Atelomycterus*, *Aulohalaelurus*, *Cephalurus*, *Figaro*, *Halaelurus*, *Haploblepharus*, *Parmaturus* and *Schroederichthys* and all other carcharhinoids examined (140:0), except *Triakis semifasciata*. In the latter *Triakis semifasciata* and in all scyliorhinids and the pentanchids *Apristurus*, *Galeus antillensis*, *Galeus polli*, *Holohalaelurus regani* and *Pentanchus*, clasper siphons are shorter than half the distance between the coracoid and cloaca [140:1; Soares & de Carvalho (2020): fig. 28].

Colour pattern

141. Colour pattern composed of saddles: (0) present; (1) absent (CI = 10; RI = 75) [extracted from Soares & de Carvalho (2020): ch. 82].

In the orectoloboids, the proscylliid *Proscyllium habereri* and the scyliorhinoids *Akheilos*, *Asymbolus*, *Atelomycterus*, *Aulohalaelurus*, *Cephaloscyllium*, *Figaro*, *Halaelurus*, *Haploblepharus*, *Holohalaelurus*, *Schroederichthys bivius* (Smith, 1838), *Schroederichthys saurisqualus* and most *Scyliorhinus*

species (except *Scyliorhinus duhamelii* and *Scyliorhinus garmani*), transverse bands darker than the background colour, known as saddles, are found over most of the body dorsolateral surface (141:0; Compagno & Stevens, 1993a; Last *et al.*, 1999; Human, 2006b, 2007; Gledhill *et al.*, 2008; Last & Séret, 2008; Last & White, 2008; Soares & de Carvalho, 2019). Saddles are absent in all other taxa examined [141:1; Compagno & Stevens (1993b); Soares & de Carvalho (2020): fig. 29].

142. Black spots over the body dorsolateral surfaces: (0) present; (1) absent (CI = 6; RI = 51) [extracted from Soares & de Carvalho (2020): ch. 83].

Black spots on body dorsolateral surfaces are observed in the orectoloboids, the proscylliid *Proscyllium habereri* and the scyliorhinoids *Akheilos*, *Asymbolus*, *Atelomycterus*, *Aulohalaelurus*, *Cephaloscyllium*, *Galeus antillensis*, *Galeus nipponensis*, *Galeus sauteri*, *Halaelurus sellus*, *Holohalaelurus*, *Poroderma pantherinum*, *Schroederichthys bivius*, *Schroederichthys saurisqualus* and most *Scyliorhinus* species (except *Scyliorhinus capensis*, *Scyliorhinus comoroensis*, *Scyliorhinus hesperius*, *Scyliorhinus meadi* Springer, 1966, *Scyliorhinus torazame* and *Scyliorhinus torrei*) (142:0; Compagno & Stevens, 1993a, b; Last *et al.*, 1999; Human, 2006a, b, 2007; Gledhill *et al.*, 2008; Last & White, 2008; Nakaya *et al.*, 2013; Soares & de Carvalho, 2019, 2020). All other taxa examined lack black spots over the body (142:1; Compagno & Stevens, 1993b; Nakaya & Sato, 1999; Nakaya & Séret, 2000).

143. Black stripes over the body dorsolateral surfaces: (0) absent; (1) present (CI = 50; RI = 0) [extracted from Soares & de Carvalho (2020): ch. 84].

Among taxa examined, only in *Poroderma africanum* and *Scyliorhinus retifer* are black stripes found (143:1; Human, 2006a; Soares & de Carvalho, 2019).

Table 3. Summary of maximum parsimony analyses

Dataset	Weighting	Fit	Number of trees	Total steps
1	Equal	88.4	1	550.7
1	Implied	89.9	7	560.6
2	Equal	239	3	3833
3	Equal	320.6	270	4416
3	SEP	321.6	133	4422
4	Equal	326.2	6	4444.2
4	SEP	327.8	1	4441.8
4	BLK	336	1	4458.6

SEP, each column weighted separately according to its own homoplasy; BLK, all characters of each molecular block weighted according to the average homoplasy of the whole marker.

Comparisons among analyses and datasets

The complete dataset presents 1187 characters, of which 143 are morphological and 1044 molecular characters; 463 of the 1044 molecular characters are phylogenetically informative. Most-parsimonious trees have between 4446.2 (equal weighing) and 4459 (extended implied weighting) steps (Table 3). Here, we chose the cladistic analysis weighting each column separately (SEP, $k = 3$) and including morphological and molecular data as the preferred hypothesis of catshark relationships, considering its greatest internal resolution of clades and stronger support. This analysis resulted in one most-parsimonious tree with 4441 steps, CI = 0.26 and RI = 0.54 (Fig. 16). The average consistency index (CI) of the morphological characters in the combined dataset is 0.41, and 45 of the 143 characters present CI values ≥ 0.5.

Examination of phylogenetic incongruence among the datasets, as measured by the incongruence–length difference test, is presented in Figure 17. Comparisons between the morphological data partition (excluding quantitative characters) and DNA did not result in a significant *P*-value, but a significant incongruence was detected between quantitative and molecular datasets ($P < 0.05$). This heterogeneity might explain the incongruences observed in tree topologies yielded when morphological (set 1) and *NADH2* (set 2) characters are analysed separately (Fig. 17). Nevertheless, resulting topologies from both datasets do not differ with regard to the position and scope of Scyliorhinidae (new definition). The inclusion of meristic characters improved the resolution between *Aulohalaelurus* and *Atelomycterus* species and of infrageneric relationships of *Cephaloscyllium* and *Parmaturus* (Figs 18, 19). Most analyses recovered the family Scyliorhinidae *s.l.* as paraphyletic, separated into three different lineages: (1) *Cephaloscyllium*, *Poroderma* and *Scyliorhinus*; (2) *Atelomycterus*, *Aulohalaelurus* and *Schroederichthys*; and (3) *Akheilos*, *Apristurus*, *Asymbolus*, *Bythaelurus*, *Cephalurus*, *Figaro*, *Galeus*, *Halaelurus*, *Haploblepharus*, *Holohalaelurus*, *Parmaturus* and *Pentanchus* (Figs 16, 17). Of the 13 genera represented by more than one species, ten are hypothesized to be monophyletic.

Total-evidence most-parsimonious trees from the different searches (EQW, SEP and BLK) were highly congruent, differing in the internal resolution of Scyliorhinidae, *Cephaloscyllium* and *Scyliorhinus*, the relationships within *Bythaelurus* and the placement of *Akheilos* (Figs 18, 19). In the topologies yielded under $k < 7$ (Fig. 18A, B), *Scyliorhinus* is resolved as more closely related to *Cephaloscyllium* than to *Poroderma*, whereas the opposite is recovered under $k > 10$ (Fig. 18C). In

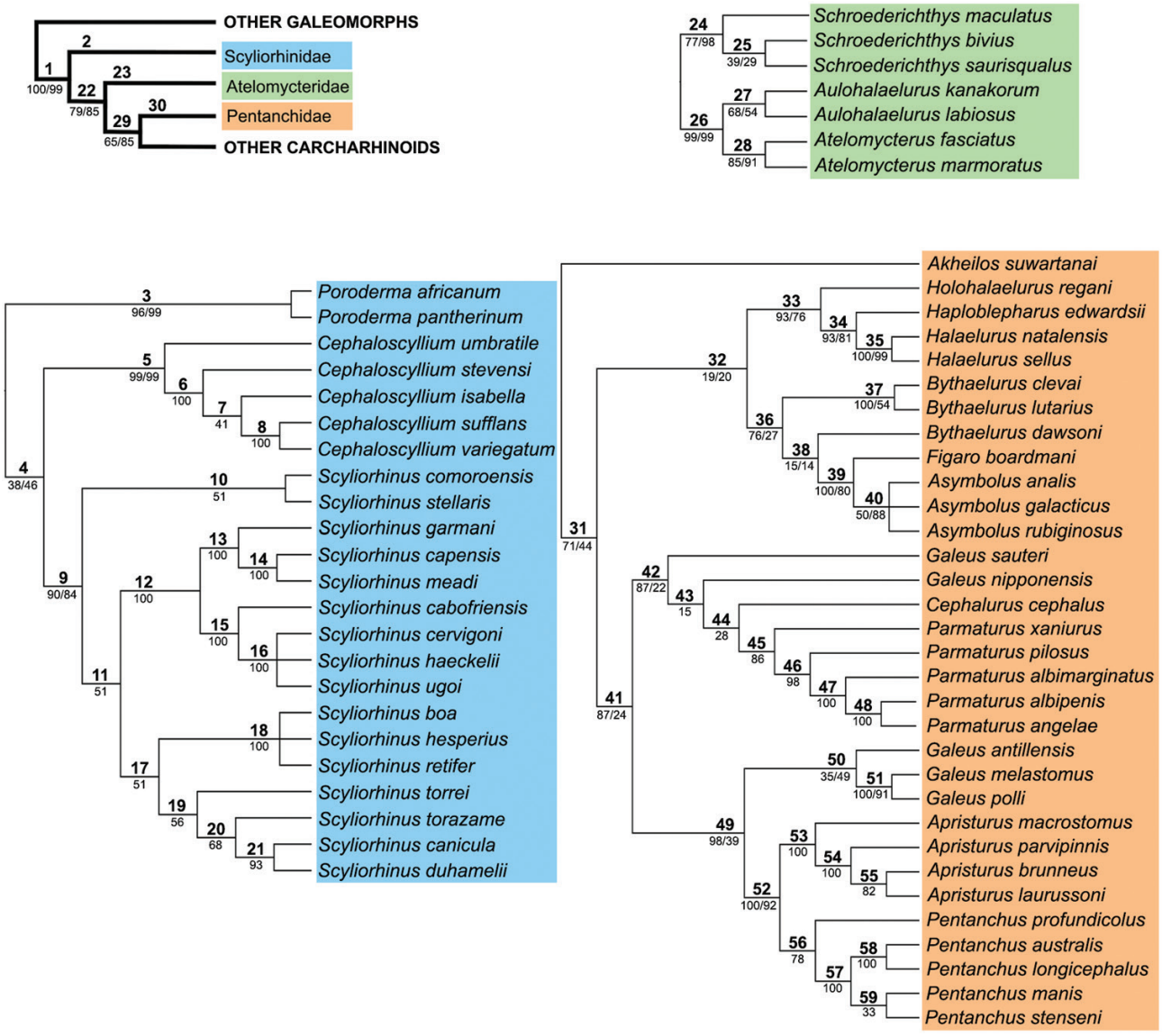

Figure 16. Most-parsimonious tree (length = 4459 bp, consistency index = 0.26, retention index = 0.54) resulting from the combined meristic, *NADH2*, morphological data partitions under extended implied weighting (SEP, each column weighted separately according to its own homoplasy $k = 3$). Numbers above branches correspond to the clades discussed throughout the text. Relative Bremer supports and GC values (differences of frequencies "Group present/Contradicted") are shown below branches. Key: blue, Scyliorhinidae; green, Atelomycteridae; orange, Pentanchidae.

addition, relationships among species of *Scyliorhinus* differ deeply with different k values (Fig. 18). *Cephaloscyllium isabella* and *Cephaloscyllium stevensi* are resolved as a sister group with $k < 3$ (Fig. 18A), whereas *Cephaloscyllium isabella* is recovered as a sister group of *Cephaloscyllium variegatum* + *Cephaloscyllium sufflans* with $k > 3$ (Fig. 18B, C). In all searches under different weighting schemes and strengths, the monophyly of *Galeus* was potentially compromised by the placement of *Galeus sauteri* and *Galeus nipponensis* as more closely related to *Cephalurus* and *Parmaturus* species than to other species of *Galeus* (Fig. 19). *Bythaelurus* is resolved as monophyletic only when k values higher than seven are considered (Fig. 19B, C); with $k < 7$, its monophyly is compromised by the placement of *B. dawsoni* in a closer relationship to *Figaro* and *Asymbolus* than to *B. clevai* and *Bythaelurus lutarius* (Springer & D'Aubrey, 1972) (Fig. 19A). *Akheilos* is placed at the base of Pentanchidae in most analyses (Fig. 19A, B); with $k > 10$, *Akheilos* is resolved as closely related to *Bythaelurus*, *Figaro* and *Asymbolus* (Fig. 19C).

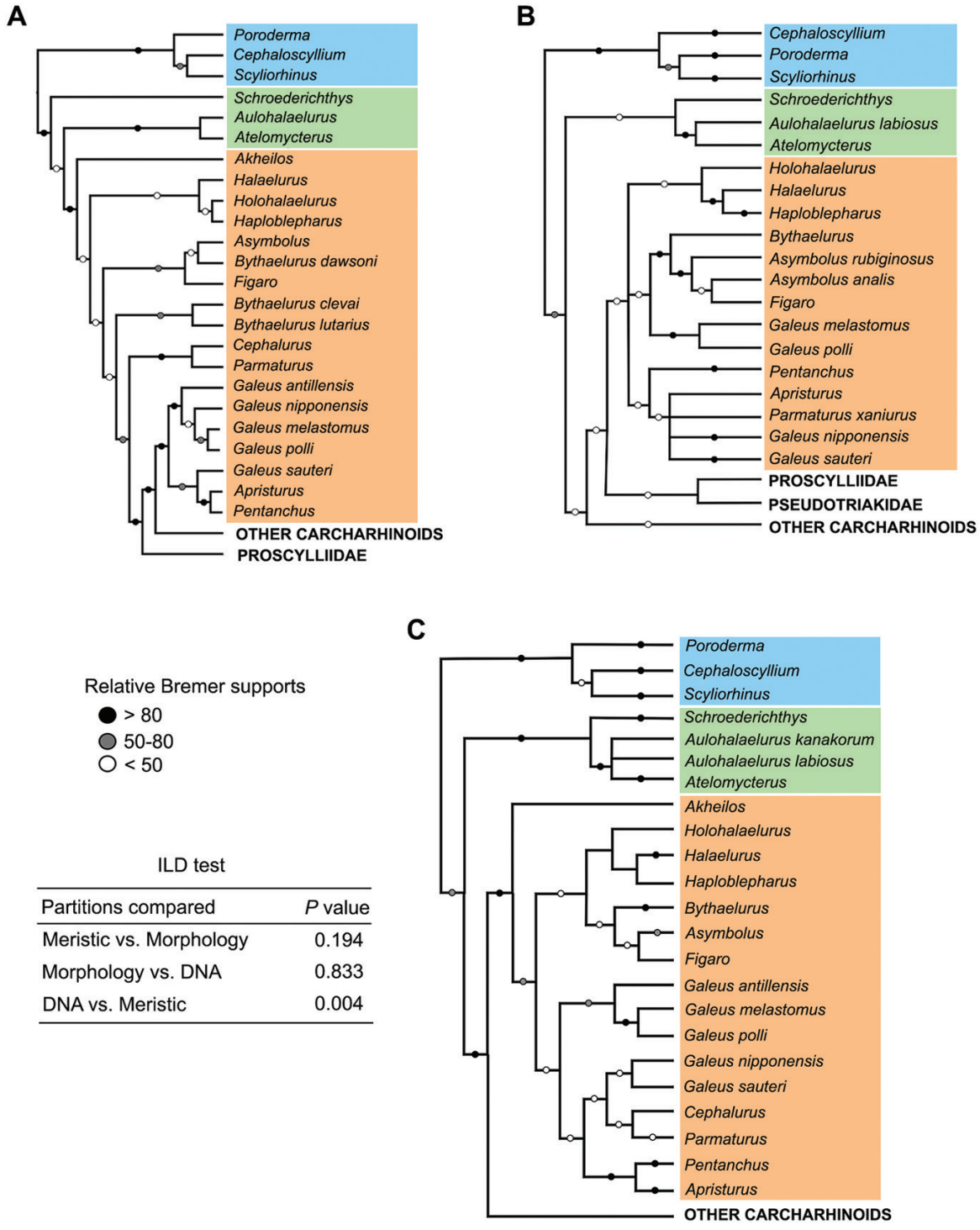

ILD test

Partitions compared	*P* value
Meristic vs. Morphology	0.194
Morphology vs. DNA	0.833
DNA vs. Meristic	0.004

Figure 17. Strict consensus of analyses using different datasets. A, morphological data (qualitative and quantitative) under implied weighting ($k = 3$). B, molecular data under equal weighting. C, qualitative morphological characters plus DNA sequences under extended implied weighting (SEP, each column weighted separately according to its own homoplasy $k = 3$). Key: blue, Scyliorhinidae; green, Atelomycteridae; orange, Pentanchidae. The *P*-values of partitions compared through the incongruence–length difference test are displayed in the inset table.

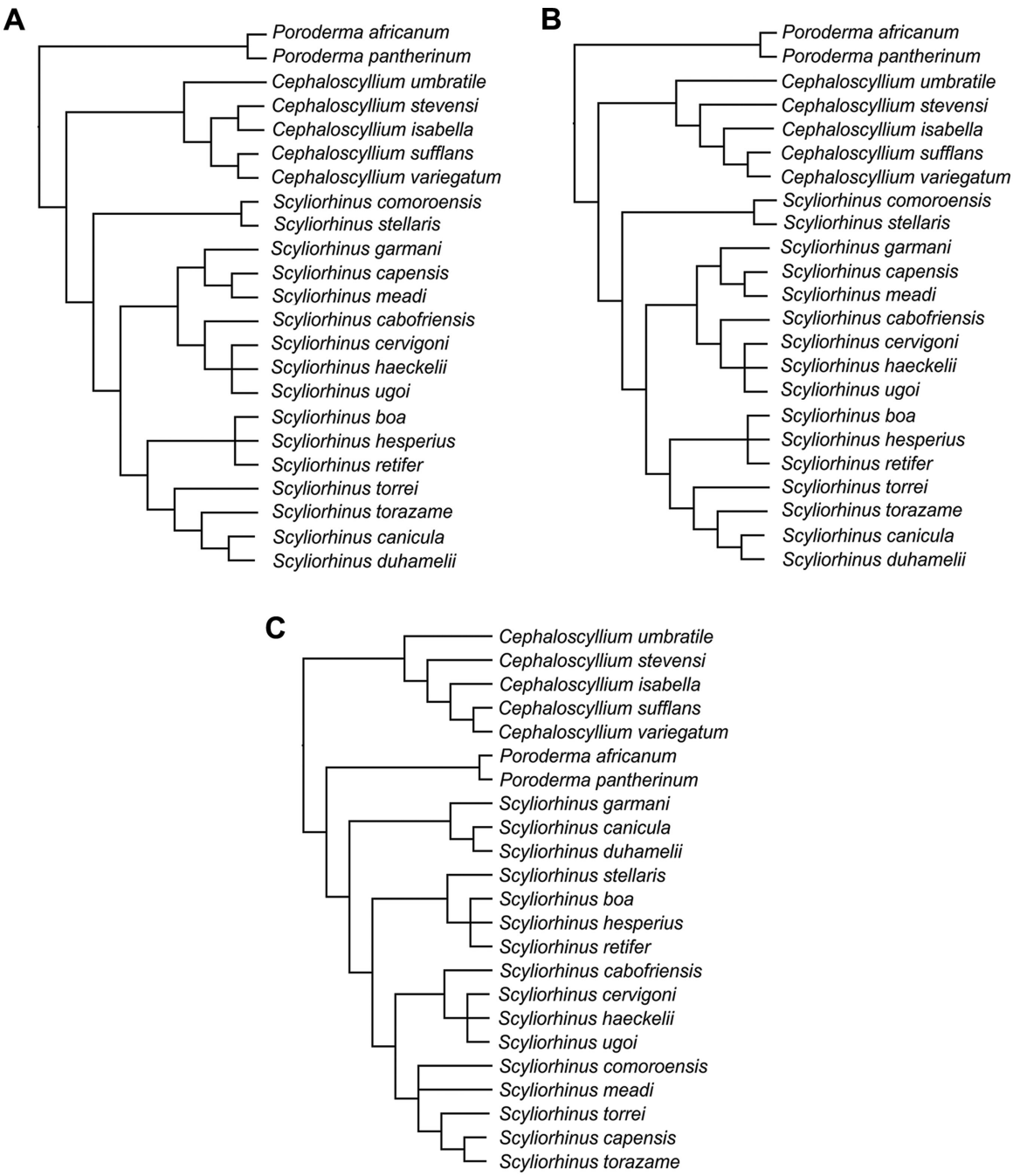

Figure 18. Phylogenetic relationships within Scyliorhinidae with different *k*-values. A, extended implied weighting ($k = 1$). B, extended implied weighting ($k = 7$). C, extended implied weighting ($k > 10$).

Phylogenetic reconstruction

Here, we list the non-ambiguous synapomorphies of clades resulting from our analyses, mostly focused on the total-evidence hypothesis, beginning in Carcharhiniformes (clade 1; Fig. 16) and continuing to include all catsharks families and genera as proposed herein (Table 2). Numbers of the morphological characters that support each node are given in parentheses along with their respective states (values for quantitative characters correspond to the meristic counts unstandardized; see Supporting Information, Supplementary Material 2). Complete lists of all synapomorphies of clades (including molecular characters), as numbered in Figure 16, and of morphological character transformations are presented in the Supporting Information (Supplementary

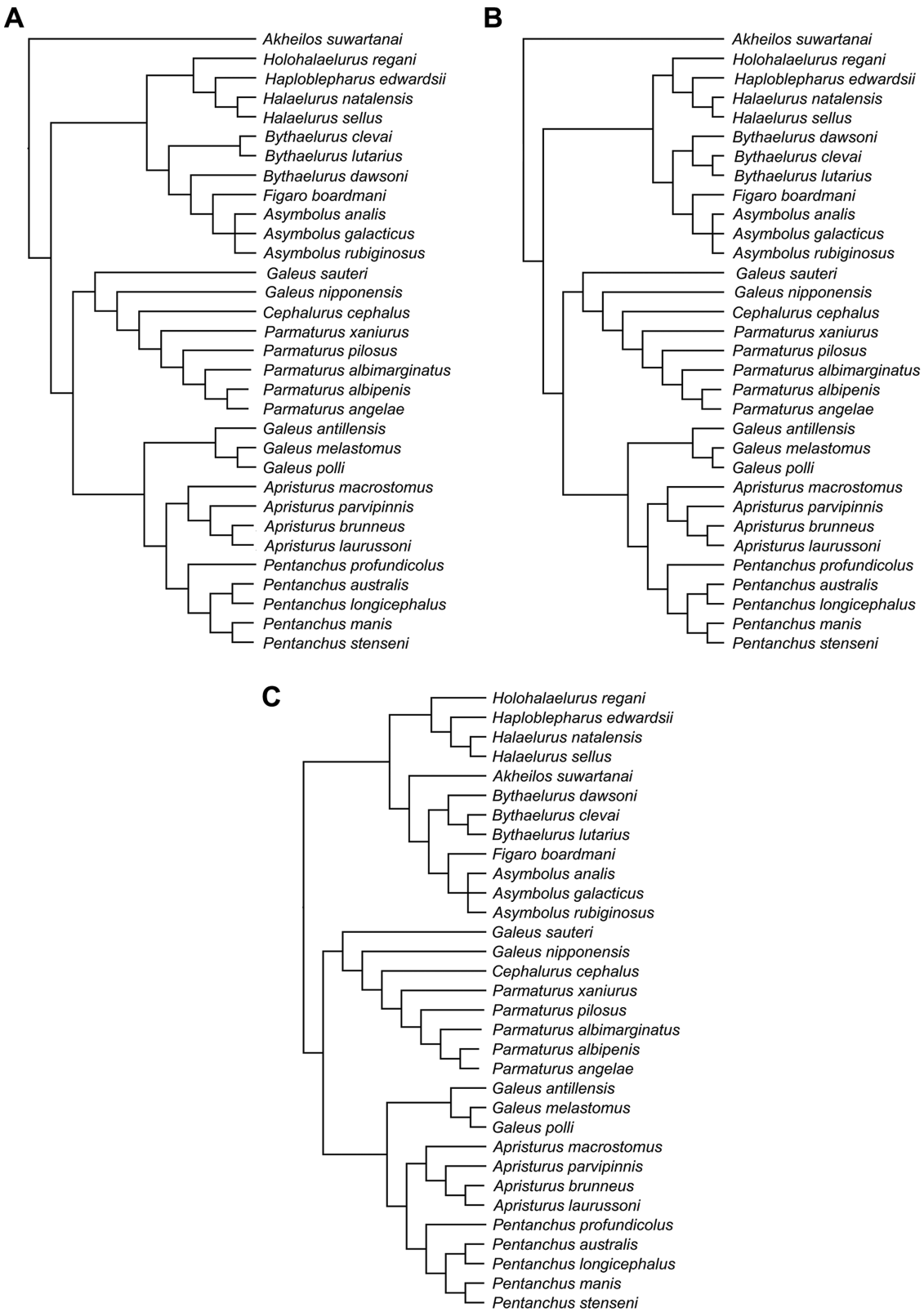

Figure 19. Phylogenetic relationships within Pentanchidae with different k-values. A, extended implied weighting (k = 1). B, extended implied weighting (k = 7). E, extended implied weighting (k > 10).

Materials 5 and 6, respectively). The general topology depicting relationships among all analysed terminal taxa (including outgroups) is available in the Supporting Information (Supplementary Material 7).

Clade 1, Carcharhiniformes: The monophyly of the order Carcharhiniformes is supported by ten synapomorphies: lower diplospondylous vertebrae counts (2:69–142), higher upper (3:25–110) and lower tooth counts (4:22–115), lower number of pectoral radials (8:11–25), presence of a nictitating lower eyelid (37:1) and muscles levator and retractor palpebrae nictitantis (52:1), ectodermal pits on dermal denticles (49:1), muscle bundles of coracohyoideus separated throughout their extension (61:2), muscle epaxialis posterior to the parietal fossa (65:1) and foramen for glossopharyngeal nerve on the posterior wall of otic capsule (89:1).

Clade 2, Scyliorhinidae: This family is resolved as the most basal group in Carcharhiniformes and sister group of all remaining ground sharks. Scyliorhinidae is restricted here to include only the genera *Cephaloscyllium*, *Poroderma* and *Scyliorhinus* (Figs 16, 17; Table 2). In all analyses, the monophyly of this family is supported strongly by a lower diplospondylous vertebral count (2:69–96), rostral cartilages not fused (68:1), presence of a thyroid foramen on the basihyal (101:1) and of three extrabranchial ventral cartilages (107:1). Differences in the relationships amongst *Cephaloscyllium*, *Poroderma* and *Scyliorhinus* were observed in hypotheses generated from different datasets (Figs 16, 17). Considering only molecular characters, *Cephaloscyllium* is resolved as the sister group of *Poroderma* + *Scyliorhinus* (Fig. 17B). Both combined and morphological datasets retrieved a closer relationship between *Cephaloscyllium* and *Scyliorhinus* rather than *Poroderma* (Figs 16, 17A, C). The monophyly of the three scyliorhinid genera is well supported in all analyses (Figs 16, 17).

Clade 3, Poroderma: The monophyly of *Poroderma* is supported by an anterior nasal flap divided into lateral and medial portions (12:1), nasal barbel present (15:1), presence of lateral processi rastriformis (104:1), oropharyngeal denticles well developed along epi- and ceratobranchials (105:1), medial border of the exorhipidion covered by clasper hooks (119:1), claspers with a ventral marginal 2 cartilage (131:0), no accessory terminal cartilage on clasper (128:1) and ventral terminal 2 cartilage posteriorly situated on the clasper (137:1).

Poroderma africanum is characterized by the following autapomorphies: presence of a projected flap on the upper lip margin (27:1; independently acquired in *Scyliorhinus* spp.), muscle coracomandibularis inserting on anteromedial borders of Meckel's cartilage (60:1), presence of an accessory cartilage on mandibular symphysis (96:1; also present in *Pentanchus longicephalus*), black spots absent (142:1) but black stripes present over the body (143:1). *Poroderma pantherinum* is characterized by a lower number of hyomandibular pores (6:13).

Clade 4: A close relationship between *Cephaloscyllium* and *Scyliorhinus* (Fig. 16) is supported by a mesonarial crest on the anterior nasal flap (14:1), one upper labial cartilage (30:1) and a well-developed medial projection of the coracoid bar (115:1).

Clade 5, Cephaloscyllium: The monophyly of *Cephaloscyllium* (Fig. 16) is supported strongly by a higher monospondylous vertebral count (1:44), upper (3:68–70) and lower (4:65–68) tooth row counts, absence of a lower labial furrow (24:1), presence of a postoral groove (31:1), origin of the second dorsal fin anterior to the vertical line that passes through the mipoint of the anal fin base (43:1) and muscle bundles of coracohyoideus widely separated (60:1).

Cephaloscyllium umbratile is resolved as the most basal species of the genus under all k values and characterized by higher numbers of diplospondylous vertebrae (2:110–131), upper (3:77–110) and lower tooth counts (4:71–102). Under $k < 3$, all other species of *Cephaloscyllium* (clade 6) are successively related and share lower counts of diplospondylous vertebrae (2:69–91). *Cephaloscyllium stevensi* has no autapomorphies and is hypothesized as a sister group of the clade formed by *Cephaloscyllium isabella*, *Cephaloscyllium variegatum* and *Cephaloscyllium sufflans* (clade 7), which is supported by a higher number of monospondylous vertebrae (1:44–58). *Cephaloscyllium isabella* is characterized by a lower number of diplospondylous vertebrae (2:71–72) and higher counts of hyomandibular pores (6:3). A sister-group relationship between *Cephaloscyllium variegatum* and *Cephaloscyllium sufflans* (clade 8) is hypothesized by the presence of oropharyngeal denticles large and forming rows on the internal face of gill components (105:1). *Cephaloscyllium sufflans* is characterized by a higher number of monospondylous vertebrae (1:49), whereas *Cephaloscyllium variegatum* has no autapomorphies.

Clade 9, Scyliorhinus: The genus *Scyliorhinus* is resolved as monophyletic in all analyses (Figs 16, 17) and diagnosed by the presence of a projected flap on the upper lip margin (27:1), a pelvic apron (40:1), an epiphyseal notch on the neurocranium (78:1) and an elongated and sling-like gill pickax (106:1). A sister-group relationship between *Scyliorhinus comoroensis*

and *Scyliorhinus stellaris* is hypothesized (clade 10) and supported by the absence of an accessory terminal cartilage on the clasper (128:1); both species are placed at the base of the genus and resolved as the sister group of all remaining congeners (clade 11; Fig. 16). *Scyliorhinus comoroensis* is characterized by a higher number of diplospondylous vertebrae (2:97) and absence of a ventral terminal 2 cartilage (136:1) and of dark spots over the body (142:1), whereas no unique autapomorphy was found for *Scyliorhinus stellaris*.

Clade 11 is supported by a lower number of upper teeth (3:39–76), and its component species are divided into two clades (clades 12 and 17; Fig. 16). The monophyly of the clade formed by *Scyliorhinus garmani*, *Scyliorhinus meadi*, *Scyliorhinus capensis*, *Scyliorhinus cabofriensis*, *Scyliorhinus cervigoni*, *Scyliorhinus haeckelii* and *Scyliorhinus ugoi* (clade 12) is supported by the presence of a rhomboidal dorsal terminal 2 cartilage of the clasper (135:1). Within clade 12, two clades are hypothesized (Fig. 16): one composed by *Scyliorhinus garmani*, *Scyliorhinus capensis* and *Scyliorhinus meadi* (clade 13) and supported by a high number of monospondylous vertebrae (1:44–48) and another formed by *Scyliorhinus cabofriensis*, *Scyliorhinus cervigoni*, *Scyliorhinus haeckelii* and *Scyliorhinus ugoi* (clade 15) and characterized by lower values of intestinal valve counts (5:6–8) and the accessory terminal cartilage absent on the clasper (128:1). *Scyliorhinus garmani* is hypothesized as a sister group of the clade formed by *Scyliorhinus capensis* and *Scyliorhinus meadi* (clade 14), which is supported by the absence of black spots over the body (142:1). *Scyliorhinus garmani* is characterized by a higher number of monospodylous vertebrae (1:48), lower values of diplospondylous vertebral counts (2:83) and lower tooth counts (4:44), a long anterior nasal flap (11:1) and a colour pattern that lacks saddles (141:1). *Scyliorhinus meadi* has no autapomorphies, and *Scyliorhinus capensis* is characterized by well-developed pelvic aprons (41:2) and a rough terminal dermal cover on the posterior tip of the claspers (122:1). *Scyliorhinus cabofriensis* is resolved as a sister group of the clade formed by *Scyliorhinus cervigoni*, *Scyliorhinus haeckelii* and *Scyliorhinus ugoi* (clade 16) and presents no autapomorphies. An unsolved polytomy is observed among species of clade 16, which is supported by the presence of an envelope on the clasper (126:1). *Scyliorhinus cervigoni* is characterized by a higher number of pectoral radial counts (8:17) and cover rhipidion of the clasper lacking dermal denticles (118:0); *Scyliorhinus ugoi* presents a lower number of pectoral radials (8:13–14), and *Scyliorhinus haeckelii* has no unique autapomorphies.

The remaining species compose clade 17. Its monophyly is supported only by molecular characters (Fig. 16). The monophyly of the clade formed by *Scyliorhinus boa*, *Scyliorhinus hesperius* and *Scyliorhinus retifer* (Fig. 16) is supported by the absence of dermal denticles on cover rhipidion of the clasper (118:0) and the presence of a medially expanded envelope of the clasper (127:1). *Scyliorhinus hesperius* is characterized by lower hyomandibular pore counts (7:5–6) and dark spots absent (142:1), whereas *Scyliorhinus retifer* is characterized by the presence of black stripes over the body (143:1); no unique autapomorphies were found for *Scyliorhinus boa*. The monophyly of clade 19 (*Scyliorhinus torrei*, *Scyliorhinus torazame*, *Scyliorhinus canicula* and *Scyliorhinus duhamelii*; Fig. 16) is supported by a lower number of monospondylous vertebrae (1:30–40) and intestinal valve counts (5:4–8) and pelvic inner margins almost entirely fused in a pelvic apron (41:2). *Scyliorhinus torrei* is hypothesized as the sister group of the clade formed by *Scyliorhinus torazame*, *Scyliorhinus canicula* and *Scyliorhinus duhamelii* (clade 20) and characterized by lower values of upper tooth counts (3:33–42) and an accessory terminal cartilage of the clasper absent (128:1). The monophyly of clade 20 is supported by a poorly developed rhipidion (123:0). The autapomorphies found for *Scyliorhinus torazame* were a higher number of upper tooth counts (3:50–76) and lower intestinal valve counts (5:6–7), and this species is hypothesized as a sister group of *Scyliorhinus canicula* and *Scyliorhinus duhamelii* (clade 21). A close relationship between *Scyliorhinus canicula* and *Scyliorhinus duhamelii* is supported by anterior nasal flaps long (11:1) and closely spaced (12:1), posterior nasal flap laterally situated to the excurrent aperture (18:1), nasoral groove present (20:1) and well-developed lower labial furrows (25:0). *Scyliorhinus canicula* is characterized by a higher number of intestinal valves (5:10–11) and a rough terminal dermal cover on clasper (122:1). Two autapomorphies were found for *Scyliorhinus duhamelii*: absence of an accessory terminal cartilage (128:1) and colour pattern that lacks saddles (141:1). Despite the great differences observed in the internal resolution of *Scyliorhinus* with higher k values, some groupings do not change, such as the clade formed by *Scyliorhinus cabofriensis*, *Scyliorhinus cervigoni*, *Scyliorhinus haeckelii* and *Scyliorhinus ugoi*, the clade formed by *Scyliorhinus boa*, *Scyliorhinus hesperius* and *Scyliorhinus retifer*, and the sister-group relationship between *Scyliorhinus canicula* and *Scyliorhinus duhamelii* (Fig. 18).

Clade 22: All carcharhiniforms except scyliorhinids are hypothesized to form a clade (suborder Carcharhinoidei; Table 2), supported by a higher

number of upper teeth (3:25–130) and the presence of a muscle depressor palpebrae nictitantis (53:1) and of an elongated and sling-like gill pickax (106:1).

Clade 23, Atelomycteridae: A close relationship among *Schroederichthys*, *Atelomycterus* and *Aulohalaelurus* was recovered in most analyses, except for the morphological dataset (Fig. 17A). In the total-evidence hypothesis (Fig. 16), these genera share an anterior border of the basihyal bifurcated (103:1) and lateral processi rastriformis present (104:1; independently acquired in the new subfamily Halaelurinae). The genus *Schroederichthys* is hypothesized as a sister group of the clade formed by *Atelomycterus* and *Aulohalaelurus* (clade 26; Fig. 16).

The monophyly of *Schroederichthys* (clade 24; Fig. 16) is supported by the following synapomorphies: lower monospondylous vertebral count (1:29–40), anterior nasal flap slender and partly covering the excurrent aperture (10:1) and separated into two portions (13:1), mesonarial crest present (14:1), one labial cartilage (30:1), muscles coracobranchialis II, III and IV originating from the pericardial membrane (63:0), absence of a fenestra for the infraorbital canal of the lateral line (85:1), thyroid foramen present (101:1), lateral processes on pectoral girdle (116:0) and envelope present on the clasper (126:1). *Schroederichthys maculatus* is resolved as a sister group of *Schroederichthys bivius* and *Schroederichthys saurisqualus* (clade 25), which is supported by a higher number of mandibular pores (6:12–18). *Schroederichthys maculatus* is characterized by a lower number of monospondylous vertebral (1:29–32) and pectoral radial counts (8:13) and colour pattern not composed of saddles (141:1). *Schroederichthys bivius* presents a higher number of pectoral radials (8:17). *Schroederichthys saurisqualus* has a higher number of mandibular pores (6:17–18), orbital process of palatoquadrate closer to half-length of each antimere (93:1), no medial projection on coracoid bar (114:1) and dorsal terminal cartilage 2 of the clasper absent (134:1).

Clade 26, Atelomycterinae: A closer relationship between *Atelomycterus* and *Aulohalaelurus* is hypothesized in all analyses (Figs 16, 17) and is supported by higher numbers of monospondylous (1:39–47) and diplospondylous (2:93–115) vertebrae, higher values for upper tooth counts (3:50–89), absence of a posterior nasal flap (16:1), upper (23:0) and lower (25:0) labial furrows longer than half of mouth width, labial furrows continuous (28:1), rostral cartilages not fused (68:1), internal carotid foramina well separated (82:2) and labial ridge present on the quadrate process (90:0). When only morphological characters are considered (Fig. 17A), this clade is resolved as more closely related to the other carcharhinoids than to *Schroederichthys* by the following synapomorphies: labial furrows continuous and fused laterally (28:1), two median ridges on dermal denticles (51:1), incurrent nasal aperture anterior to excurrent one (74:0) and presence of a labial ridge on the quadrate process (90:0).

The monophyly of *Aulohalaelurus* (clade 27) is supported by a narrow postorbital groove on the neurocranium (84:1). *Aulohalaelurus kanakorum* is characterized by one autapomorphy (higher number of diplospondylous vertebrae; 2:93–106), whereas *Au. labiosus* presents a lower number of pectoral radials (8:14) and no accessory terminal cartilage of the clasper (128:1). The monophyly of *Atelomycterus* (clade 28) is supported by higher diplospondylous vertebral counts (2:110–115), a well-developed anterior nasal flap entirely covering the excurrent aperture, posterior nasal flap and upper lip (11:1), anterior nasal flaps close to each other (12:1) and presence of a nasoral groove (20:1). *Atelomycterus marmoratus* is characterized by a higher number of monospondylous vertebral (1:44–47) and lower tooth counts (4:67) and accessory terminal ventral of the clasper absent (128:1). No unique synapomorphies were found for *Au. labiosus*.

Clade 29: In the total-evidence and molecular-only analyses, a close relationship between pentanchids and higher carcharhinoids is hypothesized and supported by lower values for intestinal valve counts (5:4–21), higher values for hyomandibular pore counts (7:4–15), external nasal cartilage fused to the dorsal position of the nasal capsule (75:1) and cover rhipidion of the clasper poorly developed (124:0).

Clade 30, Pentanchidae: The monophyly of Pentanchidae is supported in most analyses by continuous labial furrows (28:1) and ectodermal pits extending through more than half the length of the crown surface of dermal denticles (50:1). Analysing only morphological characters, the monophyly of Pentanchidae is compromised by the inclusion of other carcharhinoid families (Fig. 17A). Differences in the phylogenetic placement of the family Proscylliidae are observed when comparing the hypotheses yielded by different datasets; when morphological and molecular data are analysed separately, proscylliids are resolved as more closely related to pentanchids than to other carcharhinoids (Figs 17A, B). *Akheilos suwartanai* is resolved as closely related to the remaining pentanchid catsharks in all analyses (clade 31; Figs 16, 17A) and is characterized by the presence of an envelope on the clasper (126:1). Two main clades are observed within Pentanchidae when all data are combined (Fig. 16): clades 32 (*Holohalaelurus*, *Haploblepharus*, *Halaelurus*, *Bythaelurus*, *Asymbolus* and *Figaro*) and

41 (*Apristurus*, *Cephalurus*, *Galeus*, *Parmaturus* and *Pentanchus*). Regarding the morphological dataset, a basal clade comprising *Holohalaelurus*, *Halaelurus* and *Haploblepharus* is hypothesized to be the sister group of all remaining pentanchids successively related to other carcharhinoids (Fig. 17A). When only molecular characters are analysed, three clades are recovered, with the split of clade 31 into two different clades and equally related to the remaining pentanchids (Fig. 17B).

Clade 32, ***Halaelurinae subfam. nov.****:* The monophyly of this clade is supported by the presence of a thyroid foramen on the basihyal (101:1) and of lateral processi rastriformis (104:1). *Holohalaelurus*, *Haploblepharus* and *Halaelurus* (clade 33; Fig. 16) share a lower monospondylous vertebral (1:28–40) and intestinal valve (5:6–7) counts, muscle coracobranchialis II, III and IV originating from the pericardial membrane (63:0), accessory cartilage of basibranchial copula corresponding to one-third of the cardiobranchial cartilage (109:1) and presence of dorsal marginal 3 (130:1) and ventral marginal 2 cartilages on the clasper (131:0). When only morphological characters are considered, *Haploblepharus* is resolved as more closely related to *Holohalaelurus* than to *Halaelurus* (Fig. 17A), and this relationship is supported by a median rostral cartilage confluent with the anterior fontanelle (72:1), two Meckelian condyles on the articular region of the quadratomandibular joint (98:1) and medial projection of the coracoid bar absent (114:1). *Holohalaelurus regani* is hypothesized as a sister group of *Haploblepharus* + *Halaelurus* when molecular-only and combined datasets are analysed (Figs 16, 17B); this species is characterized by a higher number of lower teeth (4:62–67), absence of upper (22:1) and lower (24:1) labial furrows, upper labial cartilages absent (29:1), pelvic apron present (40:1), presence of a connective tissue adjacent to the basihyal (100:1), long (121:1) and rough (122:1) terminal dermal cover on the clasper, accessory terminal cartilage of the clasper absent (128:1) and short clasper siphons (140:1).

A closer relationship between *Haploblepharus* and *Halaelurus* (clade 34; Fig. 16) is supported by a muscle coracomandibularis inserting on the anteromedial borders of Meckel's cartilage (60:0), lateral processes present on the pectoral girdle (116:0) and the dorsomedial surface of clasper glans with no dermal denticles (117:1). *Haploblepharus edwardsii* is characterized by the following autapomorphies: higher number of upper teeth (3:66–75), anterior nasal flaps long (11:1) and closely spaced (12:1), posterior nasal flap absent (16:1), nasoral groove present (20:1), long lower labial furrow (25:1), crown surface of dermal denticles almost entirely covered by ectodermal pits (50:1), muscle interhyoideus extending to half the length of Meckel's cartilage (64:1), distance between internal carotid foramina greater than the distance between internal carotid and stapedial foramina (82:0), orbital process of palatoquadrate and ethmoidal region of neurocranium near to each other (95:1), accessory cartilage present on mandibular symphysis (96:1) and thyroid foramen present (101:1).

Halaelurus species (clade 35; Fig. 16) share lower values for upper (3:55–56) and lower (4:46–47) tooth counts, muscle bundles of muscle coracohyoideus distant from each other (62:1), distance between internal carotid foramina equal to the distance between internal carotid and stapedial foramina (82:2), lateral processi rastriformis present (104:1) and the absence of dorsal terminal 2 (134:1) and ventral terminal 2 (136:1) cartilages on the clasper. *Halaleurus natalensis* is characterized by a higher number of hyomandibular pores (7:25) and envelope present on the clasper (126:1), whereas *Halaelurus sellus* is characterized by lower numbers of upper (3:55) and lower (4:46) tooth counts and hyomandibular pores (7:16–18) and two median ridges on dermal denticles (51:1).

The clade composed by *Bythaelurus*, *Asymbolus* and *Figaro* (clade 36; Fig. 16) is supported by the presence of an envelope (126:1). The monophyly of *Bythaelurus* is potentially compromised by the placement of *B. dawsoni* more closely related to *Figaro* and *Asymbolus* than to its congeners. In the morphology-only dataset (Fig. 17A), *B. clevai* and *B. dawsoni* are resolved as more closely related to other pentanchids and higher carcharhinoids by the anterior position of their first and dorsal fins (42:1; 43:1). A close relationship between *B. clevai* and *B. lutarius* (clade 37) is supported by a higher number of upper teeth (3:72–76). *Bythaelurus lutarius* presents higher numbers of upper (3:76) and lower (4:86) teeth. No unique autapomorphies were found for *B. clevai*. *Bythaelurus dawsoni* is placed at the base of clade 38 (Fig. 16) and shares with *F. boardmani* and *Asymbolus* spp. a higher number of diplospondylous vertebrae (2:88–142), lower number of hyomandibular pores (7:14–17) and a ventral terminal 2 cartilage of the clasper sigmoid and concave ventrally (138:1). *Bythaelurus dawsoni* is characterized by a higher number of diplospondylous vertebrae (2:129–142), lower number of hyomandibular pores (7:14–15) and absence of a dorsal terminal 2 cartilage on the clasper (134:1).

A close relationship between *Asymbolus* and *Figaro* (clade 39; Fig. 16) is supported by a lower number of upper teeth (3:54–62). *Asymbolus* is resolved as closely related to *Halaelurus* and *Holohalaelurus*, and *Figaro* as closer to *Parmaturus*, when morphological characters are analysed separately (Fig. 17A). Six autapomorphies were found for *F. boardmani*: lower number of upper tooth counts (3:54–57), anterior

nasal flap slender (10:1), presence of upper (47:1) and lower (48:1) caudal crests of dermal denticles, rostral cartilages confluent with lateral borders of anterior fontanelle (71:1) and medial portion of Meckel's cartilage less calcified than the rest (97:1). Species of *Asymbolus* (clade 40; Fig. 16) share a well-developed posterior nasal flap (17:0), hyomandibular pores medial to the mouth commissure (32:1), presence of a pelvic apron (34:1), muscle epaxialis reaching the postorbital process (65:0), well-developed rhipidion of the clasper (123:1), presence of a ventral terminal 3 cartilage on the clasper (139:1) and black spots over the body (142:0). *Asymbolus analis* is characterized by a higher number of lower teeth (4:62) and ventral terminal 2 cartilage of the clasper trapezoidal or rod-like and not concave ventrally (138:1); *As. galacticus* by a lower number of lower teeth (4:54–59); and *As. rubiginosus* by a poorly developed cover rhipidion of the clasper (124:0).

Clade 41, ***Galeinae subfam. nov.****:* The monophyly of this clade is supported by a lower number of hyomandibular pores (7:11–25), anterior nasal flap partly covering excurrent nasal aperture and not covering posterior nasal flap or upper lip (10:1), one median ridge on dermal denticles (51:0), rostral cartilages confluent with the lateral borders of the anterior fontanelle (71:1), medial portion of Meckel's cartilage less calcified (97:1) and a poorly developed exorhipidion of the clasper (125:0).

The monophyly of *Galeus* was potentially compromised in all analyses performed (Figs 16, 17). When only morphology is analysed (Fig. 17A), all *Galeus* species except *Galeus sauteri* form a clade supported by the presence of an upper and lower caudal crest of the denticles (47:1; 48:1). In the combined analysis, *Galeus nipponensis* and *Galeus sauteri* are resolved as more closely related to *Cephalurus* and *Parmaturus* (clade 44) than to other *Galeus* species (Fig. 16). The monophyly of clade 42 is supported by higher numbers of upper (3:54–106) and lower (4:54–97) teeth. *Galeus sauteri* is placed at the base of this clade, and this species is characterized by lower numbers of monospondylous vertebrae (1:31– 34) and hyomandibular pores (7:11–13) and higher values for lower tooth (4:82) and pectoral radial (8:18) counts. *Galeus nipponensis* is resolved as a sister group of *Cephalurus* and *Parmaturus* (clade 43) and shares with these species a lower number of intestinal valves (5:5–8); this species is characterized by a horizontally elongated spiracle (36:1), terminal dermal cover corresponding up to one-third of the clasper glans (121:1) and presence of a ventral marginal 2 cartilage of the clasper (131:0).

A close relationship between *Cephalurus cephalus* and *Parmaturus* spp. (clade 44) is supported by first (42:1) and second (43:1) dorsal fins more anteriorly situated, muscle coracomandibularis inserting on the anteromedial borders of Meckel's cartilage (60:0) and absence of dermal denticles on the dorsomedial surface of the clasper glans (117:0). *Cephalurus* presents the following autapomorphies: lower numbers of vertebrae (1:28–35; 2:67–71), intestinal valves (5:5–6) and pectoral radials (8:11–12), a higher number of hyomandibular pores (7:15), upper caudal crest of denticles absent (47:0), ectodermal pits restricted to the anterior portion of crown denticles (50:0), muscle bundles of coracohyoideus distant from each other (62:1), coracobranchialis II, III and IV originating on the pericardial membrane (63:0), rostral cartilages distant from the anterior fontanelle (71:0), median rostral cartilage confluent with the anterior fontanelle (72:1), narrow postorbital groove (84:1), orbital process absent (91:0), well-developed medial projection of coracoid bar (115:1), absence of a terminal dermal cover (120:1) and a ventral terminal 2 cartilage (136:1) on the clasper.

The monophyly of *Parmaturus* is highly supported in all analyses (Figs 16, 17). In the total-evidence analysis, species of *Parmaturus* (clade 45; Fig. 16) share a broad anterior nasal flap that entirely covers the excurrent nasal aperture (10:1), exorhipidion of the clasper medially expanded (125:1) and envelope of the clasper present (126:1). *Parmaturus xaniurus* is placed at the base of the genus and is characterized by the presence of a ventral marginal 2 cartilage on the clasper (131:0). *Parmaturus pilosus*, *Parmaturus albimarginatus*, *Parmaturus angelae* and *Parmaturus albipenis* (clade 46) share higher upper tooth row counts (3:82–130) and the presence of a lower caudal crest of enlarged dermal denticles (48:1). *Parmaturus pilosus* is characterized by a higher number of monospondylous vertebrae (1:42) and resolved as the sister group of a clade formed by *Parmaturus albimarginatus*, *Parmaturus angelae* and *Parmaturus albipenis* (clade 47). The monophyly of clade 46 is supported by higher numbers of upper (3:92–106) and lower (4:92–97) teeth. *Parmaturus angelae* and *Parmaturus albipenis* (clade 48) are hypothesized to be closely related by having lower diplospondylous vertebrae counts (1:83–84), higher upper tooth row counts (3:102–130) and labial furrows continuous and fused laterally (28:0). *Parmaturus albimarginatus* is characterized by more posteriorly situated dorsal fins (42:0; 43:0), *Parmaturus albipenis* by a higher number of upper teeth (3:130) and *Parmaturus angelae* by a lower number of monospondylous vertebrae (1:38).

A clade formed by species of *Apristurus* and *Pentanchus*, *Galeus antillensis*, *Galeus melastomus* and *Galeus polli* (clade 49) is supported by lower pectoral radial counts (8:10–17), muscle epaxialis

extending anteriorly (65:0), nasal capsules oblique (73:1), laterally expanded and united to the lateral border of the nasal capsule (76:1), nasal fontanelle divided into two (77:1), internal carotid foramina distant from each other (82:0), long accessory cartilage of basibranchial (109:1) and short clasper siphons (140:1). *Galeus antillensis*, *Galeus melastomus* and *Galeus polli* (clade 50) share a ventral terminal 2 cartilage of the clasper sigmoid and concave ventrally (138:1) and no accessory dorsal marginal cartilage on the clasper (129:1). *Galeus antillensis* is hypothesized as the sister group of *Galeus melastomus* and *Galeus polli* (clade 51) and is characterized by lower numbers of upper (3:56) and lower tooth (4:52) and mandibular pore (6:3–4) counts, clasper hooks on the medial border of the exorhipidion (119:1), terminal dermal cover absent on clasper glans (120:1), an accessory terminal cartilage of the clasper absent (128:1) and ventral terminal cartilage of the clasper present (139:1). The monophyly of clade 52 (Fig. 16) is supported by a spiracle horizontally elongated (36:1) and long rostral cartilages (70:1). *Galeus melastomus* is characterized by a higher number of diplospondylous vertebrae (2:106) and lower hyomandibular pore counts (7:12), whereas *Galeus polli* is characterized by a lower number of monospondylous vertebrae (1:32–35), higher pectoral radial counts (8:16) and two median ridges on dermal denticles (51:1). When only morphological characters are considered (Fig. 17A), a closer relationship between a clade formed by *Galeus*, *Apristurus* and *Pentanchus* and another composed by higher carcharhinoids except proscylliids is supported by labial furrows discontinuous (28:0), two median ridges on dermal denticles (51:1) and labial ridge absent on the quadrate process (90:1).

Apristurus and *Pentanchus* (clade 52) are hypothesized to be closely related to each other in most analyses (Figs 16, 17) and share the absence of a posterior nasal flap (16:1), upper (23:0) and lower (25:0) labial furrows greater than one-half of mouth width, posterior condyle opposite to the facet in the articular region of quadratomandibular joint (99:1), fusion of pectoral propterygium and mesopterygium proximal segments (110:1) and presence of ventral marginal 2 (131:0) and ventral marginal 3 (133:1) cartilages on the clasper. Analysing only molecular characters, *Pentanchus* is resolved as a sister group of the clade formed by *Galeus nipponensis* + *Galeus sauteri* + *Parmaturus xaniurus* + *Apristurus* (Fig. 17B). Species of *Apristurus* (*Ap. brunneus*, *Ap. laurussonii*, *Ap. macrostomus* and *Ap. parvipinnis*; clade 53) are diagnosed by presenting the origin of second dorsal fin anterior to the vertical line that passes through the midpoint of the anal-fin base (43:1). *Apristurus macrostomus* is placed at the base of the genus (Fig. 16) and is characterized by only molecular characters. *Apristurus parvipinnis*, *Ap. laurussonii* and *Ap. brunneus* (clade 54) share labial furrows discontinuous and upper furrow ventral to the lower (28:0); *Ap. parvipinnis* presents a higher number of lower teeth (4:90) and an accessory cartilage not differentiated from the cardiobranchial cartilage of basibranchial copula (108:0). A closer relationship between *Ap. brunneus* and *Ap. laurussonii* (clade 55) is supported by lower diplospondylous vertebrae counts (2:75–82) and a higher number of hyomandibular pores (7:18–21). *Apristurus brunneus* is characterized by a lower number of diplospondylous vertebrae (2:75–78) and higher mandibular pore counts (6:6), whereas *Ap. laurussonii* presents a lower number of lower teeth (4:47–54).

Species previously classified in the genus *Apristurus* are reclassified in *Pentanchus* (*Pentanchus australis*, *Pentanchus longicephalus*, *Pentanchus manis* and *Pentanchus stenseni*; clade 56) by sharing a lower number of monospondylous vertebrae (1:29–35; Fig. 16). *Pentanchus profundicolus* is resolved as a sister group of all other congeners and has no autapomorphies. *Pentanchus australis*, *Pentanchus longicephalus*, *Pentanchus manis* and *Pentanchus stenseni* (clade 57) share lower values for upper (3:35–64) and lower (4:48–68) tooth row counts, and muscle coracomandibularis originating on the lateral borders of the coracoid (59:1). *Pentanchus longicephalus* and *Pentanchus australis* (clade 58) share higher pectoral radial counts (8:16–17) and an accessory cartilage of the basibranchial not distinct from the cardiobranchial cartilage (108:0), whereas *Pentanchus stenseni* and *Pentanchus manis* (clade 59) share an upper caudal crest of enlarged dermal denticles (47:1). *Pentanchus australis* is characterized by lower intestinal valve counts (5:8–9); *Pentanchus longicephalus* has lower values for upper tooth counts (3:35–45), higher pectoral radial counts (8:17) and an accessory cartilage present on the mandibular symphysis (96:1); *Pentanchus manis* presents a lower number of lower tooth counts (4:52) and *Pentanchus stenseni* presents a second dorsal fin more anteriorly situated (43:1).

DISCUSSION

A hypothesis of phylogenetic relationships of scyliorhinoids based on morphological characters and *NADH2* sequences and including the most comprehensive catshark taxon sampling published to date is presented here (Fig. 16). Over the past decades, molecular phylogenetics has had a central role in the establishment of systematic and evolutionary hypotheses of carcharhinoids (Iglésias *et al.*, 2005; Human *et al.*, 2006; Vélez-Zuazo & Agnarsson, 2011;

Naylor *et al.*, 2012a). Clades proposed by molecular inferences have been diagnosed subsequently by morphological characters (e.g. Scyliorhinidae and Pentanchidae in the study by Iglésias *et al.*, 2005), which were mapped onto the tree and used incorrectly to diagnose clades. De Queiroz *et al.* (1995) pointed out that there is no compelling reason not to include morphological characters to estimate phylogeny. In the present study, the greatest phylogenetic resolution was achieved when morphological and molecular data were combined into a single analysis, which also provided a more efficient summary of the available evidence for catsharks.

One of the main challenges in combining data from different sources is the availability of data for each taxon. More than one-third of the terminal taxa included here lack *NADH2* sequences, and for some of them (e.g. *Ak. suwartanai*, *Pentanchus profundicolus* and *Scyliorhinus garmani*) only external morphological characters were available. Even with 46% missing entries in the molecular partition, the combined analysis yielded better support and resolution of the topology than when morphological and molecular data were analysed separately. Flynn *et al.* (2005) suggested that excluding missing data might generate a decrease in nodal support and resolution, and many works have demonstrated that the amount of missing data is not a problem as long as enough informative characters (Maddison, 1993; Wiens, 1998, 2003, 2006) and monophyletic lineages (Graybeal, 1998; Rannala *et al.*, 1998; Dillman *et al.*, 2015; Mirande, 2019) are included in the cladistic analysis. Several authors have argued that the effects of missing data are not absolute and are dependent of the phylogenetic signal, numbers of terminal taxa and characters, and sampling of close relatives of taxa with little information available (e.g. Dragoo & Honeycutt, 1997; Wiens, 1998, 2003, 2006; Driskell *et al.*, 2004; Philippe *et al.*, 2004; Wiens & Morrill, 2011). The inclusion of *Ak. suwartanai*, *Cephalurus cephalus* and *Pentanchus profundicolus*, for which only morphological data were available, improved the tree resolution and our understanding of the relationships within Pentanchidae. It is noteworthy that the placement of *Pentanchus profundicolus* close to *Apristurus* species agrees with previous works (Compagno, 1988; Nakaya & Sato, 1999) even with 81% missing data entries.

The new hypothesis of relationships presented here is highly compatible with previous phylogenies (Vélez-Zuazo & Agnarsson, 2011; Naylor *et al.*, 2012a), differing in the relationships amongst *Cephaloscyllium*, *Poroderma* and *Scyliorhinus* and the placement of Proscylliidae. In the study by Naylor *et al.* (2012a), *Scyliorhinus* was hypothesized to be more closely related to *Poroderma* than to *Cephaloscyllium*, whereas the opposite was recovered by Vélez-Zuazo & Agnarsson (2011), Soares & de Carvalho (2020) and our analysis. *Proscyllium habereri* was resolved as a sister group of pentanchids and distantly related to the proscylliid *E. barbouri* and higher carcharhinoids in the molecular analyses of Vélez-Zuazo & Agnarsson (2011) and Naylor *et al.* (2012a). When morphological and molecular data are combined, both *Proscyllium* and *Eridacnis* are closer to higher carcharhinoids than to pentanchids (Fig. 16), but the examination of *Ctenacis* is imperative in order to elucidate the phylogeny of Proscylliidae.

Despite of the large number of *COI* sequences available in repositories such as GenBank and BOLD Systems, the inclusion of this gene in phylogenetic analyses of chondrichthyans has resulted in highly incongruent hypotheses in comparison to the relationships previously known (Vélez-Zuazo & Agnarsson, 2011; Naylor *et al.*, 2012a). The evolutionary history of *COI* might not reflect the phylogenetic history of catsharks. Furthermore, there is a disagreement between species and gene trees (Degnan & Rosenberg, 2009; Padial *et al.*, 2010). The use of *NADH2* sequences in phylogenetic analysis has proved to be reliable in recovering evolutionary history in different analyses, whether Bayesian inferences (Vélez-Zuazo & Agnarsson, 2011; Naylor *et al.*, 2012a) or under parsimony, as demonstrated herein. Thus, the more *NADH2* sequences that are obtained, the greater will be our understanding about the relationships within Carcharhiniformes.

Naylor *et al.* (2012a) highlighted the relevance of a good taxonomy to reflect the reliability of DNA sequences. In addition, taxonomic works have provided morphometric and meristic data that could be used to infer phylogenetic relationships. Meristic characters have been little used in cladistic analysis owing to difficulties in their coding (Colles, 1980; Thorpe, 1984; Archie, 1985; Chappil, 1989; Rae, 1998), and some authors have argued that these characters might not be useful for systematic purposes (Crisp & Weston, 1987; Pimentel & Riggins, 1987; Cranston & Humphries, 1988). Here, meristic characters such as vertebrae, intestinal valves and tooth counts contributed positively to the internal resolution of the genera *Cephaloscyllium* and *Scyliorhinus* and within the family Pentanchidae (see Results). Our results suggest that quantitative characters coded and analysed as such carry phylogenetic information, as stated by Goloboff *et al.* (2006).

Our analysis emphasizes the importance of including morphological characters to infer the interrelationships of scyliorhinoids and thus improve our understanding of the evolutionary history of anatomical features (Fig. 16). The phylogenetic significance of characters such as the caudal crest of dermal denticles, length of labial furrows, nasal flaps and ectodermal pits

on scales that have long been used to diagnose taxa (Garman, 1913; Bigelow & Schroeder, 1948; Springer, 1966, 1979; Muñoz-Chápuli, 1985; Compagno, 1988) is tested cladistically in the present study. The posteriormost position of dorsal fins, long used to diagnose scyliorhinoids, proved not to be a reliable character because catsharks do not form a natural group and are divided into three distinct lineages. Compagno (1988) and Shirai (1996) pointed out that carcharhinoid sharks contain many convergences and reversals, but many of the characters included in their analysis needed to be redefined and investigated better (e.g. nictitating lower eyelid, neurocranium, visceral arches and claspers). Here, we propose 20 new morphological characters and clarify many others, redefined from previous works or analysed cladistically for the first time. Nonetheless, much remains to be done to comprehend the evolution of higher carcharhinoids.

Despite the high number of homoplasies in the morphological characters analysed herein, as evidenced by low values of consistency indices (98 characters with CI < 0.5), synapomorphic characters for higher taxa, such as the great extension of ectodermal pits on dorsal surface of the crown denticles (50:1) in Pentanchidae and the presence of lateral processi rastriformis (104:1) in Atelomycteridae, proved to be informative, as demonstrated by their high retention indices (68 and 82, respectively). Of the 15 characters from musculature, eight presented high values of CI and RI; amongst these are the origin of m. levator palatoquadrati and the configuration of muscle bundles of coracohyoideus. The presence of a muscle depressor palpebrae nictitantis is hypothesized to be an apomorphic character shared by all carcharhiniforms but Scyliorhinidae. Although Compagno (1988) and Soares & de Carvalho (2020) listed the absence of this muscle as a synapomorphy for the clade formed by *Cephaloscyllium*, *Poroderma* and *Scyliorhinus*, we report this muscle also absent in lamnoids and orectoloboids. All carcharhiniforms, including Scyliorhinidae, share the presence of retractor and levator muscles. The presence of a muscle coracomandibularis originating directly on the coracoid diagnoses a group within *Pentanchus*; its condition in *Pentanchus profundicolus* is unknown.

Rostral cartilages and components of the viscerocranium (e.g. jaws, thyroid foramen and gill pickax) have proved to be useful character sources for diagnosing family and subfamily groups as proposed herein. Clasper skeleton characters have shown to be important to infer relationships, not only within *Scyliorhinus* as already stated by Soares & de Carvalho (2020), but also within scyliorhinoid families (e.g. presence of a dorsal marginal 3 cartilage in Halaelurinae, a ventral marginal 3 cartilage in *Apristurus* and *Pentanchus*, and ventral terminal 2 cartilage posteriorly situated in *Poroderma*).

Systematics of catsharks

The 'phenetic' classification proposed by Compagno (1988) is revisited and revised in light of the morphological evidence provided herein and the combination of these characters with DNA sequences in a total-evidence analysis. Scyliorhinidae *s.l.* is resolved as paraphyletic and divided into three different lineages, closely resembling the results of Vélez-Zuazo & Agnarsson (2011) and Naylor *et al.* (2012a). The arrangement proposed by Iglésias *et al.* (2005), which restricted the family Scyliorhinidae to the crestless catshark genera, is not corroborated, revealing the need to propose a new scope and definition for the family. The clade formed by *Cephaloscyllium*, *Poroderma* and *Scyliorhinus*, previously recognized as subfamily Scyliorhininae (Compagno, 1988; Naylor *et al.*, 2012a), is here equated to the family Scyliorhinidae, aiming to reflect the phylogenetic relationships amongst catsharks better.

The monophyly of Scyliorhinidae is supported here by lower diplospondylous vertebral counts, rostral cartilages not fused, presence of a thyroid foramen and of three extrabranchial ventral cartilages (Compagno, 1988; Soares & de Carvalho, 2020). This family was found to occupy the most basal position in Carcharhiniformes, corroborating other works (White, 1936b, 1937; Nakaya, 1975; Iglésias *et al.*, 2005; Human *et al.*, 2006; Vélez-Zuazo & Agnarsson, 2011; Nakaya *et al.*, 2012a). Yet, Compagno (1988) pointed out that scyliorhinoids could be a derived group by possessing a posterior first dorsal fin and hypothesized its closer relationship to *Proscyllium*. This is true for the family Pentanchidae (subfamily Pentanchinae of Compagno, 1988), which has been recovered as more closely related to proscylliids than other catshark groups in the present study and in recent molecular phylogenies (Iglésias *et al.*, 2005; Human *et al.*, 2006; Vélez-Zuazo & Agnarsson, 2011; Naylor *et al.*, 2012a).

Morphological and molecular studies have diverged on the relationships among scyliorhinids (Compagno, 1988; Vélez-Zuazo & Agnarsson, 2011; Naylor *et al.*, 2012a; Soares & de Carvalho, 2020). Our results suggest a close relationship between *Cephaloscyllium* and *Scyliorhinus*, supported by oronasal characters and a well-developed medial projection of the coracoid bar. Four of the seven synapomorphies proposed by Soares & de Carvalho (2020: 378) for the clade *Cephaloscyllium* + *Scyliorhinus* were recovered in the present study. However, considering the low support for this clade and the molecular support for *Scyliorhinus* + *Poroderma*, we recommend that more

species of *Cephaloscyllium* and DNA sequences should be included in future analyses and that a taxonomic review of the genus should be performed.

Intrageneric relationships of *Scyliorhinus* obtained here differed from the results of Soares & de Carvalho (2020). A clade formed by *Scyliorhinus comoroensis* and *Scyliorhinus stellaris* is resolved as the most basal group of the genus, whereas in the study by Soares & de Carvalho (2020), the clade formed by *Scyliorhinus boa*, *Scyliorhinus hesperius* and *Scyliorhinus retifer* is placed at the base; this clade was supported by the presence of a medially expanded envelope in their study, which is also recovered here. Species of *Scyliorhinus* from the south-western (*Scyliorhinus cabofriensis*, *Scyliorhinus haeckelii* and *Scyliorhinus ugoi*) and south-eastern (*Scyliorhinus cervigoni*) Atlantic are resolved as closely related to each other and to a clade formed by *Scyliorhinus capensis* (South Africa), *Scyliorhinus meadi* (south-eastern coast of the USA) and *Scyliorhinus garmani* (East Indies) by sharing a rhomboidal dorsal terminal 2 cartilage. In contrast, Soares & de Carvalho (2020) hypothesized a close relationship between *Scyliorhinus garmani* and *Scyliorhinus canicula* + *Scyliorhinus duhamelii* based on the extension of the anterior nasal flap and the colour pattern. The placement of *Scyliorhinus garmani* remains questionable owing to lack of information on clasper morphology and molecular data. In the present study, a close relationship amongst *Scyliorhinus torrei* (western Central Atlantic), *Scyliorhinus torazame* (Japan and East China Seas), *Scyliorhinus canicula* and *Scyliorhinus duhamelii* (Mediterranean Sea and north-eastern Atlantic) is hypothesized based on meristic characters and a well-developed pelvic apron. Soares & de Carvalho (2020) recovered a close relationship amongst *Scyliorhinus torazame*, *Scyliorhinus canicula* and *Scyliorhinus duhamelii*, which is also supported here by a short and poorly developed rhipidion. It is important to highlight that *NADH2* sequences for only four of the 16 species of *Scyliorhinus* are available to date, and efforts should be directed toward obtaining molecular data for more species.

Schroederichthys is hypothesized to be closely related to *Atelomycterus* and *Aulohalaelurus*, similar to the results of Vélez-Zuazo & Agnarsson (2011) and Naylor *et al.* (2012a). Compagno (1988) stated that *Aulohalaelurus* is the 'primitive sister genus' of *Atelomycterus* but also close to *Schroederichthys* (Compagno, 1984). Nevertheless, he isolated *Schroederichthys* in the subfamily Schroederichthyinae, considering the genus as more generalized and central in his family Scyliorhinidae (Compagno, 1988). In the present study, we propose to resurrect the family name Atelomycteridae (White, 1936b) to include these three genera. Atelomycteridae is hypothesized to be more closely related to Pentanchidae than to Scyliorhinidae (Vélez-Zuazo & Agnarsson, 2011; Naylor *et al.*, 2012a) and is diagnosed by lateral processi rastriformis longer than those surrounding and an anterior border of the basihyal bifurcated. The intermediary position of *Atelomycterus* and its close relatives between scyliorhinids and pentanchids was first proposed by White (1937) and is corroborated here.

Gomes *et al.* (2006) questioned the monophyly of *Schroederichthys*, arguing that the removal of *Schroederichthys bivius* and *Schroederichthys chilensis* (Guichenot, 1848) would be desirable. According to our results, a close relationship among *Schroederichthys bivius*, *Schroederichthys maculatus* and *Schroederichthys saurisqualus* is supported by oronasal characters and the monospondylous vertebral count. However, the inclusion of *Schroederichthys chilensis* and Schroederichthys tenuis Springer, 1966 in future analysis and a taxonomic review of the genus are needed.

Akheilos suwartanai is hypothesized to be more closely related to pentanchids than to *Schroederichthys* by sharing continuous labial furrows and ectodermal pits extending more than half the length of the crown denticles. A close relationship between *Akheilos* and *Schroederichthys* was proposed by White *et al.* (2019), but a detailed explanation for this was not provided by the authors, nor was a cladistic analysis performed. Also, only a few specimens of *Schroederichthys bivius* and *Schroederichthys saurisqualus* were examined in their study. According to White *et al.* (2019), the presence of a supraorbital crest on the neurocranium could justify the allocation of *Akheilos* in the family Scyliorhinidae (*sensu* Iglésias *et al.*, 2005). However, the description of *Ak. suwartanai* was based on a single specimen, and only external morphological characters were examined precisely (White *et al.*, 2019). *Akheilos* is tentatively included in Pentanchidae herein, but its internal anatomical characters (e.g. neurocranium, hyoid arch and clasper skeleton) must be investigated in order to corroborate its placement. The subfamily Schroederichthyinae as recognized here has a distribution restricted to the Americas and is composed of only one genus, *Schroederichthys*.

The close relationship between *Atelomycterus* and *Aulohalaelurus* demonstrated by our analysis was also proposed by Compagno (1984, 1988), who reunited both genera in his subfamily Atelomycterinae. Both genera share similarities in external morphology, oronasal characters and neurocranial structure and were also placed together by molecular inferences (Vélez-Zuazo & Agnarsson, 2011; Naylor *et al.*, 2012a). The monophyly of *Atelomycterus* was called into question by Vélez-Zuazo & Agnarsson (2011), who demonstrated the inclusion of *Au. labiosus* amongst

species of *Atelomycterus*. Such results revealed the need for a systematic revision of the subfamily Atelomycterinae, in which more representatives and characters of internal anatomy and molecular data are included.

The monophyly of the family Pentanchidae is supported by continuous labial furrows and ectodermal pits extending more than half the length of the crown denticles. The absence of a supraorbital crest on the neurocranium was used by Iglésias *et al.* (2005) to diagnose the family, but the occurrence of this crest in *Akheilos* needs to be confirmed. In the hypothesis of Vélez-Zuazo & Agnarsson (2011), the monophyly of Pentanchidae was potentially compromised by the placement of species of Proscylliidae and Pseudotriakidae close to *Apristurus*. In our analysis, Pentanchidae is recovered as the sister group to all other carcharhinoid families, including proscylliids and pseudotriakids. Generic relationships within Pentanchidae hypothesized here differ from those of Naylor *et al.* (2012a) by the division of the family into two main clades instead of the placement of *Halaelurus*, *Holohalaelurus* and *Haploblepharus* at the base.

A close relationship amongst *Halaelurus*, *Holohalaelurus* and *Haploblepharus* is strongly supported by meristic, neurocranial and clasper characters, in agreement with previous morphological (Compagno, 1988; tribe Halaelurini) and molecular (Human *et al.*, 2006; Naylor *et al.*, 2012a) hypotheses. In the present study, these genera are hypothesized to be closely related to *Bythaelurus*, *Figaro* and *Asymbolus*. Soares (2020) suggested a close relationship between *Halaelurus* and *Holohalaelurus* by the presence of a dorsal marginal 3 cartilage on the claspers, which is proposed here as synapomorphy for the clade formed by *Halaelurus*, *Holohalaelurus* and *Haploblepharus*. In contrast to Naylor *et al.* (2012a), *Halaelurus natalensis* is resolved as more closely related to *Halaelurus sellus* than *Haploblepharus edwardsii* by sharing neurocranial, jaw articulation and clasper characters.

Bythaelurus, *Figaro* and *Asymbolus* are grouped into the same clade, agreeing with Naylor *et al.* (2012a) and differing from Compagno (1988), who proposed *Asymbolus* as the most basal genus of Pentanchidae. In our analysis, *Asymbolus* is deeply nested with *Figaro*, *Bythaelurus*, *Haploblepharus*, *Halaelurus* and *Holohalaelurus*. A closer relationship between *Asymbolus* and *Figaro* was hypothesized by Compagno (1988), Vélez-Zuazo & Agnarsson (2011) and Naylor *et al.* (2012a) and corroborated by the present study. The paraphyly of *Bythaelurus* was hypothesized in morphology-only and total-evidence analyses; further studies are necessary to review both taxonomy and phylogenetic relationships within this genus.

The paraphyly of *Galeus* was recovered by Vélez-Zuazo & Agnarsson (2011) and Naylor *et al.* (2012a) and corroborated here because *Galeus sauteri* and *Galeus nipponensis* are more closely related to *Cephalurus* and *Parmaturus* than to other species of *Galeus*. Those species are distributed in the Indo-Pacific region, whereas *Galeus antillensis*, *Galeus melastomus* and *Galeus polli* are recorded from the North Atlantic Ocean. *Galeus sauteri* and *Galeus gracilis*: Compagno & Stevens, 1993 present a dorsal terminal cartilage on the clasper different from that observed in their congeners (Soares, 2020: 11–12). Compagno (1988) pointed out that the inclusion of *Galeus murinus* (Collett, 1904), *Galeus nipponensis* and *Galeus schultzi* Springer, 1979 in the genus would be undesirable because they differ from the 'typical' species of *Galeus* [*Galeus arae* (Nichols, 1927), *G. atlanticus*, *G. melastomus* and *G. polli*]. Compagno & Stevens (1993b) pointed out that several species of *Galeus* are incompletely known in relationship to anatomical structures, such as the neurocranium and claspers. A taxonomic review and anatomical assessment of all *Galeus* species is essential to update the classification of the genus and enlarge our knowledge about its infrageneric relationships.

A close relationship between *Cephalurus* and *Parmaturus* was proposed by Iglésias *et al.* (2005) and is weakly supported here by the position of dorsal fins and insertion of the muscle coracomandibularis. Compagno (1988) suggested a close relationship between both genera, mainly based on the enlarged branchial region and cranial morphology shared by *Cephalurus cephalus* and *Parmaturus xaniurus*. The scope of *Parmaturus* has been revised over the years, and its definition is still unclear because some species are considered as intermediates between *Galeus*, *Parmaturus* and *Apristurus* (Garman, 1906, 1913; Regan, 1908; Springer, 1979; Compagno, 1988). Furthermore, Compagno (1988) and Soares *et al.* (2019) mentioned that the lack of anatomical information on most *Parmaturus* species has impeded its proper separation from other genera, such as *Figaro* and *Galeus*. Although the genus *Parmaturus* has been resolved as monophyletic in the present study, intrageneric relationships need to be re-evaluated with the inclusion of internal anatomical characters and molecular sequences for most of its species.

Garman (1913) recognized *Pentanchus* as a monotypic genus and proposed the genus *Apristurus* for *Ap. indicus* (Brauer, 1906), *Ap. brunneus*, *Ap. platyrhynchus* (Tanaka, 1909), *Ap. macrorhynchus* (Tanaka, 1909) and *Ap. profundorum* (Smith & Radcliffe, 1912). Discussion on the validity of *Pentanchus* as a genus separated from *Apristurus* was presented by Springer (1979), Compagno (1984, 1988) and Nakaya & Séret (2000). Compagno (1988) presented an extensive list of

characters to illustrate the close resemblance between *Pentanchus profundicolus* and *Apristurus herklotsi* (Fowler, 1934) (= *Pentanchus herklotsi*), despite the lack of a first dorsal fin in the former (perhaps abnormally). The author also included *Pentanchus profundicolus*, *P. longicephalus* and *P. herklotsi* in his *Apristurus longicephalus* group based on the description of *P. longicephalus* provided by Nakaya (1975). In contrast, Nakaya & Séret (2000) proposed a close relationship between *Pentanchus profundicolus* and *Ap. macrorhynchus* based on the configuration of the supraorbital canal of lateral line system.

Species of *Apristurus* have been grouped in different ways by previous authors (Fowler, 1934; Springer, 1979; Compagno, 1988; Nakaya & Sato, 1999). Fowler (1934) proposed the subgenus *Parapristurus* to include *Catulus spongiceps* (Gilbert, 1905) based on nasal flap characters, and Springer (1979) elevated it to the rank of genus based on denticle-free anterior gill slits. Additionally, Springer (1979) proposed the subgenus *Compagnoia* to include *P. manis* and *P. stenseni* by having soft bodies and supracaudal crests of denticles. Bigelow & Schroeder (1948) reported differences in the shape of gill openings of *Ap. atlanticus, Ap. platyrhynchus*, *Ap. verweyi*, *Pentanchus herklotsi*, *Pe. microps*, *Pe. profundorum* and *Pe. spongiceps*, and suggested that these taxa could be generically separated from species similar to *Ap. brunneus*. Nakaya & Sato (1999) divided the genus *Apristurus* in three groups (*brunneus*, *longicephalus* and *spongiceps*), using snout length, intestinal valve counts, length of labial furrows and supraorbital sensory canal of lateral line system to distinguish among species. Most of those characters were included in the present analysis (characters 5, 23, 25 and 70), with the exception of the supraorbital sensory canal. A close relationship between *brunneus* and *spongiceps* groups, mainly based on snout length, was also proposed by Nakaya & Sato (1999). Later, Sato (2000) revisited the *Apristurus* relationships and hypothesized that the *spongiceps* group would be more closely related to the *longicephalus* group than to the *brunneus* group, which has been corroborated by recent phylogenies (Iglésias *et al.*, 2005; Vélez-Zuazo & Agnarsson, 2011; Naylor *et al.*, 2012a). The monophyly of *Apristurus* was contested by Naylor *et al.* (2012a) with the recovery of a polytomy amongst *Apristurus* species groups, *Galeus sauteri* and *Parmaturus xaniurus*.

According to our examination, species assigned to the *Apristurus* species groups *spongiceps* and *longicephalus* present the muscle coracomandibularis originating on the medial surface of the coracoid bar; a condition unique among carcharhinoids (Soares & de Carvalho, 2020: p. 358, fig. 11D). Furthermore, a close relationship between *Pentanchus profundicolus* and *Apristurus* species of *spongiceps* and *longicephalus* groups is strongly supported by our analysis. Both groups of *Apristurus* and *Pentanchus* have soft bodies, a long caudal fin and lower monospondylous vertebral counts. Based on this evidence, three nomenclatural alternatives were evaluated: (1) synonymize *Pentanchus* and *Apristurus*; (2) revalidate *Parapristurus* or *Compagnoia* to include species of *Apristurus* closely related to *Pentanchus*; or (3) redefine the scope of *Pentanchus* to include *Apristurus* species of *spongiceps* and *longicephalus* groups. Alternative 1 implies overlooking the uniqueness of muscular features in species of *spongiceps* and *longicephalus* groups, whereas alternative 2 does not take into account the similarities between *Pentanchus* and *Apristurus* species closely related to it. Thus, alternative 3 was preferred: we propose the reallocation of species previously assigned to *Apristurus* in *Pentanchus*, restricting the scope of *Apristurus* to include only species of the *brunneus* group (Table 2).

Lastly, we aim to provide a phylogeny-based classification for catshark genera using as much information as possible. It must be pointed out that this analysis excludes information from extinct species and genera mostly diagnosed from tooth characters (Cappetta, 2012). Efforts should be directed toward the investigation of morphological variation in teeth and the inclusion of extinct representatives of carcharhinoids in future analyses in order to increase our understanding of the phylogeny of these sharks. We hope that this study can inspire future works on the evolution of morphological characters among carcharhiniforms.

ACKNOWLEDGEMENTS

The authors acknowledge Barbara Brown (AMNH), Mark McGrouther (AMS), Oliver Crimmen (BMNH), David Catania (CAS), Alastair Graham (CSIRO), Rob Robbins (FLMNH), Toshio Kawai (HUMZ), Karsten Hartel and Andrew Williston (MCZ), Patrice Pruvost (MNHN), Alessio Datovo (MZUSP), Sven Kullander (NRM), Masanori Nakae and Gento Shinohara (NSMT), Ofer Gon and Nkosinathi Mazungula (SAIAB), Albe Bosman (SAM), Ulisses Gomes and Hugo Santos (UERJ), Lynne Parenti, Jeffrey Williams, Kris Murphy and Sandra Raredon (USNM), Ralf Thiel (ZMH) and Marcus Krag (ZMUC) for permission to visit the collections and examine the specimens under their care. We thank José Ortiz (USAC) for sending photographs of specimens of *Scyliorhinus hesperius*. We also thank Ulisses Gomes (UERJ), Marcos Mirande (CONICET) and two anonymous referees for providing valuable comments that improved this paper. We also thank Ênio Matos and Phillip Lentitakis (IBUSP)

for the scanning electron microscope images, and Hugo Idalgo and Reginaldo Silva (Hospital Veterinário da Universidade de São Paulo) for the radiographs. Part of this work was included in the Ph.D. thesis of K.D.A.S., which was supervised by Marcelo R. de Carvalho. K.D.A.S. was supported by Coordenação de Aperfeiçoamento de Pessoal de Nível Superior (CAPES) (Código de Financiamento 001) and Fundação de Amparo à Ciência do Estado de São Paulo (FAPESP) (processes 2014/20316-5, 2015/21314-9 and 2016/22214-0). K.M. was funded by a Masters and PhD fellowship by CAPES-PROEX (process 8749764832218320).

DATA AVAILABILITY

All data generated or analyzed during this study are included in this published article.

REFERENCES

Archie KW. 1985. Methods for coding variable morphological features for numerical taxonomic analysis. *Systematic Zoology* **3:** 326–345.

Aschliman N, **Claeson KM**, **McEachran JD. 2012.** Phylogeny of Batoidea. In: Carrier JC, Musick JA, Heithaus MR, eds. *Biology of sharks and their relatives, Vol. 2*. Boca Raton: CRC Press, 57–96.

Artedi P. 1738. *Ichthyologia sive opera omnia de piscibus, scilicet: bibliotheca ichthyologica. Philosophia ichthyologica. Genera piscium. Synonymia specierum. Descriptiones specierum. Omnia in hoc genere perfectiora, quam antea ulla*. Leiden: Conrad Wishof.

Bass AJ, **D'Aubrey JD**, **Kistnasamy N. 1975.** Sharks of the east coast of southern Africa. II. The families Scyliorhinidae and Pseudotriakidae. *Investigational Report. Oceanographic Research Institute, Durban* **37:** 1–64.

Berkenhout J. 1769. *Outlines of the natural history of Great Britain and Ireland, containing a systematic arrangement and concise description of all the animals, vegetables and fossils which have hitherto been discovered in these kingdoms*. London: P. Elmsly.

Bigelow HB, **Schroeder WC. 1948.** *Fishes of the western North Atlantic. Part I. Lancelets, cyclostomes and sharks*. New Haven: Yale University.

Bloch ME. 1785. *Naturgeschichte der ausländischen Fische*. Berlin: Hesse.

Bloch ME. 1796. *Ichthyologie ou histoire naturelle des poissons: en six parties avec 216 planches dessinées et enluminées d'après nature. Part III*. Berlin: published by the author.

Bremer K. 1994. Branch support and tree stability. *Cladistics* **10:** 295–304.

Cappetta H. 2012. *Handbook of paleoichthyology. Vol. 3E: Chondrichthyes. Mesozoic and Cenozoic Elasmobranchii: teeth*. Munich: Dr Friedrich Pfeil.

de Carvalho MR. 1996. Higher-lever elasmobranch phylogeny, basal squaleans, and paraphyly. In: Stiassny MLJ, Parenti LR, Johnson GD, eds. *Interrelationships of fishes*. New York: Academic Press, 35–62.

Cavalcanti M. 2007. A phylogenetic supertree of the hammerhead sharks (Carcharhiniformes: Sphyrnidae). *Zoological Studies* **46:** 6–11.

Chappil JA. 1989. Quantitative characters in phylogenetic analysis. *Cladistics* **5:** 217–234.

Chu YT, **Wen MC. 1979.** *A study of the lateral-line canal system and that of Lorenzini ampullae and tubules of elasmobranchiate fishes of China. Monograph of fishes of China*. Shanghai: Academic Press.

Colless DH. 1980. Congruence between morphometric and allozyme data for meridian species: a reappraisal. *Systematic Zoology* **3:** 280–299.

Compagno LJV. 1970. Systematics of the genus *Hemitriakis* (Selachii: Carcharinidae), and related genera. *Proceedings of the California Academy of Sciences* **38:** 63–98.

Compagno LJV. 1973. Interrelationships of living elasmobranchs. *Zoological Journal of the Linnean Society* **53:** 15–61.

Compagno LJV. 1977. Phyletic relationships of living sharks and rays. *American Zoologist* **17:** 303–322.

Compagno LJV. 1984. FAO species catalogue. Vol. 4. Sharks of the world: an annotated and illustrated catalogue of shark species known to date. Part 2. Carcharhiniformes. In: *FAO Fisheries Synopsis 125, Vol. 4. Part 2*. Rome: FAO, 251–655.

Compagno LJV. 1988. *Sharks of the order Carcharhiniformes*. Princeton: Princeton University Press.

Compagno LJV. 1999. Systematics and body form. In: Hamlett WC, ed. *Sharks, skates and rays: the biology of elasmobranch fishes*. Baltimore: Johns Hopkins University Press, 1–42.

Compagno LJV, **Dando M**, **Fowler S. 2005.** *Sharks of the world*. Princeton: Princeton University Press.

Compagno LJV, **Stevens JD. 1993a.** *Atelomycterus fasciatus* n.sp., a new catshark (Chondrichthyes: Carcharhiniformes: Scyliorhinidae) from tropical Australia. *Records of the Australian Museum* **45:** 147–169.

Compagno LJV, **Stevens JD. 1993b.** *Galeus gracilis* n. sp., a new sawtail catshark from Australia, with comments on the systematics of the genus *Galeus* Rafinesque, 1810 (Carcharhiniformes: Scyliorhinidae). *Records of the Australian Museum* **45:** 171–194.

Corrigan S, **Beheregaray LB. 2009.** A recent shark radiation: molecular phylogeny, biogeography and speciation of wobbegong sharks (family: Orectolobidae). *Molecular Phylogenetics and Evolution* **52:** 205–216.

Cranston PS, **Humphries CJ. 1988.** Cladistics and computers: a chironomid conundrum? *Cladistics* **4:** 72–92.

Crisp MD, **Wiston PH. 1987.** Cladistics and legume systematics, with an analysis of the Bossiaeeae, Brongniartieae and Mirbelieae. In: Stirton ZC, ed. *Advances in legume systematics. Part 3*. Kew: Royal Botanical Gardens, 65–130.

De Beer GR. 1937. *The development of the vertebrate skull*. Chicago: University of Chicago Press.

Degnan JH, **Rosenberg NA. 2009.** Gene tree discordance, phylogenetic inference and the multispecies coalescent. *Trends in Ecology & Evolution* **24:** 332–340.

Dillman CB, **Sidlauskas BL**, **Vari RP. 2015.** A morphological supermatrix-based phylogeny for the Neotropical fish superfamily Anostomoidea (Ostariophysi: Characiformes): phylogeny, missing data and homoplasy. *Cladistics* **32:** 276–296.

Douady CJ, **Dosay M**, **Shivji MS**, **Stanhope MJ. 2003.** Molecular phylogenetic evidence refuting the hypothesis of Batoidea (rays and skates) as derived sharks. *Molecular Phylogenetics and Evolution* **26:** 215–221.

Dragoo JW, **Honeycutt RL. 1997.** Systematics of mustelid-like carnivores. *Journal of Mammalogy* **78:** 426–443.

Driskell AC, **Ane C**, **Burleigh JG**, **McMahon MM**, **O'Meara BC**, **Sanderson MJ. 2004.** Prospects for building the tree of life from large sequence databases. *Science* **306:** 1172–1174.

Drummond AJ, Ashton B, Buxton S, Cheung M, Cooper A, ***et al***. **2010.** Geneious v5.5, Available at: http://www.geneious.com. Accessed 2020.

Ebert DA, **Fowler S**, **Compagno LJV**, **Dando M. 2013.** *Sharks of the world: a fully illustrated guide*. Plymouth: Wild Nature Press.

Edgar RC. 2004. MUSCLE: multiple sequence alignment with high accuracy and high throughput. *Nucleic Acids Research* **32:** 1792–1797.

Eernisse DJ, **Kluge G. 1993.** Taxonomic congruence versus total evidence, and amniote phylogeny inferred from fossils, molecules, and morphology. *Molecular Biology and Evolution* **10:** 1170–1195.

Eitner BJ. 1995. Systematics of the genus *Alopias* (Lamniformes: Alopiidae) with evidence for the existence of an unrecognized species. *Copeia* **3:** 562–571.

Farris JS, **Kallersjo M**, **Kluge AG**, **Bult C. 1994.** Testing significance of incongruence. *Cladistics* **10:** 315–319.

Flynn JJ, **Wesley-Hunt GD. 2005.** Carnivora. In: Rose KD, Archibald JD, eds. *The rise of placental mammals*. Baltimore: John Hopkins University Press, 175–198.

Fowler HW. 1934. Descriptions of new fishes obtained 1907 to 1910, chiefly in the Philippine Islands and adjacent seas. *Proceedings of the Academy of Natural Sciences of Philadelphia* **85:** 233–367.

Fowler HW. 1941. The fishes of the groups Elasmobranchi, Holocephali, Isospondyli, and Ostariophysi obtained by the United States Bureau of Fisheries steamer 'Albattross' in 1907 to 1910, chiefly in the Philippine Islands and adjacent seas. *Bulletin of the United States National Museum* **13:** 1–879.

Garman S. 1906. New Plagiostoma. *Bulletin of the Museum of Comparative Zoology at Harvard College* **46:** 203–208.

Garman S. 1913. The Plagiostomia (sharks, skates and rays). *Memoirs of the Museum of Comparative Zoology at Harvard College* **36:** 1–528, 77 plates.

Garrick JAF, **Schultz LP. 1963.** A guide to the kinds of potentially dangerous sharks. In: Gilbert PW, ed. *Sharks and survival*. Boston: Heath, 36–60.

Gesner C. 1586. *Conr. Gesneri Tigurini medicinæ et philosophiae professoris in Schola Tigurina, historiæ animalium liber II: qui est de quadrupedibus ouiparis*. Frankfurt: Wechel & Cambier.

Gill TN. 1862. Analytical synopsis of the order of Squali; and revision of the nomenclature of the genera. *Annals of the Lyceum of Natural History of New York* **7:** 367–408.

Gledhill DC, **Last PR**, **White WT. 2008.** Resurrection of the genus *Figaro* Whitley (Carcharhiniformes: Scyliorhinidae) with the description of a new species from northeastern Australia. *CSIRO Marine and Atmospheric Research Paper* **22:** 179–188.

Goloboff PA. 1993. Estimating character weights during tree search. *Cladistics* **9:** 83–91.

Goloboff PA. 2014. Extended implied weighting. *Cladistics* **30:** 260–272.

Goloboff PA, **Carpenter JM**, **Arias JS**, **Esquivel DRM. 2008a.** Weighting against homoplasy improves phylogenetic analysis of morphological data sets. *Cladistics* **24:** 1–16.

Goloboff PA, **Farris J**, **Nixon K. 2003.** *T.N.T.: tree analysis using new technology*. Program and documentation, available from the authors. Available at: http://www.lillo.org.ar/phylogeny/tnt/

Goloboff PA, **Farris JS**, **Nixon KC. 2008b.** TNT, a free program for phylogenetic analysis. *Cladistics* **24:** 774–786.

Goloboff PA, **Mattoni CM**, **Quinteros AS. 2006.** Continuous characters analyzed as such. *Cladistics* **22:** 589–601.

Gomes UL, **Peters GO**, **de Carvalho MR**, **Gadig OBF. 2006.** Anatomical investigation of the slender catshark *Schroederichthys tenuis* Springer, 1966, with notes on intrageneric relationships (Chondrichthyes: Carcharhiniformes: Scyliorhinidae). *Zootaxa* **1119:** 29–58.

Goto T. 2001. Comparative anatomy, phylogeny and cladistic classification of the order Orectolobiformes (Chondrichthyes, Elasmobranchii). *Memoirs of the Graduate School of Fisheries Sciences Hokkaido University* **48:** 1–100.

Graybeal A. 1998. Is it better to add taxa or characters to a difficult phylogenetic problem? *Systematic Biology* **47:** 9–17.

Griffiths AM, **Miller DD**, **Egan A**, **Fox J**, **Greenfield A**, **Mariani S. 2013.** DNA barcoding unveils skate (Chondrichthyes: Rajidae) species diversity in 'ray' products sold across Ireland and the UK. *PeerJ* **1:** e129.

Gronovius LT. 1756. *Bibliotheca regni animalis atque lapidei, seu, recensio auctorum et librorum: qui de regno animali & lapideo methodice, physice, medice, chymice, philologice, vel theologice tractant, in usum naturalis historiae studiosorum*. Leiden: published by the author.

Herman J, **Hovestadt-Euler M**, **Hovestadt DC. 1990.** Contributions to the study of the comparative morphology of teeth and other relevant ichthyodorulites in living supraspecific taxa of Chondrichthyan fishes. In: Stehmann M, ed. Part A: Selachii. No. 2b: order: Carcharhiniformes—family: Scyliorhinidae. *Bulletin de l'Institut Royal des Sciences Naturelles de Belgique* **60:** 181–230.

Hillis DM. 1987. Molecular versus morphological approaches to systematics. *Annual Review of Ecology and Systematics* **18:** 23–42.

Hoffman HA, **Jordan DS. 1892.** A catalogue of the fishes of Greece with notes on the names now in use and those

employed by classical authors. *Academy of Natural Sciences of Philadelphia* **44:** 230–286.

Holmes BH, **Steinke D**, **Ward RD. 2009.** Identification of shark and ray fins using DNA barcoding. *Fisheries Research* **95:** 280–288.

Huber DR, **Soares MC**, **de Carvalho MR. 2011.** Cartilaginous fishes cranial muscles. In: Farrell AP, ed. *Encyclopedia of fish physiology: from genome to environment*. San Diego: Academic Press, 449–462.

Human BA. 2006a. A taxonomic revision of the catshark genus *Poroderma* Smith, 1837 (Chondrichthyes: Carcharhiniformes: Scyliorhinidae). *Zootaxa* **1229:** 1–32.

Human BA. 2006b. A taxonomic revision of the catshark genus *Holohalaelurus* Fowler 1934 (Chondrichthyes: Carcharhiniformes: Scyliorhinidae), with descriptions of two new species. *Zootaxa* **1315:** 1–56.

Human BA. 2007. A taxonomic revision of the catshark genus *Haploblepharus* Garman 1913 (Chondrichthyes: Carcharhiniformes: Scyliorhinidae). *Zootaxa* **1451:** 1–40.

Human BA, **Owen EP**, **Compagno LJV**, **Harley EH. 2006.** Testing morphologically based phylogenetic theories within the cartilaginous fishes with molecular data, with special reference to the catshark family (Chondrichthyes; Scyliorhinidae) and the interrelationships within them. *Molecular Phylogenetics and Evolution* **39:** 384–391.

Iglésias SP, **Lecointre G**, **Sellos DY. 2005.** Extensive paraphylies within sharks of the order Carcharhiniformes inferred from nuclear and mitochondrial genes. *Molecular Phylogenetics and Evolution* **34:** 569–583.

Jungersen HFE. 1899. *On the apendices genitales in the Greenland shark Somniosus microcephalus (Bl. Schn.) and another selachians. Danish Ingolf Expedition, Vol. II*. Copenhagen: Bianco luno.

Kluge AG. 1989. A concern for evidence and a phylogenetic hypothesis of relationships among *Epicrates* (Boidae, Serpentes). *Systematic Zoology* **38:** 7–25.

Kluge AG, **Wolf AJ. 1993.** Cladistics: whats's in a word? *Cladistics* **9:** 183–199.

Lana FO, **Soares KDA**, **Hazin FHV**, **Gomes UL. 2021.** Description of the chondrocranium of the silky shark *Carcharhinus falciformis* with comments on the cranial terminology and phylogenetic implications in carcharhinids (Chondrichthyes, Carcharhiniformes, Carcharhinidae). *Journal of Morphology* **2021:** 1–16.

Last PR, **Gomon MF**, **Gledhill DC. 1999.** Australian spotted catsharks of the genus *Asymbolus* (Carcharhiniformes: Scyliorphinidae). Part 2: descriptions of three new, dark-spotted species. *CSIRO Marine Laboratories* **239:** 19–35.

Last PR, **Séret B**, **White WL. 2008.** New swellsharks (*Cephaloscyllium*: Scyliorhinidae) from the Indo-Australian region. *CSIRO Marine and Atmospheric Research Paper* **22:** 129–146.

Last PR, **White WL. 2008.** Two new saddled swellsharks (*Cephaloscyllium*: Scyliorhinidae) from eastern Australia. *CSIRO Marine and Atmospheric Research Paper* **22:** 159–170.

Leigh-Sharpe WH. 1926. The comparative morphology of the secondary sexual characters of elasmobranch fishes. The claspers, clasper siphons, and clasper glands. Memoir VIII. *Journal of Morphology and Physiology* **42:** 307–320.

Linnaeus C. 1758. *Systema naturae per regna tria naturae, secundum classes, ordines, geneera, species, cum characteribus, differentiis. Synonymis, locis, editio decima, reformata*. Stockholm: Salvius.

López J, **Ryburn J**, **Fedrigo O**, **Naylor G. 2006.** Phylogeny of sharks of the family Triakidae (Carcharhiniformes) and its implications for the evolution of carcharhiniform placental viviparity. *Molecular Phylogenetics and Evolution* **40:** 50–60.

Maddison W. 1993. Missing data versus missing characters in phylogenetic analysis. *Systematic Biology* **42:** 576–581.

Madduppa H, **Ayuningtyas RU**, **Subhan B**, **Arafat D**, **Prehadi P. 2016.** Exploited but unevaluated: DNA barcoding reveals skates and stingrays (Chordata, Chondrichthyes) species landed in the Indonesian fish market. *Ilmu Kelautan Maret (IJMS)* **21:** 29–36.

Maisey JG. 1980. An evaluation of jaw suspension in sharks. *American Museum Novitates* **2706:** 1–17.

Maisey JG. 1984. Higher elasmobranch phylogeny: a look at the evidence. *Journal of Vertebrate Paleontology* **4:** 359–371.

Mariguela TC, **De-Franco B**, **Almeida TVV**, **Mendonça FF**, **Gadig OBF**, **Foresti F**, **Oliveira C. 2009.** Identification of guitarfish species *Rhinobatos percellens*, *R. horkelli*, and *Zapteryx brevirostris* (Chondrichthyes) using mitochondrial genes and RFLP technique. *Conservation Genetics Resources* **1:** 393–396.

Maruska KP. 2001. Morphology of the mechanosensory lateral line system in elasmobranch fishes: ecological and behavioral considerations. *Environmental Biology of Fishes* **60:** 47–75.

Mirande JM. 2019. Morphology, molecules and the phylogeny of Characidae (Teleostei, Characiformes). *Cladistics* **35:** 282–300.

Motta PJ, **Wilga CD. 1995.** Anatomy of the feeding apparatus of the lemon shark, *Negaprion brevirostris*. *Journal of Morphology* **226:** 309–329.

Muñoz-Chápuli R. 1985. Ornamentación ultraestructural del esqueleto dérmico en algumas espécies de Carcharhiniformes. *Miscellània Zoològica* **9:** 394–396.

Müller J, **Henle J. 1838–1841.** *Systematische Beschreibung der Plagiostomen*. Berlin: Viet und Comp.

Nakaya K. 1975. Taxonomy, comparative anatomy and phylogeny of Japanese catsharks, Scyliorhinidae. *Memoirs of the Faculty of Fisheries, Hokkaido University* **23:** 1–94.

Nakaya K, **Inoue S**, **Ho H-C. 2013.** A review of the genus *Cephaloscyllium* (Chondrichthyes: Carcharhiniformes: Scyliorhinidae) from Taiwanese waters. *Zootaxa* **3752:** 101–129.

Nakaya K, **Sato K. 1999.** Species grouping within the genus *Apristurus* (Elasmobranchii: Scyliorhinidae). In: Séret B, Sire J-Y, eds. *Proceedings of the 5th Indo-Pacific Fish Conference, Nouméa*. Paris: Société Française d'Ichtyologie, 307–320.

Nakaya K, **Séret B. 2000.** Re-description and taxonomy of *Pentanchus profundicolus* Smith & Radcliffe, based on a

second specimen from the Philippines (Chondrichthyes, Carcharhiniformes, Scyliorhinidae). *Ichthyological Research* **47:** 373–378.

Naylor GJP, **Caira JN**, **Jensen K**, **Rosana KAM**, **Straube N**, **Lakner C. 2012a.** Elasmobranch phylogeny: a mitochondrial estimate based on 595 species. In: Carrier JC, Musick JA, Heithaus MR, eds. *Biology of sharks and their relatives*, *2nd edn*. Boca Raton: CRC Press, 31–56.

Naylor GJP, **Caira JN**, **Jensen K**, **Rosana KAM**, **White WT**, **Last PR. 2012b.** A sequence-based approach to the identification of shark and ray species and its implications for global elasmobranch diversity and parasitology. *Bulletin of the American Museum of Natural History* **367:** 1–262.

Naylor GJP, **Ryburn JA**, **Fedrigo O**, **López JA. 2005.** Phylogenetic relationships among the major lineages of modern elasmobranchs. In: Hamlett WC, Jamieson BGM, eds. *Reproductive biology and phylogeny, Vol. 3*. EnWeld: Science Publishers, 1–25.

Nelson JS, **Grande TC**, **Wilson MVH. 2016.** *Fishes of the world*, *5th edn*. New York: John Wiley & Sons.

Nixon KC, **Carpenter JM. 1993.** On outgroups. *Cladistics* **9:** 423–426.

Padial JM, **Miralles A**, **De la Riva I**, **Vences M. 2010.** The integrative future of taxonomy. *Frontiers in Zoology* **7:** 16.

Philippe H, **Snell EA**, **Bapteste E**, **Lopez P**, **Holland PWH**, **Casane D. 2004.** Phylogenomics of eukaryotes: impact of missing data on large alignments. *Molecular Biology and Evolution* **21:** 1740–1752.

Pimentel R, **Riggins R. 1987.** The nature of cladistic data. *Cladistics* **3:** 201–209.

Quattro JM, **Stoner DS**, **Driggers WB**, **Anderson CA**, **Priede KA**, **Hoppmann EC**, **Campbell NH**, **Duncan KM**, **Grady JM. 2006.** Genetic evidence of cryptic speciation within hammerhead sharks (genus *Sphyrna*). *Marine Biology* **148:** 1143–1155.

de Queiroz A, **Donoghue M**, **Kim J. 1995.** Separate versus combined analysis of phylogenetic evidence. *Annual Review of Ecology and Systematics* **26:** 657–681.

Rae TC. 1998. The logical basis for the use of continuous characters in phylogenetic systematics. *Cladistics* **14:** 221–228.

Rannala B, **Huelsenbeck JP**, **Yang Z**, **Nielson R. 1998.** Taxon sampling and the accuracy of large phylogenies. *Systematic Biology* **47:** 702–710.

Raschi W, **Tabit C. 1992.** Functional aspects of placoid scales: a review and update. *Australian Journal of Marine and Freshwater Research* **43:** 123–147.

Regan CT. 1908. A synopsis of the sharks of the family Scyliorhinidae. *Annals and Magazine of Natural History* **8:** 453–465.

Reif WE. 1982. Morphogenesis and function of the squamation in sharks. 1. Comparative functional morphology of shark scales, and ecology of sharks. *Neues Jahrbuch für Geologie und Paläontologie-Abhandlungen* **164:** 172–183.

Reif WE. 1985. Squamation and ecology of sharks. *Courier Forschunginstitut Senckenberg* **78:** 1–101.

Richards VP, **Henning M**, **Witzell W**, **Shivji MS. 2009.** Species delineation and evolutionary history of the globally distributed spotted eagle ray (*Aetobatus narinari*). *Journal of Heredity* **100:** 273–283.

Rondelet G. 1554. *Libri de piscibus marinis in quibus verae piscium effigies expressae sunt*. Lyon: Mathias Bonhomme.

Sabaj MH. 2016. *Standard symbolic codes for institutional resource collections in herpetology and ichthyology: an online reference. Version 6.5 (16 August 2016)*. Washington: American Society of Ichthyologists and Herpetologists. Available at: http://www.asih.org/

Salviani H. 1554. *Aquatilium animalium historiae, liber primus: cum eorumdem formis, aere excusis*. Rome: Hippolytus Saluianus.

Sato K. 2000. *Phylogenetic systematics of the deep-water catshark genus* Apristurus *(Chondrichthyes, Carcharhiniformes, Scyliorhinidae)*. Unpublished PhD Thesis, Faculty of Fisheries, Hokkaido University.

Sato K, **Nakaya K**, **Yorozu M. 2008.** *Apristurus australis* sp. nov., a new long-snout catshark (Chondrichthyes: Carcharhiniformes: Scyliorhinidae) from Australia. *CSIRO Marine and Atmospheric Research Paper* **22:** 113–122.

Sereno PC. 2007. Logical basis for morphological characters in phylogenetics. *Cladistics* **23:** 565–587.

Séret B. 1990. *Aulohalaelurus kanakorum* n.sp., a new species of catshark (Carcharhiniformes, Scyliorhinidae, Atelomycterinae) from New Caledonia. *Records of the Australian Museum* **42:** 127–136.

Séret B, **Last PR. 2007.** Four new species of deepwater catsharks of the genus *Parmaturus* (Carcharhiniformes: Scyliorhinidae) from New Caledonia, Indonesia and Australia. *Zootaxa* **1657:** 23–39.

Serra-Pereira B, **Moura T**, **Griffiths AM**, **Serrano Gordo L**, **Figueiredo I. 2010.** Molecular barcoding of skates (Chondrichthyes: Rajidae) from the southern Northeast Atlantic. *Zoologica Scripta* **40:** 76–84.

Shirai S. 1992. Identity of extra branchial arches of Hexanchiformes (Pisces, Elasmobranchii). *Bulletin of the Faculty of Fishery of the Hokkaido University* **43:** 24–32.

Shirai S. 1996. Phylogenetic interrelationships of Neoselachians (Chondrichthyes: Euselachii). In: Stiassny MLJ, Parenti LR, Johnson GD, eds. *Interrelationships of fishes*. New York: Academic Press, 9–34.

Smith PJ, **Steinke D**, **Mcveagh SM**, **Stewart AL**, **Struthers CD**, **Roberts CD. 2008.** Molecular analysis of Southern Ocean skates (*Bathyraja*) reveals a new species of Antarctic skate. *Journal of Fish Biology* **73:** 1170–1182.

Soares KDA. 2020. Comparative anatomy of the clasper of catsharks and its phylogenetic implications (Chondrichthyes: Carcharhiniformes: Scyliorhinidae). *Journal of Morphology* **2020:** 1–17.

Soares KDA, **de Carvalho MR. 2019.** The catshark genus *Scyliorhinus* (Chondrichthyes: Carcharhiniformes: Scyliorhinidae): taxonomy, morphology and distribution. *Zootaxa* **4601:** 1–147.

Soares KDA, **de Carvalho MR. 2020.** Phylogenetic relationship of catshark species of the genus *Scyliorhinus* (Chondrichthyes, Carcharhiniformes, Scyliorhinidae) based

on comparative morphology. *Zoosystematics and Evolution* **96:** 345–395.

Soares KDA, **de Carvalho MR**, **Schwingel PR**, **Gadig OBF. 2019.** A new species of *Parmaturus* (Chondrichthyes: Carcharhiniformes: Scyliorhinidae) from Brazil, southwestern Atlantic. *Copeia* **107:** 314–322.

Soares KDA, Gadig OBF, Gomes UL. 2015. *Scyliorhinus ugoi*, a new species of catshark from Brazil (Chondrichthyes: Carcharhiniformes: Scyliorhinidae). *Zootaxa* **3937:** 347–361.

Spies IB, **Gaichas S**, **Stevenson DE**, **Orr JW**, **Canino MF. 2006.** DNA-based identification of Alaska skates (*Amblyraja*, *Bathyraja* and *Raja*: Rajidae) using cytochrome *c* oxidase subunit I (coI) variation. *Journal of Fish Biology* **69:** 283–292.

Springer S. 1966. A review of Western Atlantic cat sharks, Scyliorhinidae, with descriptions of a new genus and five new species. *Fishery Bulletin, US Fish and Wildlife Service* **65:** 581–624.

Springer S. 1979. *A revision of the catsharks, family Scyliorhinidae. Circular 422*. Washington: Department of Commerce, National Oceanic and Atmospheric Administration Technical Report, National Marine Fisheries Service.

Stensiö EA. 1959. On the pectoral fin and shoulder girdle of the Arthrodires. *Kungliga Svenska Vetenskapsakademiens Handlingar* **4:** 1–299.

Straube N, **Iglésias SP**, **Sellos DY**, **Kriwet J**, **Schliewen UK. 2010.** Molecular phylogeny and node time estimation of bioluminescent lantern sharks (Elasmobranchii: Etmopteridae). *Molecular Phylogenetics and Evolution* **56:** 905–917.

Straube N, **Kriwet J**, **Schliewen UK. 2011.** Cryptic diversity and species assignment of large lantern sharks of the *Etmopterus* spinax clade from the Southern Hemisphere (Squaliformes, Etmopteridae). *Zoologica Scripta* **40:** 61–75.

Thorpe RS. 1984. Coding morphometric characters for constructing Wagner networks. *Evolution; international journal of organic evolution* **38:** 244–355.

Vélez-Zuazo X, **Agnarsson I. 2011.** Shark tales: a molecular species-level phylogeny of sharks (Selachimorpha, Chondrichthyes). *Molecular Phylogenetics and Evolution* **58:** 207–217.

Ward RD, **Bronwyn HH**, **White WT**, **Last PR. 2008.** DNA barcoding Australasian Chondrichthyans: results and potential uses in conservation. *Marine and Freshwater Research* **59:** 57–71.

Ward RD, **Hanner R**, **Hebert PDN. 2009.** The campaign to DNA barcode all fishes, FISH-BOL. *Journal of Fish Biology* **74:** 329–356.

Ward RD, **Holmes B. 2007.** An analysis of nucleotide and amino acid variability in the barcode region of cytochrome *c* oxidase I (*cox1*) in fishes. *Molecular Ecology Notes* **7:** 899–907.

Ward RD, **Holmes BA**, **Zemlak TS**, **Smith PJ. 2007.** Part 12: DNA barcoding discriminates spurdogs of the genus *Squalus*. In: Last PR, White WT, Pogonoski JJ, eds. *Descriptions of new dogfishes of the genus* Squalus *(Squaloidea: Squalidae)*. Canberra: Commonwealth Scientific and Industrial Research Organisation, 114–130.

Ward RD, **Zemlak TS**, **Innes BH**, **Last PR**, **Hebert PDN. 2005.** DNA barcoding Australia's fish species. *Philosophical Transactions of the Royal Society B: Biological Sciences* **360:** 1847–1857.

Weigmann S. 2016. Annotated checklist of the living sharks, batoids and chimaeras (Chondrichthyes) of the world, with a focus on biogeographical diversity. *Journal of Fish Biology* **88:** 837–1037.

Weigmann S, **Kaschner CJ**, **Thiel R. 2018.** A new microendemic species of the deep-water catshark genus *Bythaelurus* (Carcharhiniformes, Pentanchidae) from the northwestern Indian Ocean, with investigations of its feeding ecology, generic review and identification key. *PLoS One* **13:** e0207887.

White EG. 1936a. Some transitional elasmobranchs connecting the Catuloidea with the Carcharinoidea. *American Museum Novitates* **879:** 1–22.

White EG. 1936b. A classification and phylogeny of the elasmobranch fishes. *American Museum Novitates* **837:** 1–16.

White EG. 1937. Interrelationships of the elasmobranchs with a key to the order Galea. *Bulletin of the American Museum of Natural History* **74:** 25–138.

White WT, **Fahmi F**, **Weigmann S. 2019.** A new genus and species of catshark (Carcharhiniformes: Scyliorhinidae) from eastern Indonesia. *Zootaxa* **4691:** 444–460.

White WT, **Last PR. 2012.** A review of the taxonomy of chondrichthyan fishes: a modern perspective. *Journal of Fish Biology* **80:** 1–17.

Whitley GP. 1948. New sharks and fishes from Western Australia. Part 4. *Australian Zoologist* **11:** 259–276.

Wiens JJ. 1998. Does adding characters with missing data increase or decrease phylogenetic accuracy? *Systematic Biology* **47:** 625–640.

Wiens JJ. 2003. Missing data, incomplete taxa, and phylogenetic accuracy. *Systematic Biology* **52:** 528–538.

Wiens JJ. 2006. Missing data and the design of phylogenetic analyses. *Journal of Biomedical Informatics* **39:** 34–42.

Wiens JJ, Morrill MC. 2011. Missing data in phylogenetic analysis: reconciling results from simulations and empirical data. *Systematic Biology* **60:** 719–731.

Winchell CJ, **Martin AP**, **Mallatt J. 2004.** Phylogeny of elasmobranchs based on LSU and SSU ribosomal RNA genes. *Molecular Phylogenetics and Evolution* **31:** 214–224.

Wong EH-K, **Shivji MS**, **Hanner RH. 2009.** Identifying sharks with DNA barcodes: assessing the utility of a nucleotide diagnostic approach. *Molecular Ecology Resources* **9:** 243–256.

Wyffels J, **King BL**, **Vincent J**, **Chen C**, **Wu CH**, **Polson SW. 2014.** SkateBase, an elasmobranch genome project and collection of molecular resources for chondrichthyan fish. *F1000Research* **3:** 191.

Wynen L, **Larson H**, **Thorburn D**, **Peverell S**, **Morgan D**, **Field I**, **Gibb K. 2009.** Mitochondrial DNA supports the identification of two endangered river sharks (*Glyphis glyphis* and *Glyphis garricki*) across northern Australia. *Marine and Freshwater Research* **60:** 554–562.

Zemlak TS, **Ward RD**, **Connell AD**, **Holmes BH**, **Hebert PDN. 2009.** DNA barcoding reveals overlooked marine fishes. *Molecular Ecology Resources* **9**(Suppl.): 237–242.

SUPPORTING INFORMATION

Additional Supporting Information may be found in the online version of this article at the publisher's web-site:

Supplementary Material 1. List of material examined.
Supplementary Material 2. Matrix of quantitative characters presenting absolute and normalized values.
Supplementary Material 3. Matrix of qualitative morphological characters.
Supplementary Material 4. Molecular alignment of *NADH2* sequences.
Supplementary Material 5. List of non-ambiguous synapomorphies of clades and terminal taxa based on the most-parsimonious cladogram resulting from combined datasets and under extended implied weighting (k = 3).
Supplementary Material 6. List of morphological character transformations based on the most-parsimonious cladogram resulting from combined datasets and under extended implied weighting (k = 3).
Supplementary Material 7. General topology of the consensus of the most-parsimonious tree resulting from combined datasets and under extended implied weighting (k = 3).